Neutrino Cosmology

July 30th, 2024
YETI 2024: The 3 Neutrino Problem
Durham University

Eleonora Di Valentino
Royal Society Dorothy Hodgkin Research Fellow
School of Mathematics and Statistics
University of Sheffield (UK)

Neutrino physics and cosmology

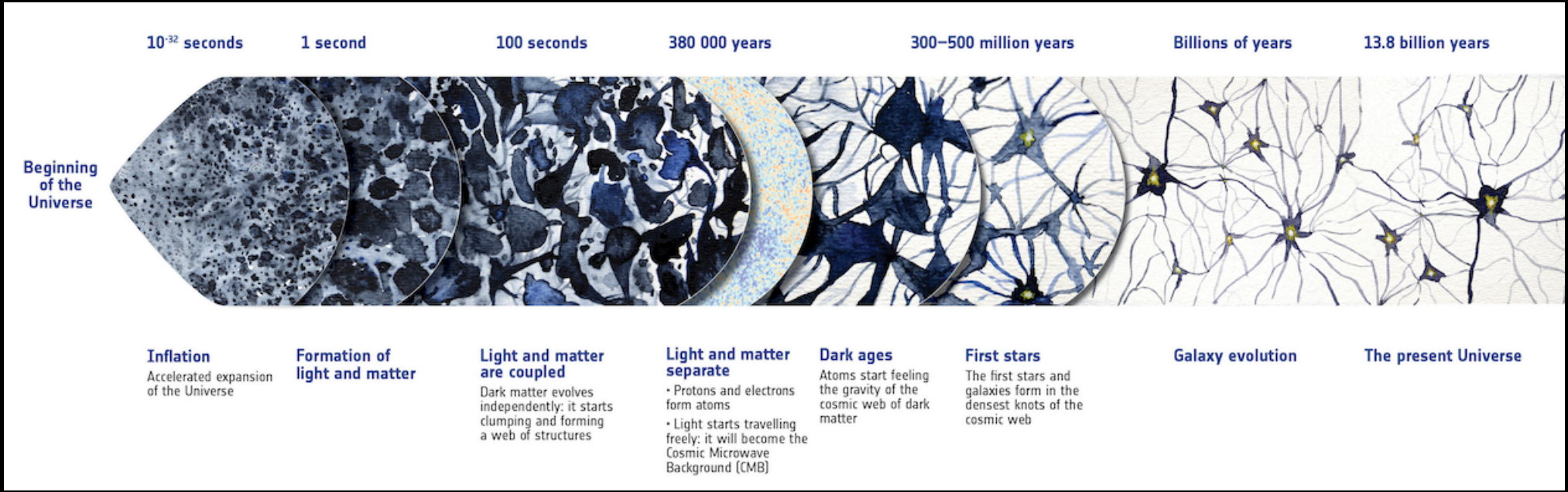

Neutrinos are the last particles of the Standard Model whose masses are unknown. To measure their total mass with the cosmological data we depend on the creation of a Cosmic Neutrino Background at early times, and the growth of structures at late times.

Therefore, the main cosmological probes that we can use are the Cosmic Microwave Background (CMB) and the Large Scale Structure (LSS) data.

With the cosmological data, we can place constraints not only on the total neutrino mass, but also on the neutrino effective number.

The Standard cosmological model

The Standard cosmological model

O'Raifeartaigh et al, arxiv:1701.07261

Modern cosmology was probably born when Albert Einstein (1917) applied general relativity for the first time to cosmology introducing the cosmological constant term.
On the 4th of February 1917 Albert Einstein wrote to Paul Ehrenfest:
”I have perpetrated something ...in gravitation theory,
which exposes me a bit to the danger of being committed to a madhouse.”

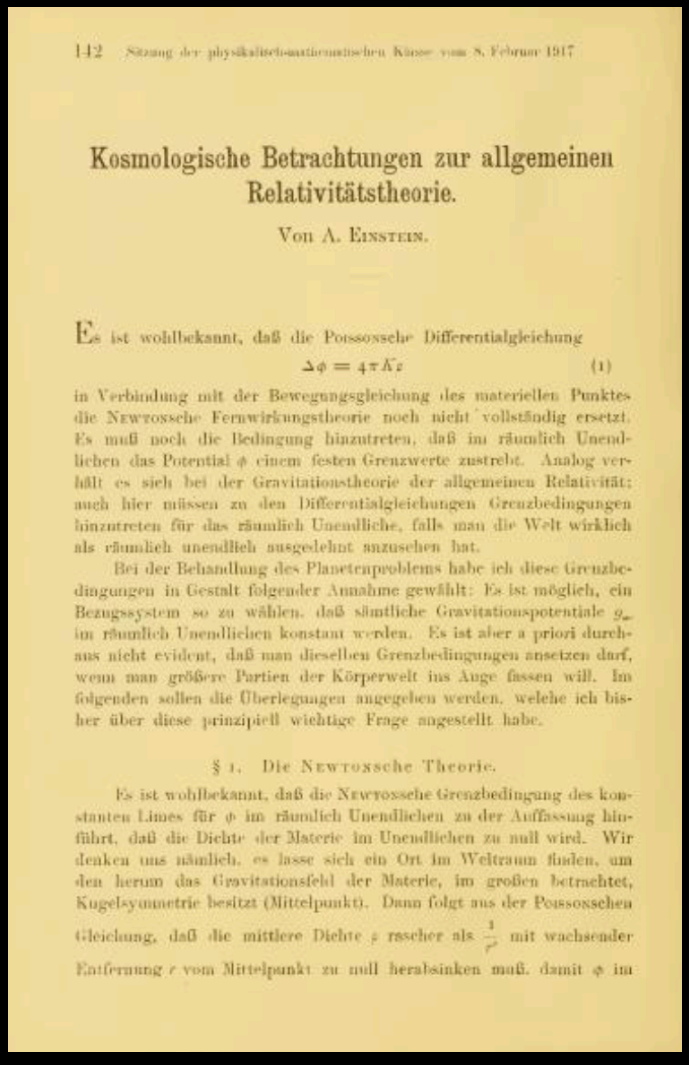

142 Sitzung der physikalisch-mathematischen Klasse vom 8. Februar 1917

Kosmologische Betrachtungen zur allgemeinen Relativitätstheorie.

Von A. Einstein.

Es ist wohlbekannt, daß die Possossche Differentialgleichung

$$\Delta\phi = 4\pi K\varrho \qquad (1)$$

in Verbindung mit der Bewegungsgleichung des materiellen Punktes die Newtonsche Fernwirkungstheorie noch nicht vollständig ersetzt. Es muß noch die Bedingung hinzutreten, daß im räumlich Unendlichen das Potential ϕ einem festen Grenzwerte zustrebt. Analog verhält es sich bei der Gravitationstheorie der allgemeinen Relativität; auch hier müssen zu den Differentialgleichungen Grenzbedingungen hinzutreten für das räumlich Unendliche, falls man die Welt wirklich als räumlich unendlich ausgelehnt anzusehen hat.

Bei der Behandlung des Planetenproblems habe ich diese Grenzbedingungen in Gestalt folgender Annahme gewählt: Es ist möglich, ein Bezugssystem so zu wählen, daß sämtliche Gravitationspotentiale $g_{\mu\nu}$ im räumlich Unendlichen konstant werden. Es ist aber a priori durchaus nicht evident, daß man dieselben Grenzbedingungen ansetzen darf, wenn man größere Partien der Körperwelt ins Auge fassen will. Im folgenden sollen die Überlegungen angegeben werden, welche ich bisher über diese prinzipiell wichtige Frage angestellt habe.

§ 1. Die Newtonsche Theorie.

Es ist wohlbekannt, daß die Newtonsche Grenzbedingung des konstanten Limes für ϕ im räumlich Unendlichen zu der Auffassung hinführt, daß die Dichte der Materie im Unendlichen zu null wird. Wir denken uns nämlich, es lasse sich ein Ort im Weltraum finden, um den herum das Gravitationsfeld der Materie, im großen betrachtet, Kugelsymmetrie besitzt (Mittelpunkt). Dann folgt aus der Possossschen Gleichung, daß die mittlere Dichte ϱ rascher als $\frac{1}{r^2}$ mit wachsender Entfernung r vom Mittelpunkt zu null herabsinken muß, damit ϕ im

Einstein published his theory in the paper ‘Cosmological Considerations in the General Theory of Relativity’ on February 15th 1917 on the Prussian Academy of Sciences.

The model proposed by Einstein was static and closed.
In order to have this possibility he extended his theory of General Relativity by including a Λ term,
the Cosmological Constant:

$$G_{\mu\nu} - \frac{1}{2} g_{\mu\nu} G = -\kappa T_{\mu\nu}$$

$$G_{\mu\nu} - \lambda g_{\mu\nu} = -\kappa \left(T_{\mu\nu} - \frac{1}{2} g_{\mu\nu} T \right)$$

The Standard cosmological model

O'Raifeartaigh et al, arxiv:1701.07261

In the meantime, around 1922 Friedmann and, independently, Lemaitre in 1927, proposed a different solution with an expanding universe, deriving what we now call the "Hubble law", and therefore no need for a cosmological constant term.

Einstein, at the beginning, rejected the idea of an expanding universe, and according to Lemaitre, he was telling him:
“Your calculations are correct, but your physics is abominable”.

The Standard cosmological model

However, two years later (1929) Hubble (and Humason) confirmed the existence of that law and determined a value for the constant that now bears Hubble's name.

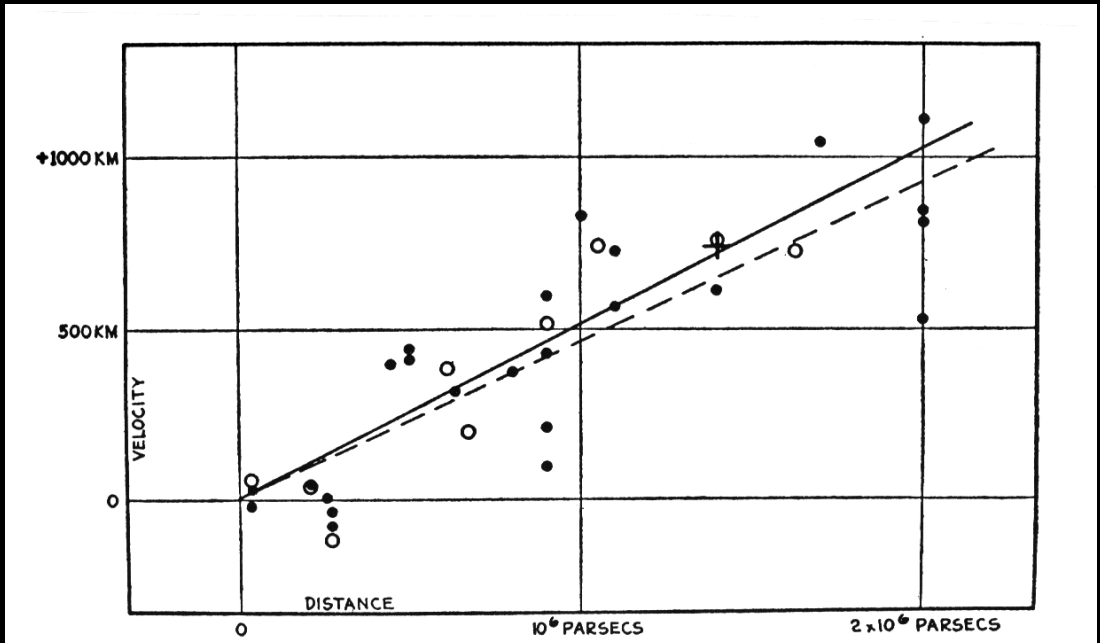

FIG. 9. *The Formulation of the Velocity-Distance Relation.*

The redshift of galaxies was directly proportional to the distance of the galaxy from Earth.
That meant that
things farther away from Earth were moving away faster.

In other words,
the universe must be expanding.

Albert Einstein then rejected the cosmological constant term as unnecessary because no longer justified, so he wrote to Weyl in 1923 (O'Raifeartaigh et al, arxiv:1701.07261):
" If there is no quasi-static world, then away with the cosmological term"

The Standard cosmological model

After 1930 the expanding universe model of Friedmann-Lemaitre started to be accepted by the majority of the people, and Einstein then published his new view in the Sitzungsberichte der Preussischen Akademie der Wissenschaften.

Einstein A. (1931). Sitzungsber. Preuss. Akad. Wiss. 235-237

As Straumann writes in his paper arXiv:gr-qc/0208027
”Many authors have quoted this paper but never read it.
As a result, the quotations gradually changed in an interesting, quite systematic fashion.

Einstein A. (1931). Sitzsber. Preuss. Akad. Wiss.
Einstein A. Sitzsber. Preuss. Akad. Wiss. (1931)
Einstein A. Sb. Preuss. Akad. Wiss. (1931)
Einstein A. and Preuss S.B. (1931) Akad. Wiss 235

Presumably, one day some historian of science will try to find out what happened with the young physicist S.B. Preuss, who apparently wrote just one important paper and then disappeared from the scene.”

But Einstein Was Wrong About Being Wrong…

Nobel Prize in Physics 2011
for the discovery of the accelerating expansion of the universe through observations of distant Supernovae!

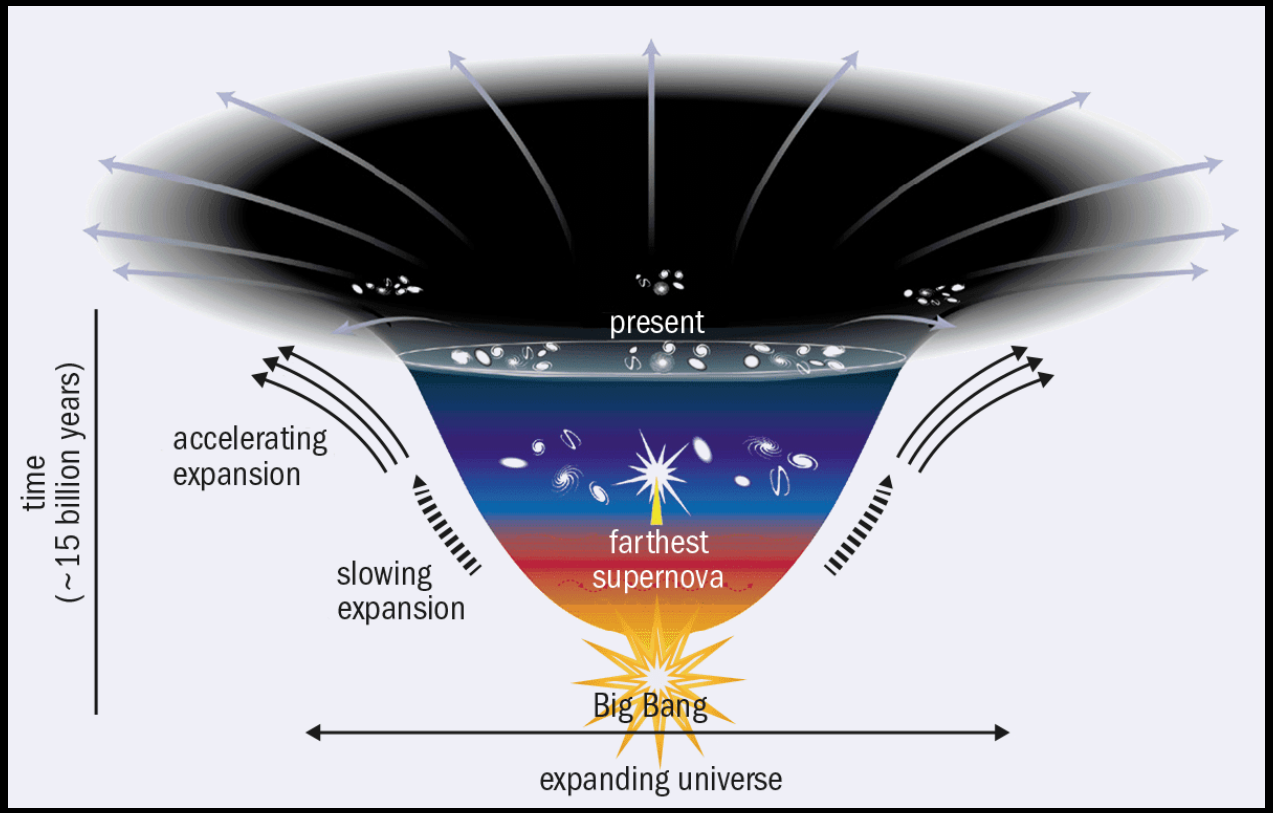

Kolb, arXiv:0709.3102 [astro-ph.CO]

The ΛCDM model

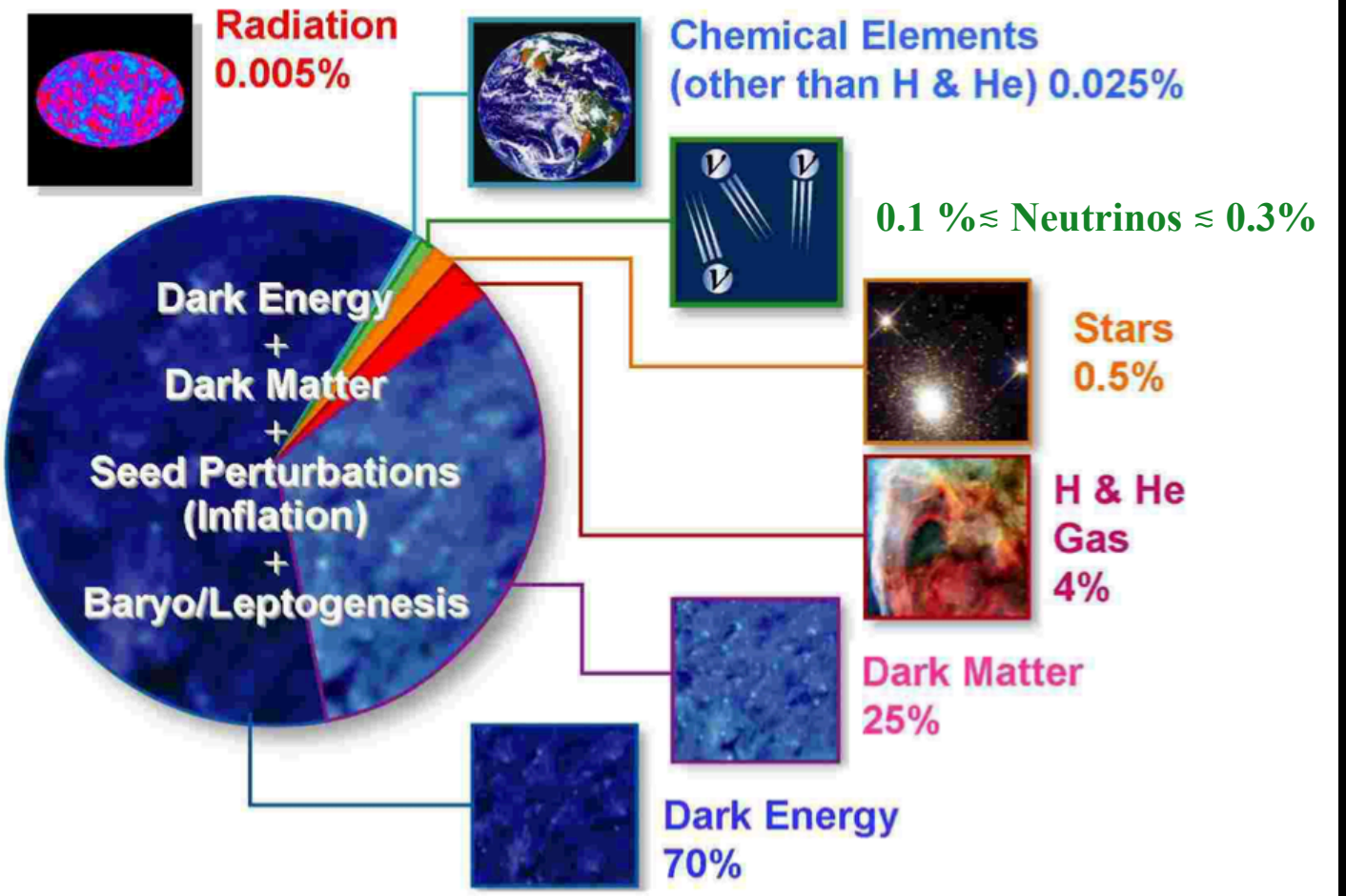

The ΛCDM model, where Λ represents Einstein's cosmological constant, and CDM means cold dark matter, has been chosen as the standard cosmological model due to its simplicity and its ability to accurately describe a wide range of observations.

In this model the radiation energy density accounts for just 0.005% of the total. Elements other than H and He constitute only about 0.025% of the total.

Neutrinos contribute around 0.1 - 0.3%.
Most of the baryons in the Universe are found as hot intracluster gas composed of hydrogen and helium.
Approximately 25% of the total mass-energy density is dark matter, and about 70% is dark energy, which causes the Universe's accelerated expansion.

Our understanding of the history of the universe today

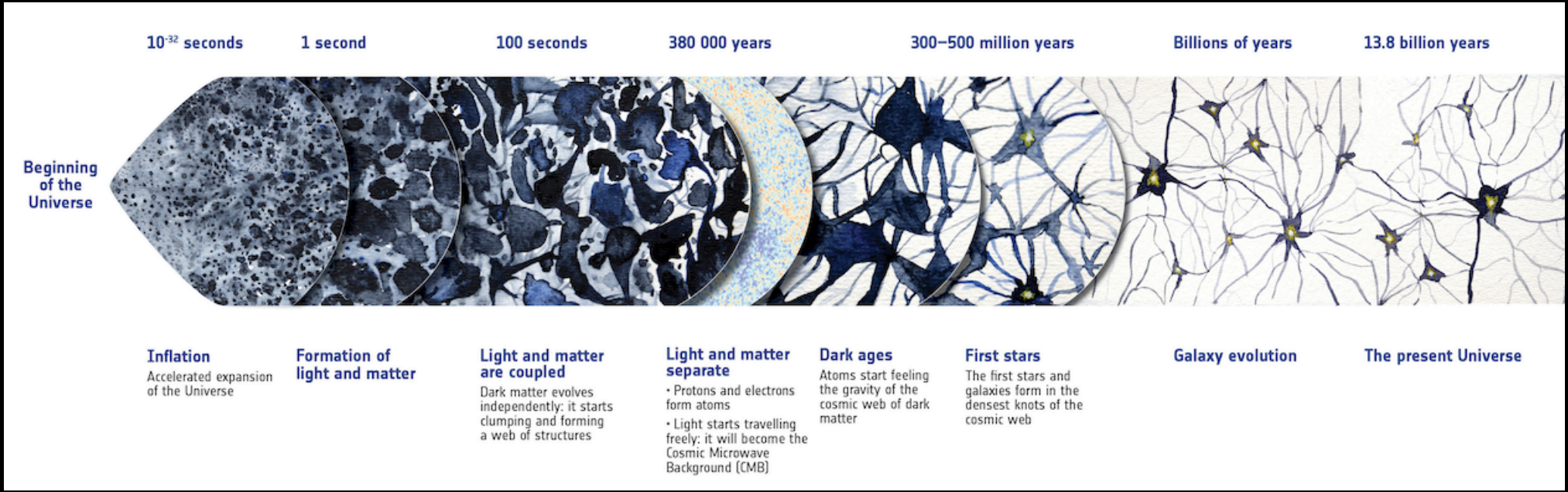

In 1948 Gamow, Alpher and Herman theorized that the Universe originates from a hot “Big Bang", explaining the observed amount of light elements in the Universe through primordial nucleosynthesis (BBN).

According to this theory, the early Universe was mainly composed of a plasma of ionized matter and electromagnetic radiation in thermodynamic equilibrium, through particle-antiparticle annihilation and pairs creation reactions.

As the Universe expanded, this primordial plasma cooled, passing through a phase of recombination, during which electrons and protons combined into neutral hydrogen atoms, and decoupling, during which the Universe subsequently became transparent to the motion of photons.

Our understanding of the history of the universe today

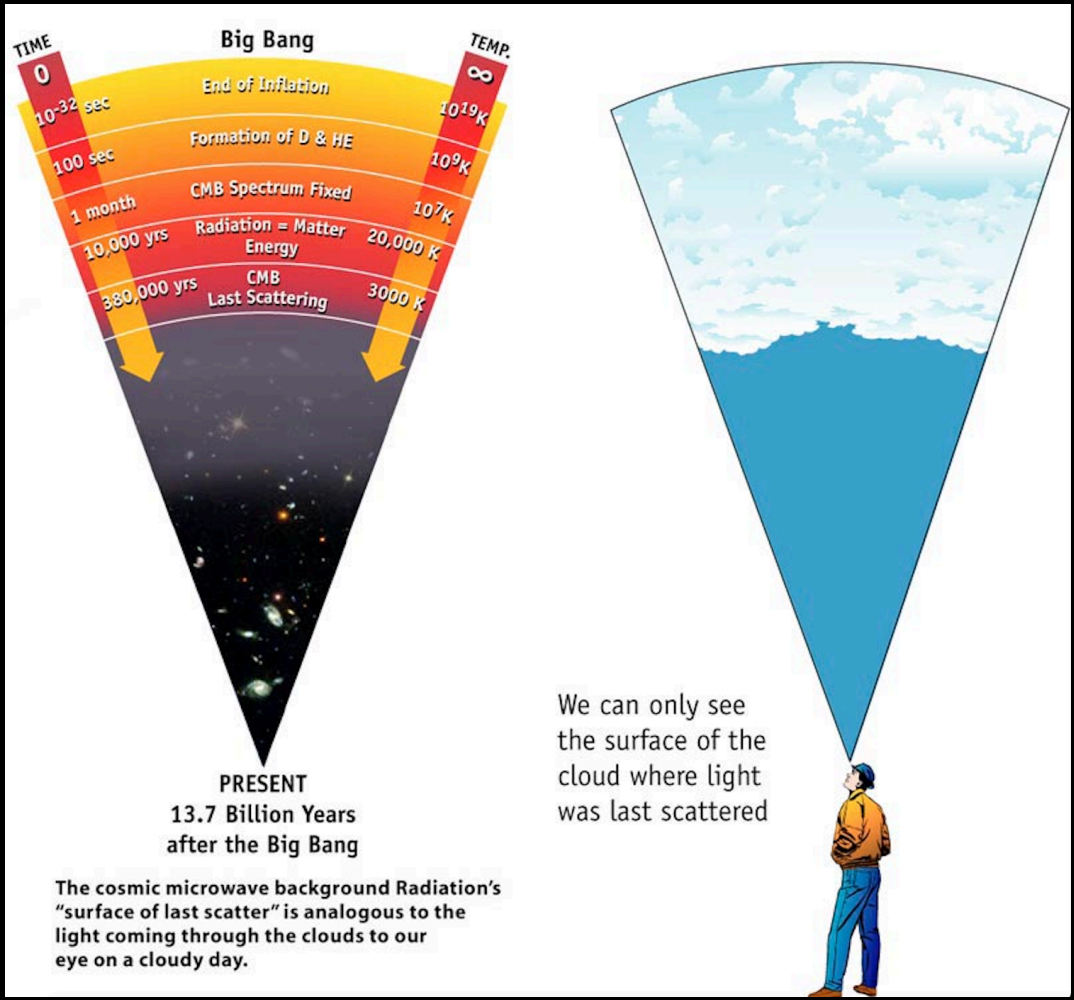

Figura: http://wmap.gsfc.nasa.gov

One of the major prediction of this theory was therefore the existence of a Cosmic Microwave Background (CMB) radiation that permeates the entire observable Universe.

The CMB is the radiation coming from recombination, emitted about 13 billion years ago, just 380,000 years after the Big Bang.
After the discovery of the CMB radiation by Penzias and Wilson in 1964, a model of cosmological structure formation started to be developed that could explain the observed structure of the local Universe, composed of galaxies and cluster of galaxies, starting from a nearly isotropic and homogeneous universe as observed from the CMB.

Our understanding of the history of the universe today

The CMB retains the shape of the primordial universe in which photons were in thermodynamic equilibrium, displaying a thermal black-body spectrum that has cooled with the expansion of the universe, reaching a temperature of T=2.725K today.
This radiation coming from all directions is almost homogeneous, but also offers an image of the minuscule density differences present at recombination and bears witness to everything that happened to photons as they traveled to us.
These effects result in small temperature variations among the photons themselves, on the order of 1/100000, known as anisotropies.

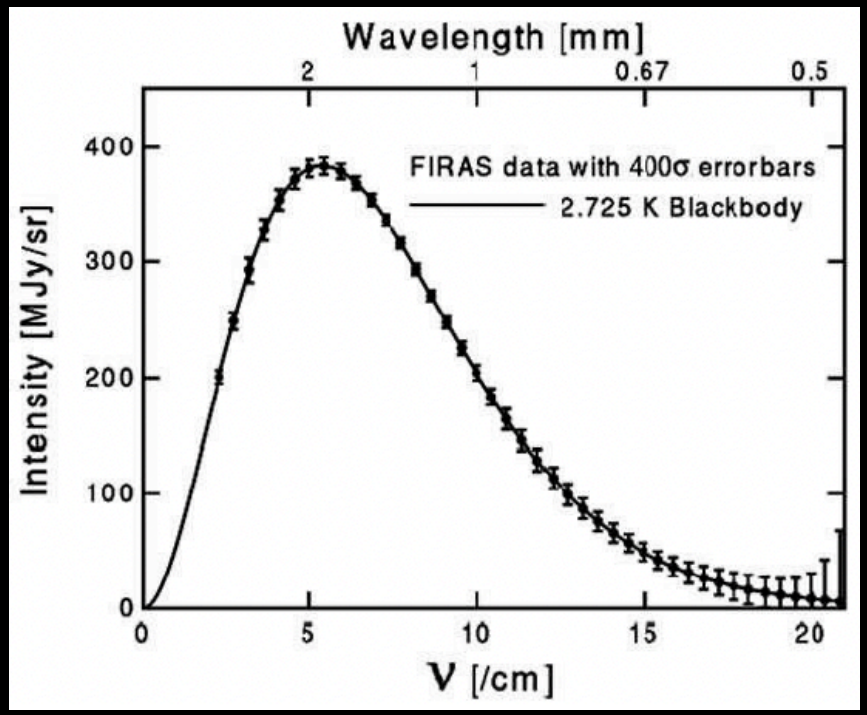

Wuensche & Villa, arXiv:1002.4902

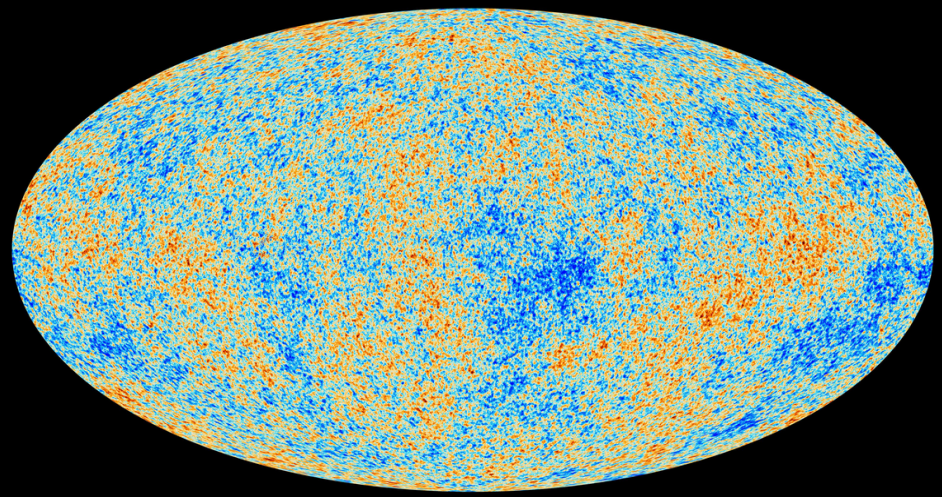

Planck collaboration, 2018

Our understanding of the history of the universe today

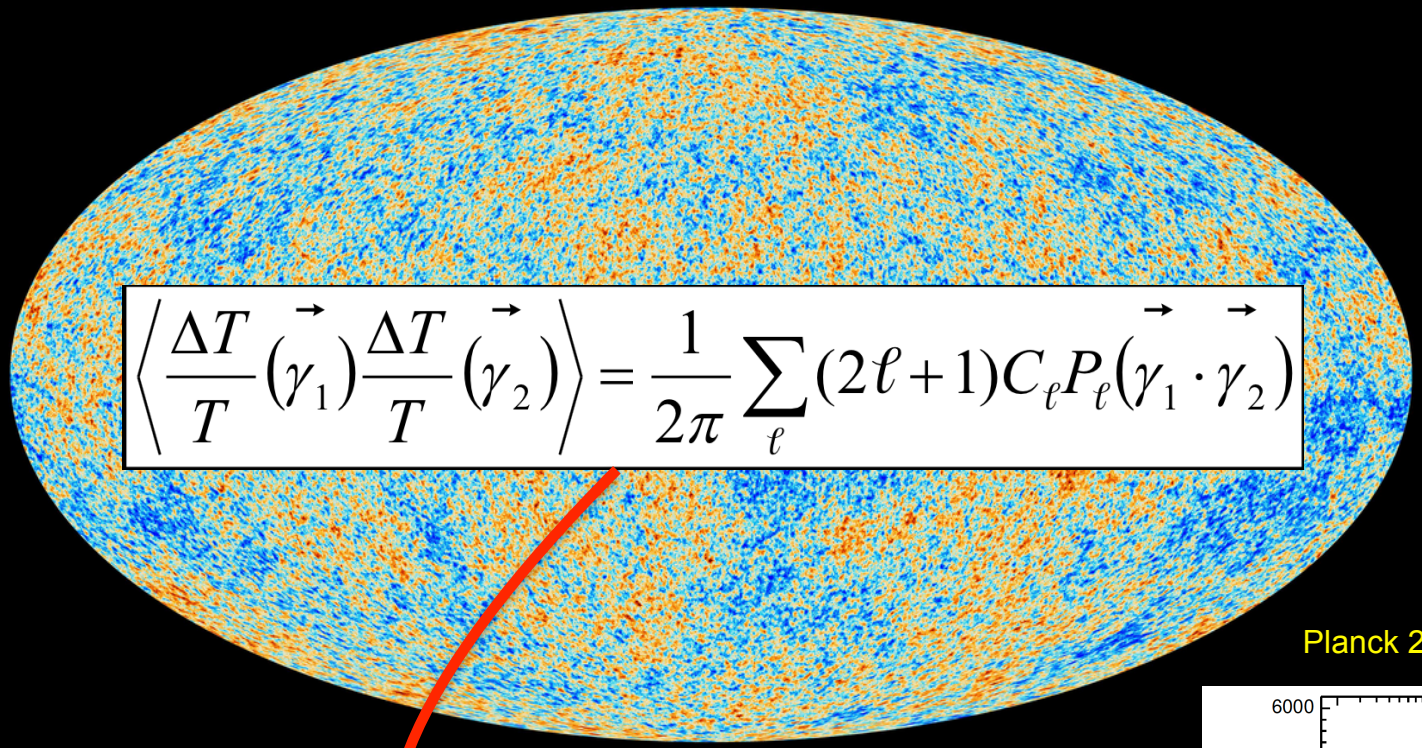

$$\left\langle \frac{\Delta T}{T}(\vec{\gamma}_1)\frac{\Delta T}{T}(\vec{\gamma}_2)\right\rangle = \frac{1}{2\pi}\sum_{\ell}(2\ell+1)C_\ell P_\ell(\vec{\gamma}_1\cdot\vec{\gamma}_2)$$

From the map of the CMB anisotropies we can extract the temperature angular power spectrum.

Planck 2018, Astron.Astrophys. 641 (2020) A6

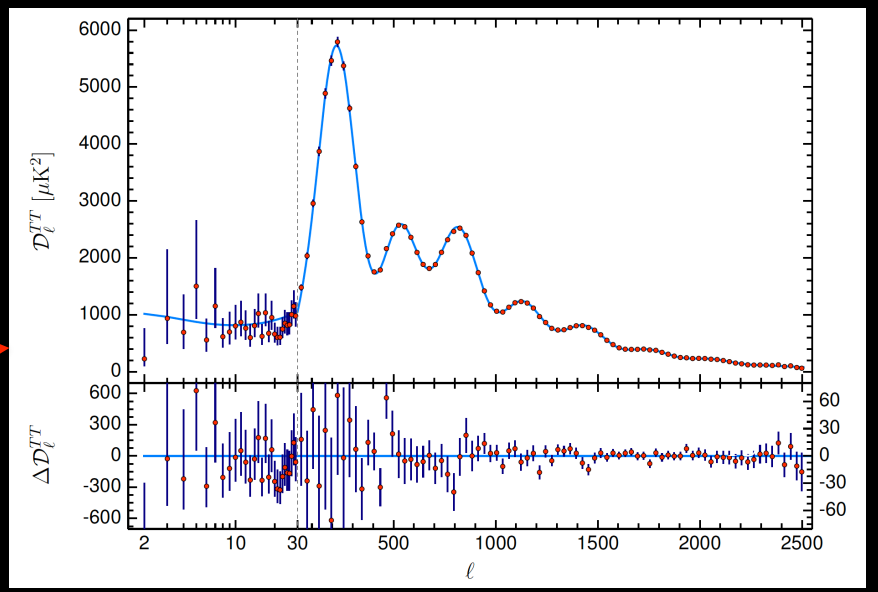

Our understanding of the history of the universe today

In this picture, the present structure of the Universe, characterized by large voids, great concentrations of matter, and filaments, formed starting from small fluctuations in matter density in a nearly homogeneous state.

The homogeneous and isotropic cosmological model provides a relatively good description of the Universe at early times and/or on very large scales, approximately more than 100 Mpc, where density fluctuations are small.
This assumption is called the 'Cosmological Principle',
meaning that there are neither preferred places nor preferred directions in the Universe.
Cosmological observations, such as the distribution of galaxy clusters in the sky and the amplitude of the CMB anisotropies, confirm that the Cosmological Principle is a very accurate zeroth-order approximation.
This allows us to treat the CMB anisotropies and density fluctuations on large scales as first-order perturbations of the homogeneous Universe.

Thanks to the Cosmological Principle, the evolution of the Universe can be described through the Friedmann equations, obtained using the Friedmann-Lemaître-Robertson-Walker metric in the Einstein equation.

Our understanding of the history of the universe today

Adopting a 4-dimensional coordinate system for the space-time $\{x^\alpha\}$, with $\alpha = 0, 1, 2, 3$, the infinitesimal distance between two events is given by the invariant line elements ds^2:

$$ds^2 = g_{\mu\nu} dx^\mu dx^\nu$$

Where dx^0 is the time-like component, the other three the spatial coordinates, and $g_{\mu\nu}$ is the metric.

We adopt the Cosmological Principle, i.e. isotropy, no preferred directions ($g_{0i}=g_{i0}=0$), and homogeneity, the density at every point depends only on time and not on the position.
(This is not true on planetary and galactic scales, where structures contrast with interstellar voids, but on a large scale >100 Mpc, it is confirmed by observations of the distribution of matter and the CMB.)
Finally, we assume the time synchronization, i.e. the time is the same everywhere.

The resulting metric is the Friedmann-Lemaitre-Robertson-Walker (FLRW), that describes the distance between two events in space-time.

$$ds^2 = c^2 dt^2 - a^2(t) \left[\frac{dr^2}{1 - kr^2} + r^2 \left(d\theta^2 + sin^2\theta d\varphi^2 \right) \right]$$

Our understanding of the history of the universe today

$$ds^2 = c^2dt^2 - a^2(t)\left[\frac{dr^2}{1-kr^2} + r^2\left(d\theta^2 + sin^2\theta d\varphi^2\right)\right]$$

Here we find the dimensionless scale factor a(t), which describes the way in which the distances in the Universe contract or expand in function of time: the separation (or convergence) is not due to movement but to the creation (or suppression) of space. It is usually normalized so that $a(t_0) = 1$ at present time.

The proper physical distance between two points in the Universe is obtained by multiplying the scale factor times their fixed distance, known as comoving distance.

$$\overrightarrow{x}(t) = a(t)\overrightarrow{r}$$

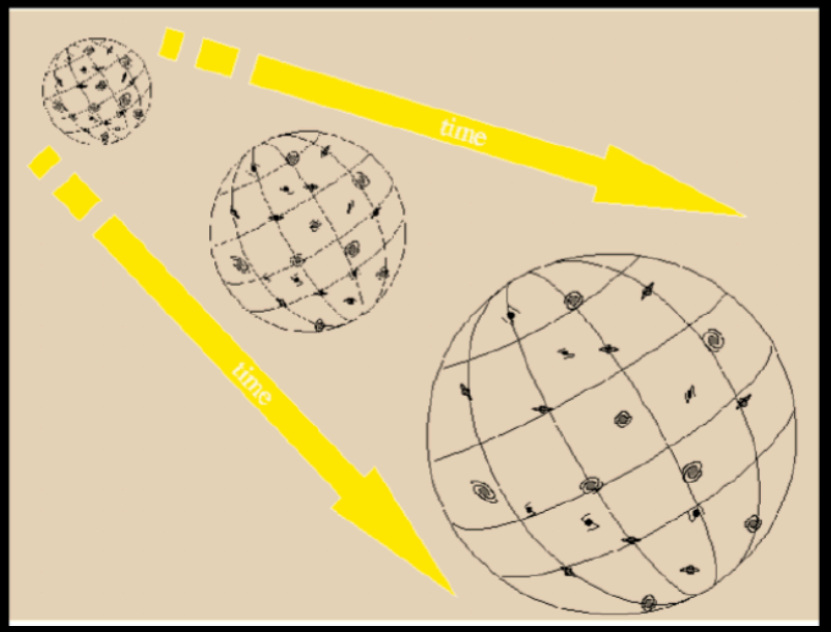

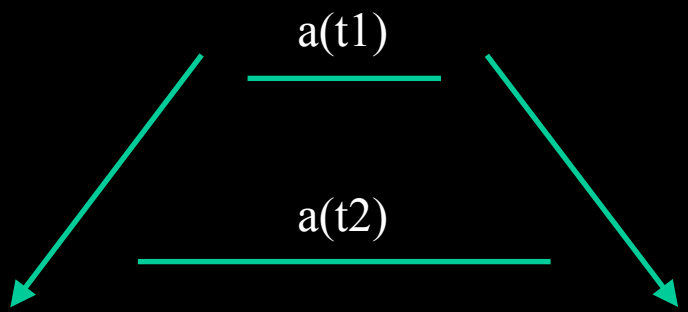

Our understanding of the history of the universe today

$$ds^2 = c^2dt^2 - a^2(t)\left[\frac{dr^2}{1-kr^2} + r^2\left(d\theta^2 + sin^2\theta d\varphi^2\right)\right]$$

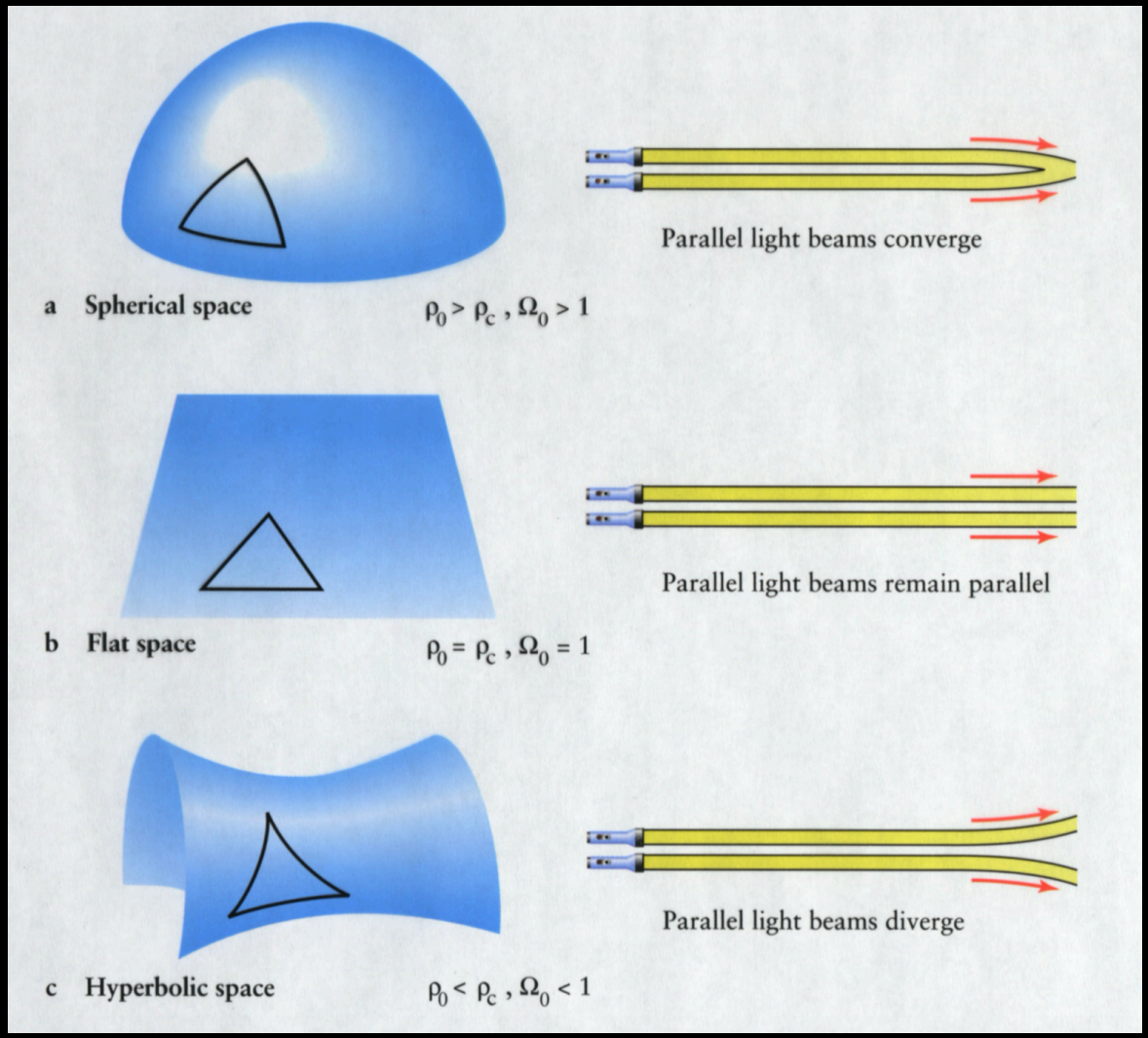

Figura: http://w3.phys.nthu.edu.tw

The curvature parameter k is proportional to the inverse of the curvature radius R squared ($k \propto R^{-2}$) and can be positive, null or negative.

At these values corresponds an open (two lines that start moving parallel diverge), spatially flat (two lines moving parallel always keep the same distance) or closed (two lines that start moving parallel converge) curvature of the Universe.

Our understanding of the history of the universe today

The scale factor a(t) will evolve in time
accordingly to the matter-energy content of the universe.

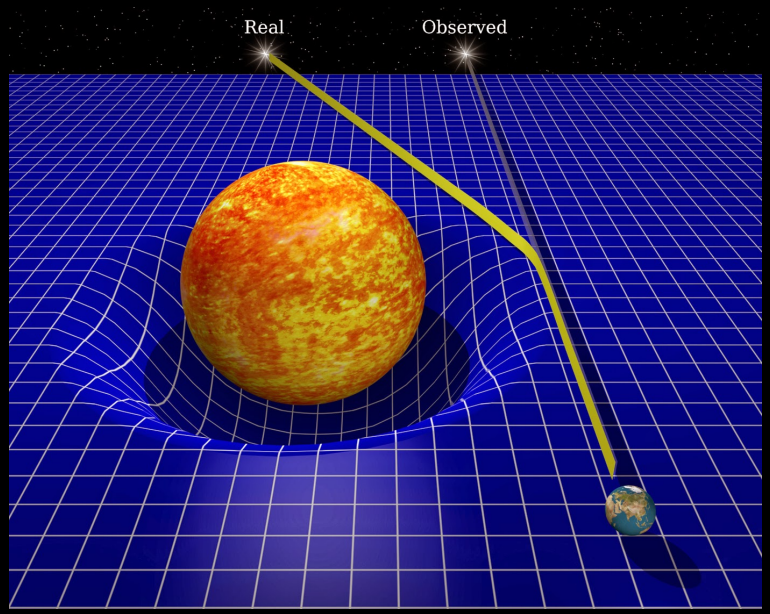

Figura: vice.com

In General Relativity a matter-energy distribution curves gravitationally the metric structure of the space-time.
The evolution over time of the geometry of the universe is described by Einstein equations:

$$R_{\mu\nu} - \frac{1}{2} g_{\mu\nu} R = \frac{8\pi G}{c^2} T_{\mu\nu} + \Lambda g_{\mu\nu}$$

which relate the purely geometric properties of space-time, to the distribution of matter-energy of the universe.
For this it is sufficient to know the energy content of the Universe to determine its geometry and vice-versa.

Our understanding of the history of the universe today

$$R_{\mu\nu} - \frac{1}{2} g_{\mu\nu} R = \frac{8\pi G}{c^2} T_{\mu\nu} + \Lambda g_{\mu\nu}$$

In the Einstein equations, $R = g^{\mu\nu} R_{\mu\nu}$ is the Ricci scalar and $R_{\mu\nu}$ the Ricci tensor, that is defined by the Christoffel symbols

$$R_{\mu\nu} = \Gamma^{\alpha}_{\mu\alpha,\nu} - \Gamma^{\alpha}_{\mu\nu,\alpha} + \Gamma^{\alpha}_{\mu\rho}\Gamma^{\rho}_{\mu\alpha} - \Gamma^{\rho}_{\mu\nu}\Gamma^{\alpha}_{\rho\alpha}$$

depending on the tensor metric $g_{\mu\nu}$.

$$\Gamma^{\alpha}_{\beta\gamma} = \frac{1}{2} g^{\alpha\rho} \left(g_{\rho\beta,\gamma} + g_{\rho\gamma,\beta} - g_{\beta\gamma,\rho} \right)$$

$T_{\mu\nu}$ is instead the energy-momentum tensor

$$T^{\mu\nu} = \begin{pmatrix} \rho & 0 & 0 & 0 \\ 0 & -P & 0 & 0 \\ 0 & 0 & -P & 0 \\ 0 & 0 & 0 & -P \end{pmatrix}$$

where we assume all the components of the Universe (radiation, matter, etc.) as perfect fluids, i.e., they can be described completely by two parameters independent of time: density ρ and pressure P, which is the same in all directions.

Our understanding of the history of the universe today

Combining together the FLRW metric and Einstein equations we obtain the Friedmann equations that describe the expansion history of the universe.

The first Friedmann equation is obtained from the first component (μ,ν) = (0, 0):

$$H^2 = \left(\frac{\dot{a}}{a}\right)^2 = \frac{8\pi G}{3}\rho - \frac{k}{a^2} + \frac{\Lambda}{3}$$

where we have introduced a possible cosmological constant Λ and defined the Hubble constant parameter H, that represents the rate of the expansion of the Universe at time t. The second Friedmann equation can be obtained combining the first Friedmann equation with the trace of the Einstein equations:

$$\frac{\ddot{a}}{a} = -\frac{4\pi G}{3}(\rho + 3P) + \frac{\Lambda}{3}$$

and represents the acceleration of the Universe.

Our understanding of the history of the universe today

In absence of external forces, the energy momentum tensor is conserved,
that implies that its covariant derivative is equal to zero in an expanding universe.

$$T^{\mu\nu}_{;\nu} = 0$$

We have therefore the continuity equation,
that is not independent on the two Friedmann equations:

$$\dot{\rho} + 3H\left(\rho + P\right) = 0.$$

We now introduce the equation of state that links pressure and density,
that for a perfect fluid reads as:

$$P = w\rho$$

where w is a constant that depends on the component considered.

$$w = \begin{cases} 0, & \text{matter} \\ \frac{1}{3}, & \text{radiation} \\ -1, & \text{cosmological constant} \end{cases}$$

Our understanding of the history of the universe today

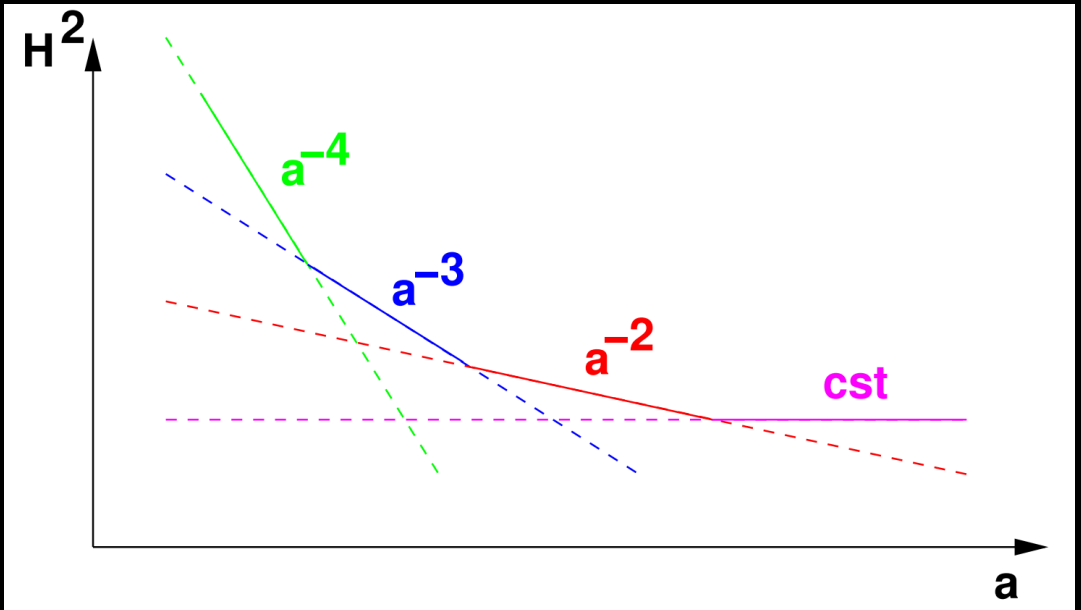

Figure 2.1: Evolution of the square of the Hubble parameter, in a scenario in which all typical contributions to the Universe expansion (radiation, matter, curvature, cosmological constant) dominate one after each other.

Lesgourgues, arxiv:astro-ph/0409426

The continuity equation becomes:

$$\frac{d\rho}{\rho} = -3\,(1+w)\,\frac{da}{a}$$

Integrating this last equation (assuming w as constant with time) we have the density as a function of the scale factor a(t):

$$\rho(a) = \rho_0 \frac{1}{a(t)^{3(1+w)}}$$

Considering the different components of matter, radiation, and cosmological constant, we have:

$$\rho_m = \frac{\rho_m^0}{a^3}, \qquad \rho_r = \frac{\rho_r^0}{a^4}, \qquad \rho_\Lambda = \rho_\Lambda^0.$$

Our understanding of the history of the universe today

If we define the critical density as follows:

$$\rho_c = \frac{3H^2}{8\pi G} = 10^{-29} h^2 g/cm^3$$

We can rewrite the 1st Friedmann equation as

$$H^2 = \left(\frac{\dot{a}}{a}\right)^2 = \frac{8\pi G}{3}\rho - \frac{k}{a^2} + \frac{\Lambda}{3} \quad \Rightarrow \quad \frac{\rho_m}{\rho_c} + \frac{\rho_r}{\rho_c} + \frac{\Lambda}{3H^2} - \frac{k}{a^2 H^2} = 1$$

or if we introduce the quantities

$$\rho_\Lambda = \frac{\Lambda}{8\pi G}, \quad \rho_k = -\frac{3k}{8\pi G a^2} = \frac{\rho_k^0}{a^2}.$$

we have:

$$\frac{\rho_m}{\rho_c} + \frac{\rho_r}{\rho_c} + \frac{\rho_\Lambda}{\rho_c} + \frac{\rho_k}{\rho_c} = 1$$

Our understanding of the history of the universe today

If we call the ratio between the critical density
and the density of each component as density parameter:

$$\Omega_x = \frac{\rho_x^0}{\rho_c^0}$$

we have at present time

$$\Omega = \sum_i \Omega_i = \Omega_m + \Omega_\Lambda + \Omega_r = 1 - \Omega_k$$

And we can rewrite the first Friedmann equation as:

$$H^2 = \left(\frac{\dot{a}}{a}\right)^2 = H_0^2 \left(\frac{\Omega_r}{a^4} + \frac{\Omega_m}{a^3} + \frac{\Omega_k}{a^2} + \Omega_\Lambda\right)$$

While the second Friedmann equations becomes:

$$-\frac{1}{H_0^2}\left(\frac{\ddot{a}}{a}\right) = \frac{\Omega_r}{a^4} + \frac{1}{2}\frac{\Omega_m}{a^3} - \Omega_\Lambda$$

The radiation component includes photons and relativistic neutrinos.
The matter component includes baryons, dark matter, and non-relativistic neutrinos.

Our understanding of the history of the universe today

From the first law of thermodynamics we know that

$$dE = d(\rho V) = -pdV + TdS$$

where E, V and S are, respectively, energy, volume, and entropy of the considered system.

Therefore, we have

$$S = \frac{E + PV}{T} = \frac{(\rho + P)V}{T}$$

and we can define the entropy density as follows:

$$s = \frac{S}{V} = \frac{\rho + P}{T}$$

Using the distribution functions

$$f = \frac{1}{e^{(E-\mu)/kT} \pm 1}$$

(- is for bosons and + is for fermions) and the energy density for relativistic particles

$$\rho_i = g_i \int \frac{d^3p}{(2\pi\hbar)^3} E(p) f_i(\vec{x}, \vec{p})$$

we obtain

$$\rho = \begin{cases} \rho_B = g_B \frac{\pi^2}{30} T^4, & bosons \\ \rho_F = \frac{7}{8} g_F \frac{\pi^2}{30} T^4, & fermions \end{cases}$$

Dodelson, Modern Cosmology, Academic Press.

Our understanding of the history of the universe today

Therefore the plasma total density will be:

$$\rho_r = g_{tot}\frac{\pi^2}{30}T^4$$ with $$g_{tot} = \sum_b g_B + \frac{7}{8}\sum_f g_F$$

Assuming a perfect fluid, the plasma will have P = (1/3) ρ, and then

$$s = \frac{4}{3}\frac{\rho}{T} = \frac{2\pi^2}{45}g_{tot}T^3$$

We can demonstrate that the entropy density of the Universe scales as a^{-3} (sa^3= const), and conclude that

$$T \propto \frac{1}{a(t)\sqrt[3]{g_{tot}}},$$

and, when g_{tot}= const, also the temperature scales as a^{-1}.

Dodelson, Modern Cosmology, Academic Press.

Our understanding of the history of the universe today

Neutrinos behave like radiation when they are relativistic,
and like matter, when they become non-relativistic.

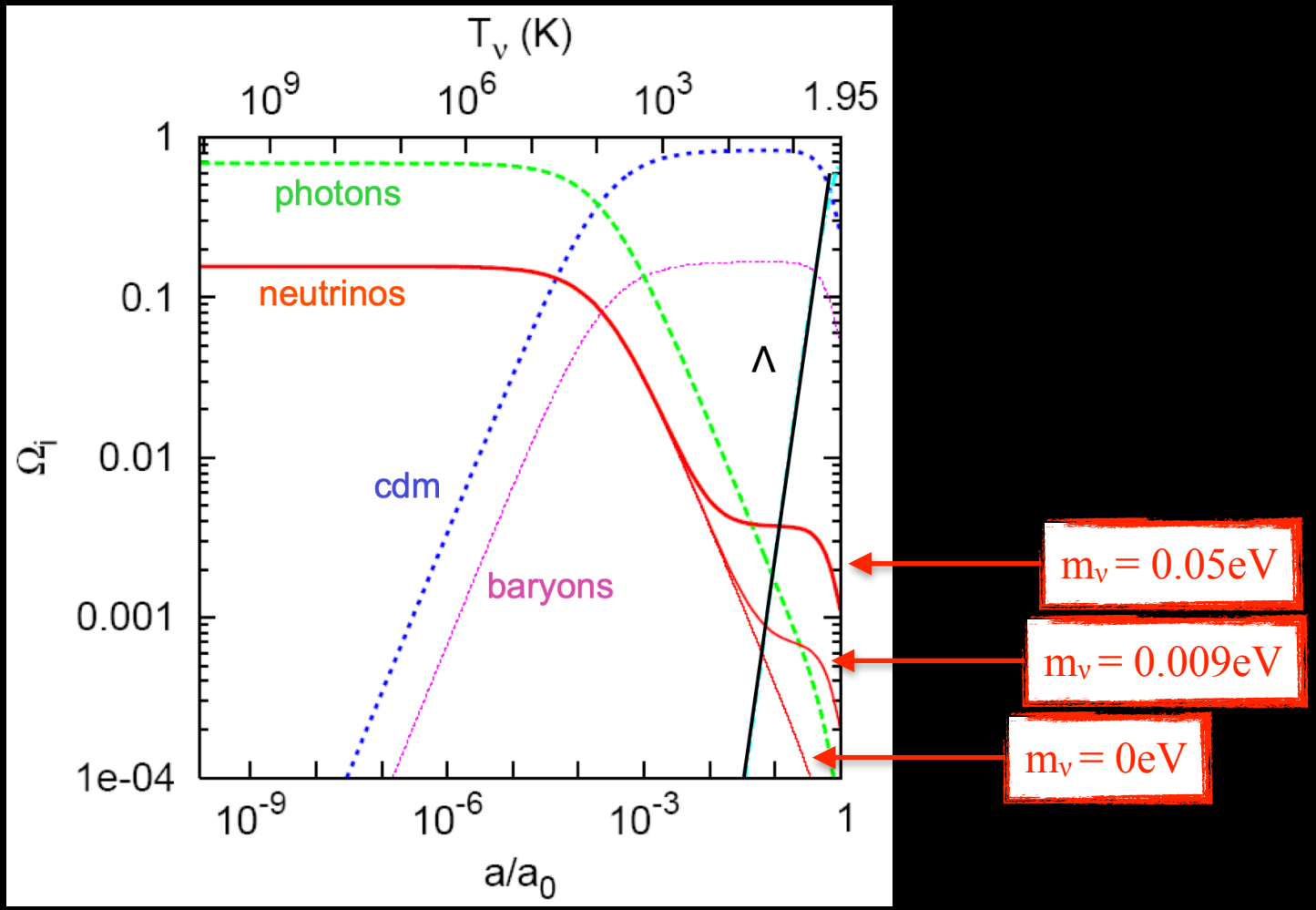

Lesgourgues and Pastor, arXiv:1404.1740

Evolution of the background energy densities in terms of the fractions Ωi,
from Tv = 1 MeV until now.

Neutrino physics and cosmology

If the total neutrino mass is of the order of 1 eV, neutrinos are radiation at the time of equality, and non-relativistic matter today.

We expect the transition to the non-relativistic regime after the time of the photon decoupling.

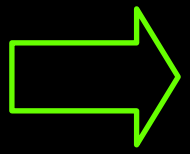

When neutrinos are relativistic, will contribute to the radiation content of the universe, through the effective number of relativistic degrees of freedom Neff.

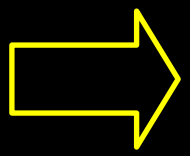

When they become non-relativistic, will only cluster at scales larger than their free streaming scale, suppressing therefore structure formation at small scales, and affecting the large scale structures.

The Cosmic Neutrino Background

Neutrinos are initially coupled to the rest of the primordial plasma through these weak interactions:

$$\nu + e^- \leftrightarrow \nu + e^-, \qquad n + \nu_e \leftrightarrow p^+ + e^-, \qquad n + e^+ \leftrightarrow p^+ + \bar{\nu}_e.$$

At that time, they have a momentum spectrum with an equilibrium Fermi-Dirac distribution at temperature T equal to:

$$f_{eq}(p) = \frac{1}{e^{(p-\mu_\nu)/T} + 1},$$

where p is the momentum and μ_ν is the neutrino chemical potential (that we assume equal to zero, i.e. no neutrino-antineutrino asymmmetry). Their weak interaction rate is

$$\Gamma(z) = n\langle\sigma v\rangle$$

with $\sigma_w \sim G_F^2 T^2$ the cross section for the weak interactions with G_F the Fermi constant, n the neutrino number density, and v the velocity of particles (and the brackets for the thermal average).

J. Lesgourgues and S. Pastor, Phys. Rept. 429, 307 (2006) [astro-ph/0603494].
S.Dodelson, Modern Cosmology, Academic Press.

The Cosmic Neutrino Background

Neutrinos decouple from the rest of the plasma, when the rate of the weak interaction reactions, which keep them in thermodynamic equilibrium with the primordial plasma, becomes smaller than the expansion rate of the Universe:

$$H = \sqrt{\frac{8\pi\rho}{3M_{Pl}^2}},$$

If we consider the weak interaction rate $\Gamma_\nu \approx G_F^2 T^5$ and $H \approx T^2/M_{Pl}$,

we obtain a decoupling temperature of about $T_{dec} \approx 1MeV$.

Therefore, in the standard cosmological model,
a Cosmic Neutrino Background (CNB) is expected to form when
the temperature falls below T~1MeV, and the Universe can no longer transform
protons into neutrons, which have a mass difference of 1.293 MeV.
From this moment, neutrinos cease to interact
and begin to propagate freely (free streaming).
Their distribution remains a Fermi-Dirac equilibrium spectrum because they do not interact anymore, a consequence of the Liouville theorem since they are ultra relativistic,
but their temperature falls as a^{-1}.

J. Lesgourgues and S. Pastor, Phys. Rept. 429, 307 (2006) [astro-ph/0603494].
S.Dodelson, Modern Cosmology, Academic Press.

The Cosmic Neutrino Background

After neutrinos decoupling, photons start to be heated by electrons-positrons annihilation:

$$e^- + e^+ \leftrightarrow \gamma + \gamma.$$

When the Universe's temperature falls below T ~ 0.5 MeV,
i.e., of the order of the electron mass,
this reaction proceeds only in the rightward direction,
producing extra photons that rapidly thermalize.

From this moment, the ratio between the temperatures of the backgrounds of neutrinos and photons will be fixed, despite the temperature decreasing with the expansion of the Universe. If neutrinos decouple instantaneously,
we can assume that the entropy transfer of this annihilation
did not affect the decoupled neutrinos, and we can calculate the ratio
between the temperature of relic photons and neutrinos.

J. Lesgourgues and S. Pastor, Phys. Rept. 429, 307 (2006) [astro-ph/0603494].
S.Dodelson, Modern Cosmology, Academic Press.

The Cosmic Neutrino Background

Before the annihilation, at the scale factor a_1,
the total entropy density s is contributed by massless bosons,
such as photons in 2 spin states, each contributing with $2\pi^2 T^3/45$ for spin state;
massless fermions, such as electrons in 2 spin states, positrons in 2 spin states,
3 generations of neutrinos and 3 of anti-neutrinos, each in 1 spin state,
each contributing with $(7/8)\times(2\pi^2 T^3/45)$ for spin state;
and massive fermions in negligible way.
The total entropy density will be:

$$s(a_1)=\frac{2\pi^2}{45}T_1^3\left[2+\frac{7}{8}(2+2+3+3)\right]=\frac{43\pi^2}{90}T_1^3,$$

with T_1 the common temperature of the several components in a_1.
After annihilation, at the scale factor a_2,
the electrons and positrons do no longer contribute to the total entropy density,
and photons and neutrinos have temperatures no longer equal
(photons are hotter than neutrinos). Therefore we have:

$$s(a_2)=\frac{2\pi^2}{45}\left[2T_\gamma^3+\frac{7}{8}6T_\nu^3\right].$$

J. Lesgourgues and S. Pastor, Phys. Rept. 429, 307 (2006) [astro-ph/0603494].
S.Dodelson, Modern Cosmology, Academic Press.

The Cosmic Neutrino Background

We know that the total entropy density scales as a^{-3}, so we can equate (assuming that during the process the total entropy is approximately constant):

$$s(a_1)a_1^3 = s(a_2)a_2^3$$

obtaining

$$\frac{43}{2}(a_1 T_1)^3 = 4\left[\left(\frac{T_\gamma}{T_\nu}\right)^3 + \frac{21}{8}\right](T_\nu(a_2)a_2)^3$$

Since neutrino temperature scales as a^{-1}, we have also

$$a_1 T_1 = a_2 T_\nu(a_2).$$

So, the ratio between the temperature of relic neutrinos and photons is:

$$T_\nu = \left(\frac{4}{11}\right)^{1/3} T_\gamma \approx 1.945K \rightarrow kT_\nu \approx 1.68 \cdot 10^{-4} eV$$

that remains the same until now.

Therefore we expect today a CNB at this temperature, with a number density of:

$$n_\nu(T_\nu) = \frac{g}{(2\pi)^3}\int \frac{d^3p}{e^{p/T_\nu}+1} = \frac{3\zeta(3)}{4\pi^2}T_\nu^3 \rightarrow n_{\nu_k,\bar{\nu}_k} \approx 0.1827 \cdot T_\nu^3 \approx 112 cm^{-3}$$

J. Lesgourgues and S. Pastor, Phys. Rept. 429, 307 (2006) [astro-ph/0603494].
S.Dodelson, Modern Cosmology, Academic Press.

Direct CNB detection

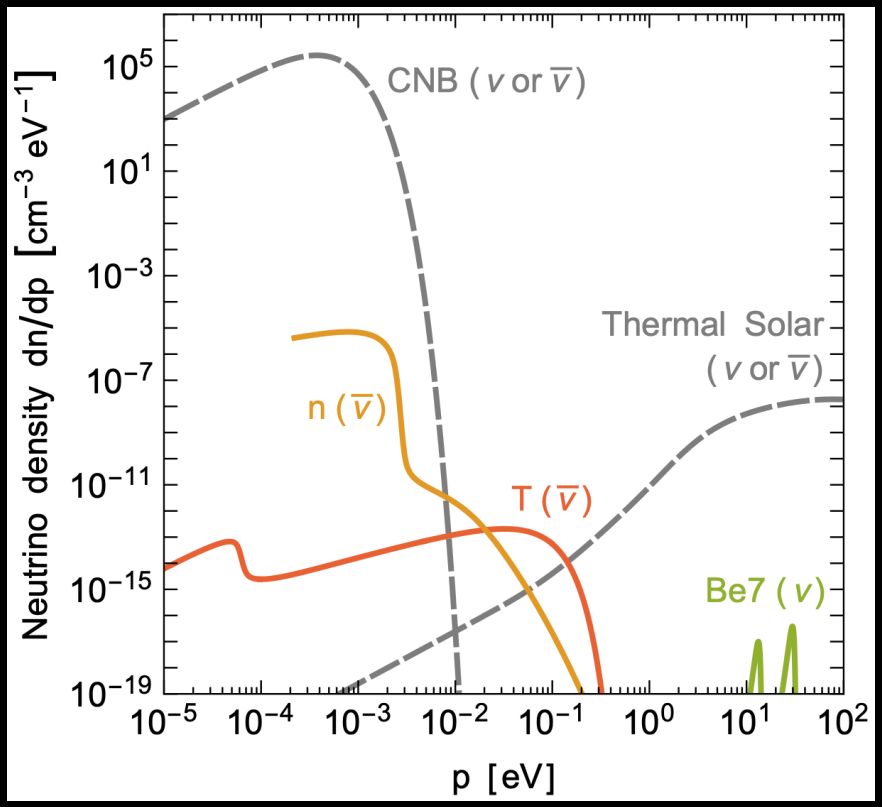

Vitagliano et al., arXiv:1910.11878

In 1962, Weinberg proposed a method to detect the presence of
"a shallow degenerate Fermi sea of neutrinos"
that fills the universe.
During those times, neutrinos were believed to be massless, and the proposed method required using a beta-decaying nucleus,
which could decay and emit an electron if capturing a neutrino from the CNB:
the process is therefore called
"neutrino capture on beta-decaying nucleus".
The original proposal considered a possible depletion in the electron (positron) energy spectrum due to a large chemical potential of the neutrino.

Di Valentino et al., arXiv:2404.19322

Direct CNB detection

In 2007, Cocco et al., arXiv:hep-ph/0703075 revisited the original proposal to properly describe the effect of neutrino capture in the absence of large chemical potentials but in the presence of neutrino masses.

One of the crucial points is that the neutrino capture process is related to standard beta-decay, with the difference that the neutrino (or antineutrino) is in the final state and the energy of the electron can exceed the end-point value E_0 of the beta-decay spectrum. Therefore, in order to build a successful experiment,

it is crucial to be able to distinguish neutrino capture events with energy above E_0 from beta-decay events with energy below E_0.

This is no easy task, because the energy separation between beta-decay and neutrino capture events is equal to twice the neutrino mass (Long et al. arXiv:1405.7654).

The authors of Cocco et al., arXiv:hep-ph/0703075 consider the half-life and cross section of different nuclei and determine that the best chances to build an experiment emerge when adopting tritium:

it provides a reasonably large event rate for neutrino capture together with a sufficiently small contamination of the signal region by beta- decay background events.

Di Valentino et al., arXiv:2404.19322

Direct CNB detection

Based on this result, the first experimental attempt at detecting the CNB by neutrino capture on tritium is being developed at Gran Sasso Laboratories in Italy.
The PTOLEMY proposal plans to reach a final setup with approximately 100 g of tritium and a final energy resolution in the ballpark of 0.1eV in order to detect ~ 5 neutrino capture events per year if their separation from the beta-decay spectrum is sufficiently large.
According to the first set of simulations, this setup could guarantee a 3σ observation of the CNB in one year if neutrino masses are above 0.2eV (Betti et al. arXiv:1902.05508).
Even if this is not true for standard neutrinos, PTOLEMY could still detect the presence of sterile neutrinos in the CNB.

Di Valentino et al., arXiv:2404.19322

Indirect CNB detection

Fortunately, we have rather clear indirect evidence of the existence of the CNB due to cosmological observables constraining the Neutrino Effective Number N_{eff}.

If the sum of the active neutrino masses is less than 1eV,
they are relativistic at the decoupling era.
The relativistic neutrinos contribute to the present energy density of the Universe:

$$\rho_{rad} = \rho_\gamma + \rho_\nu = g_\gamma \left(\frac{\pi^2}{30}\right) T_\gamma^4 + g_\nu \left(\frac{\pi^2}{30}\right) \left(\frac{7}{8}\right) T_\nu^4$$

where we considered the different behaviour of bosons and fermions,
i.e., their different distribution functions.
If we rewrite it as a function of the photon energy density,
that we know perfectly thanks to the CMB measurements, we obtain:

$$\rho_{rad} = \left(1 + \left(\frac{7}{8}\right) \left(\frac{4}{11}\right)^{\frac{4}{3}} \left(\frac{g_\nu}{g_\gamma}\right)\right) \rho_\gamma$$

that is valid only for instantaneous neutrino decoupling.

J. Lesgourgues and S. Pastor, Phys. Rept. 429, 307 (2006) [astro-ph/0603494].
S.Dodelson, Modern Cosmology, Academic Press.

Indirect CNB detection

We define the effective number of relativistic degrees of freedom as the ratio:

$$N_{\rm eff} = \frac{g_\nu}{g_\gamma}$$

with an expected value (Bennett et al. arXiv:2012.02726)

$$N_{\rm eff}^{\rm SM} = 3.0440 \pm 0.0002,$$

instead of 3, for the different neutrino flavours,
assuming standard electroweak interactions and three active massless neutrinos.
The 0.0440 correction accounts for the solution of the Boltzmann equation,
which describes how the distribution function of neutrinos evolves in time, considering:

1) A not instantaneous neutrino decoupling. The neutrino decoupling and the annihilation of electrons and positrons occur close enough in time to cause residual interactions between the photon bath and the high-momentum neutrinos that are still coupled to it. These interactions lead to a slightly smaller increase in the comoving photon temperature compared to the case of instantaneous decoupling, and distortions in the neutrino distribution function.
2) Tracking of the neutrino flavour oscillations that are active around neutrino decoupling.
3) QED radiative corrections (finite-temperature effects in the QED plasma).

Standard-model corrections to $N_{\rm eff}^{\rm SM}$	Leading-digit contribution
m_e/T_d correction	$+0.04$
$\mathcal{O}(e^2)$ FTQED correction to the QED EoS	$+0.01$
Non-instantaneous decoupling+spectral distortion	-0.005
$\mathcal{O}(e^3)$ FTQED correction to the QED EoS	-0.001
Flavour oscillations	$+0.0005$
Type (a) FTQED corrections to the weak rates	$\lesssim 10^{-4}$

Indirect CNB detection

The relic density of active neutrinos is independent of their nature,
whether they are Dirac or Majorana particles.
This is because in calculating the degrees of freedom,
we consider only those that were populated and brought into equilibrium before the time of neutrino decoupling, which are the same in both cases.

$$\rho_{rad} = \left[1 + \frac{7}{8}\left(\frac{4}{11}\right)^{4/3} N_{\rm eff}\right]\rho_\gamma$$

The value of N_{eff} is constrained at the BBN epoch, by comparing experimental data with theoretical predictions of the primordial abundances of light elements, such as helium ^{4}He and deuterium D,
which also depend on the baryon-to-photon ratio, $\eta = n_b/n_\eta$.
Additionally, independent constraints on this parameter N_{eff} at a later epoch, can be extracted from the power spectrum of CMB anisotropies.

J. Lesgourgues and S. Pastor, Phys. Rept. 429, 307 (2006) [astro-ph/0603494].
S.Dodelson, Modern Cosmology, Academic Press.

Neff at the BBN

Big Bang Nucleosynthesis (BBN) refers to the epoch when the temperature of the Universe is between 10 MeV > T > 0.1 MeV, corresponding to a time period from approximately $10^{-2} < t < 10^{2}$ seconds after the Big Bang.

BBN bounds are derived from the abundances of the first light nuclei (heavier than the lightest isotope of hydrogen).
Increasing Neff > 3.044 results in an additional contribution to the dark radiation of our universe, that will increase the expansion rate H(z) through the first Friedmann equation

$$H^2 = \left(\frac{\dot{a}}{a}\right)^2 = H_0^2 \left(\frac{\Omega_r}{a^4} + \frac{\Omega_m}{a^3} + \frac{\Omega_k}{a^2} + \Omega_\Lambda\right)$$

This will move earlier the period of weak decoupling, which implies a higher freeze-out temperature of weak interactions.

Di Valentino et al., arXiv:2404.19322

Neff at the BBN

At high temperatures, weak interactions are in thermal equilibrium,
thereby fixing the ratio of neutron and proton number densities to be
$n/p = \mathrm{e}^{-Q/T}$,
where Q = 1.293 MeV is the neutron-proton mass difference.
In other words, the neutron fraction decreases with the temperature of the universe. When the rate of the weak interactions falls below the expansion rate of the Universe, the weak interactions freeze-out at a temperature T_{fr},
which will fix the neutron fraction $n/p = \mathrm{e}^{-Q/T_{\mathrm{fr}}}$.

As a result of a higher freeze-out temperature,
there will be a higher neutron-to-proton ratio, and consequently,
more neutrons are present at the BBN,
leading to a larger fraction of primordial Helium and Deuterium
(as well as a higher fraction of other primordial elements)
with respect to hydrogen.

This makes BBN a laboratory to test for additional contributions to Neff.

Neff at the BBN

In concrete models, solving a set of differential equations that govern nuclear interactions in the primordial plasma
(Pisanti et al. arXiv:0705.0290, Consiglio et al. arXiv:1712.04378, Gariazzo et al. arXiv:2103.05027),
allows for the computation of light element abundances.
A very well know tool is PArthENoPE
(Public Algorithm Evaluating the Nucleosynthesis of Primordial Elements),
which is publicly available at http://parthenope.na.infn.it/.

$$Y_p = 0.2469\, R_{pn\gamma}^{0.005}\, R_{dp\gamma}^{0.0002}\, R_{ddn}^{0.006}\, R_{ddp}^{0.005} \left(\frac{\omega_b}{0.02242}\right)^{0.04} \left(\frac{\tau_n}{879.4\,\mathrm{s}}\right)^{0.72} \left(1+\frac{\Delta N_{\mathrm{eff}}}{3.045}\right)^{0.16}$$

$$\frac{D}{\mathrm{H}} = 2.51\times 10^{-5}\, R_{pn\gamma}^{-0.20}\, R_{dp\gamma}^{-0.31}\, R_{ddn}^{-0.51}\, R_{ddp}^{-0.42} \left(\frac{\omega_b}{0.02242}\right)^{-1.61} \left(\frac{\tau_n}{879.4\,\mathrm{s}}\right)^{0.43} \left(1+\frac{\Delta N_{\mathrm{eff}}}{3.045}\right)^{0.41}$$

Pisanti et al. arXiv:2011.11537

Neff at the BBN

These results can then be compared to values inferred from astrophysical and cosmological observations. From the direct measurements of primordial abundances of both Deuterium and Helium we can infer the constraints on Neff.

Pisanti et al. arXiv:2011.11537

	ω_b	$N_{\rm eff}$
Planck	0.02237 ± 0.00015	3.045
Planck+BAO	0.02242 ± 0.00014	3.045
D-3ν	0.02233 ± 0.00036	3.045
D+Planck	0.02224 ± 0.00022	2.95 ± 0.22
BBN [5]	0.0220 ± 0.0005	2.84 ± 0.20
BBN [6]	0.0221 ± 0.0006	2.86 ± 0.28
BBN [7]	0.0234 ± 0.0005	3.60 ± 0.17
BBN [8]	0.0219 ± 0.0006	2.78 ± 0.28

$Y_p = 0.2446 \pm 0.0029$ [5]

$Y_p = 0.2449 \pm 0.0040$ [6]

$Y_p = 0.2551 \pm 0.0022$ [7]

$Y_p = 0.2436 \pm 0.0040$ [8]

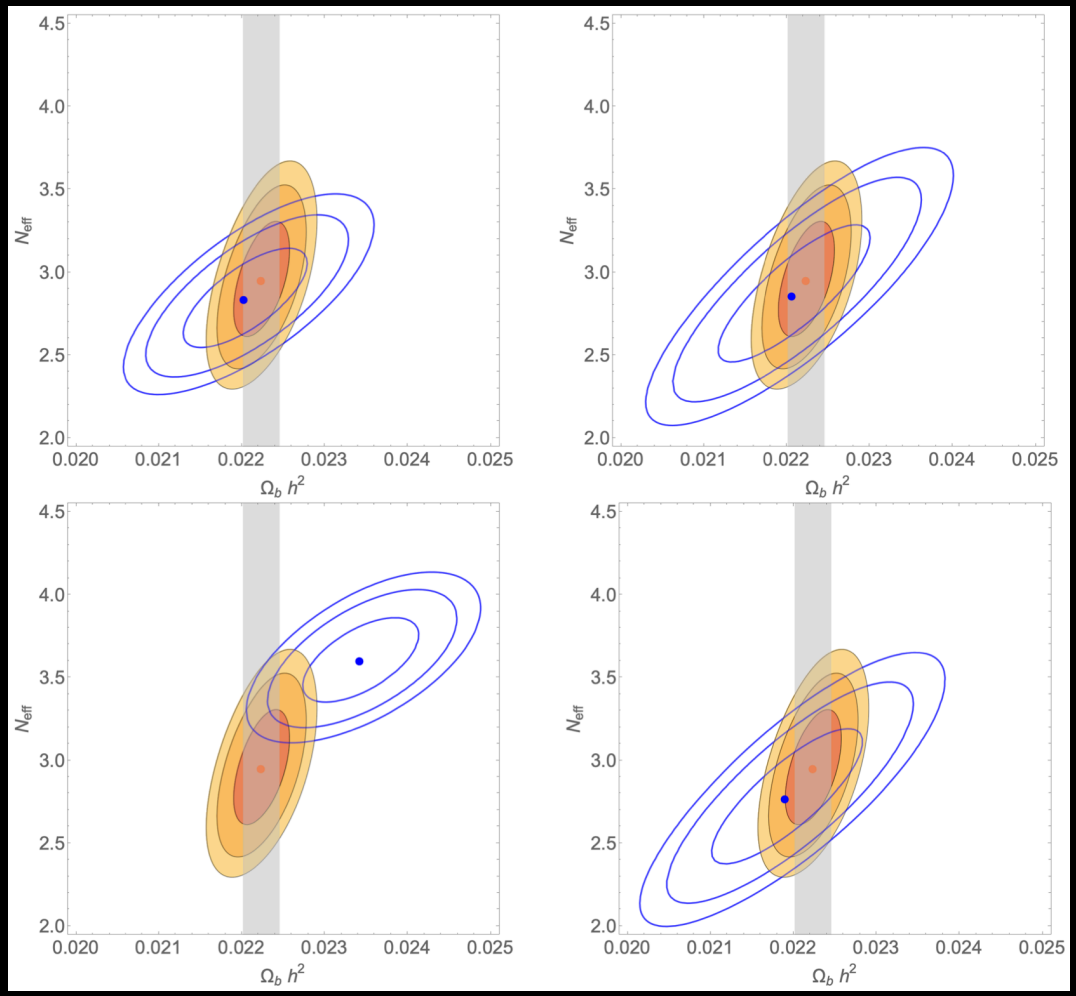

see also Yeh et al. arXiv:2011.13874

Hou et al., arXiv:1104.2333

Neff at the CMB

Concerning the CMB temperature power spectrum, first of all,
varying N_{eff} changes the time of the matter to radiation equivalence:
a higher radiation content due to the presence of additional relativistic species
leads to a delay in z_{eq}:

$$1 + z_{\rm eq} = \frac{\Omega_m}{\Omega_r} = \frac{\Omega_m h^2}{\Omega_\gamma h^2} \frac{1}{(1 + 0.2271 N_{\rm eff})}$$

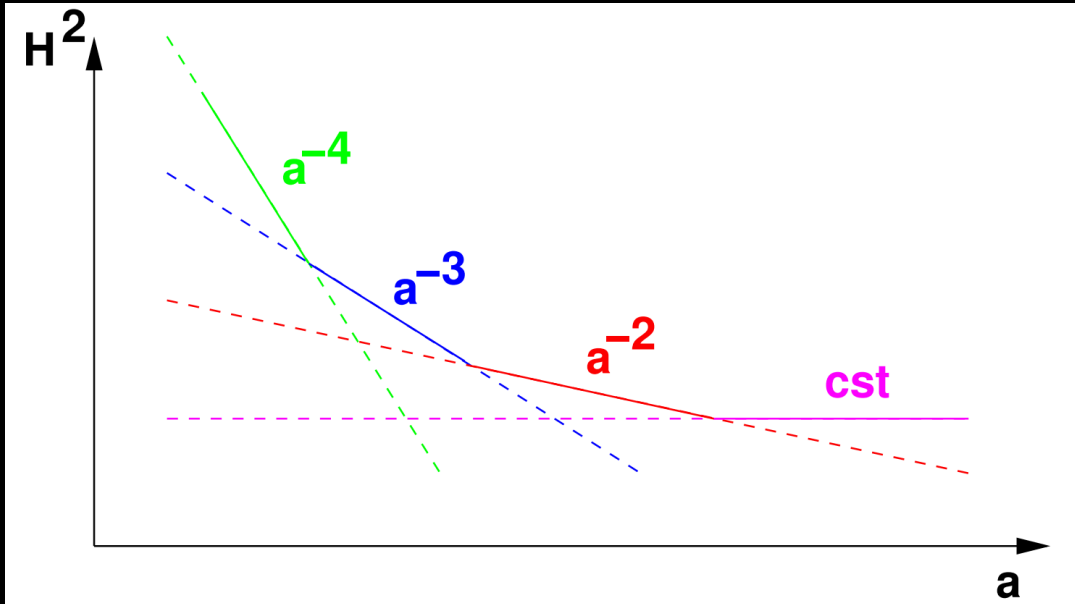

Figure 2.1: Evolution of the square of the Hubble parameter, in a scenario in which all typical contributions to the Universe expansion (radiation, matter, curvature, cosmological constant) dominate one after each other.

$$a(t) = \frac{1}{1+z}$$

Lesgourgues, arxiv:astro-ph/0409426

Hou et al., arXiv:1104.2333

Neff at the CMB

During the fully matter-dominated period, gravitational potentials remain nearly constant over time. Consequently, the Integrated Sachs-Wolfe (ISW) effect, which is sensitive to the time variation of gravitational potentials, will be very small.

The ISW effect (Sachs and Wolfe, ApJ 1967) occurs when photons are gravitationally redshifted or blueshifted while crossing a gravitational potential that changes over time. Unlike the primary Sachs-Wolfe (SW) effect, which occurs at the last scattering surface, the ISW effect is integrated along the photon's path from the last scattering surface to the observer.

If the matter-radiation equivalence occurs later, it implies that at the time of decoupling, radiation is not yet negligible and still a (subdominant) component, and the gravitational potential is still slowly decreasing. Since the matter does not completely dominate over radiation, this gradual decrease in the gravitational potential would continue to affect the photons' paths, contributing to the early ISW effect.

Hou et al., arXiv:1104.2333

Neff at the CMB

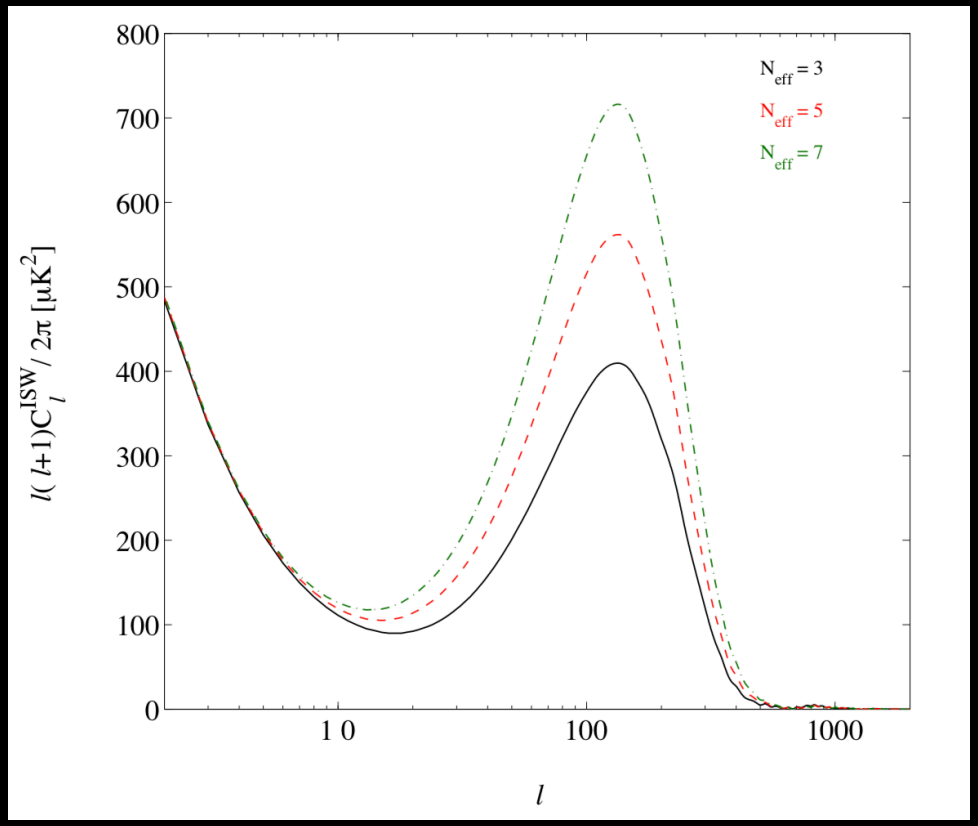

Archidiacono et al. Adv.High Energy Phys. 2013 (2013) 191047

Therefore, a higher Neff will show up as an enhancement of the early ISW effect.

Since the early ISW effect adds in phase with the primary anisotropy, it increases the height of the first acoustic peaks. Consequently, a higher Neff will increase the CMB perturbation peaks at l ~ 200.

Hou et al., arXiv:1104.2333

Neff at the CMB

However, the main effect of increasing Neff is located at high multipoles ell (the CMB damping tail) rather than at the very first peaks.
If ΔNeff increases, the H(z) will increase as well.

This will decrease the sound horizon at recombination, i.e., the distance that sound waves could have traveled in the time before recombination,

$$r_s = \int_0^{t_*} c_s\, dt/a = \int_0^{a_*} \frac{c_s\, da}{a^2 H}$$

and the diffusion scale (Silk damping scale), which arises because baryon-photon decoupling is not an instantaneous process, leading to a diffusion damping of oscillations in the plasma.

$$r_d^2 = (2\pi)^2 \int_0^{a_*} \frac{da}{a^3 \sigma_T n_e H} \left[\frac{R^2 + \frac{16}{15}(1+R)}{6(1+R^2)}\right]$$

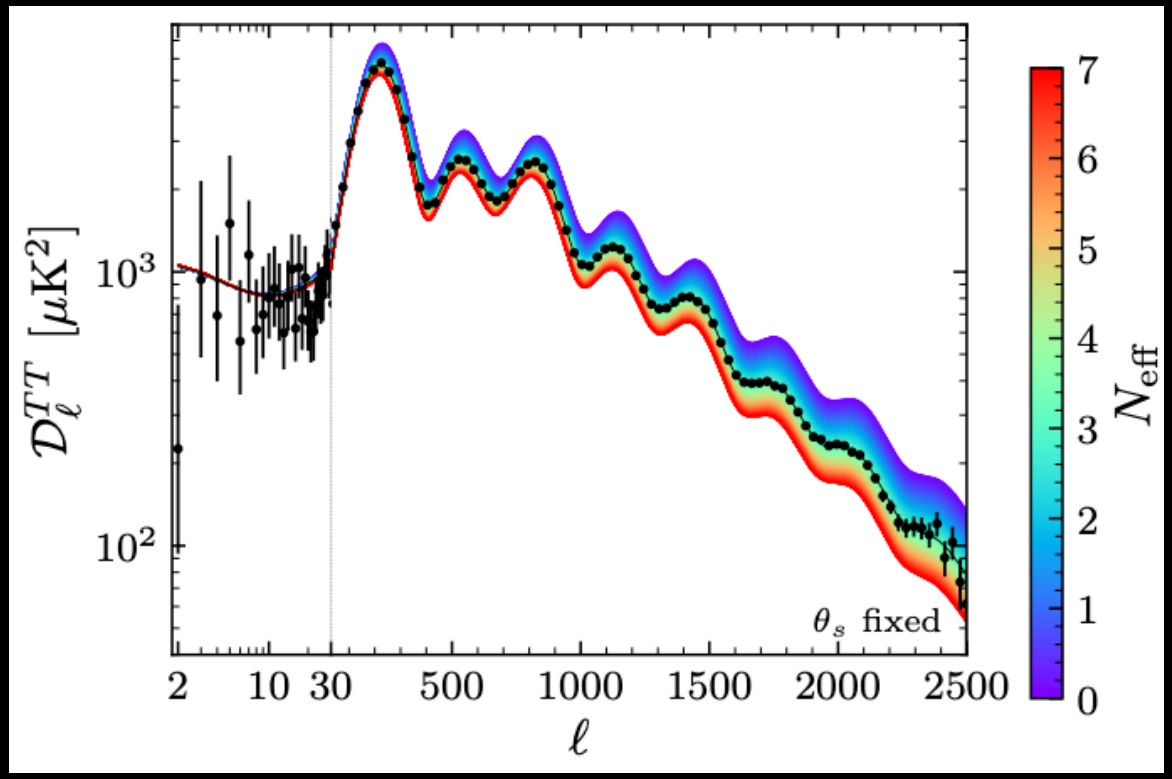

Abazajian et al. 2022, SNOWMASS, arXiv:2203.07377

CMB acoustic peaks in the damping tail will be then shifted and suppressed, and the oscillations will be smeared when increasing Neff.

Cosmological parameters:
($\Omega_b h^2$, $\Omega_m h^2$, H0 , n_s , τ, As)

Theoretical model

We choose a set of cosmological parameters that describes our theoretical model and compute the angular power spectra. Because of the correlations present between the parameters, variation of different quantities can produce similar effects on the CMB.

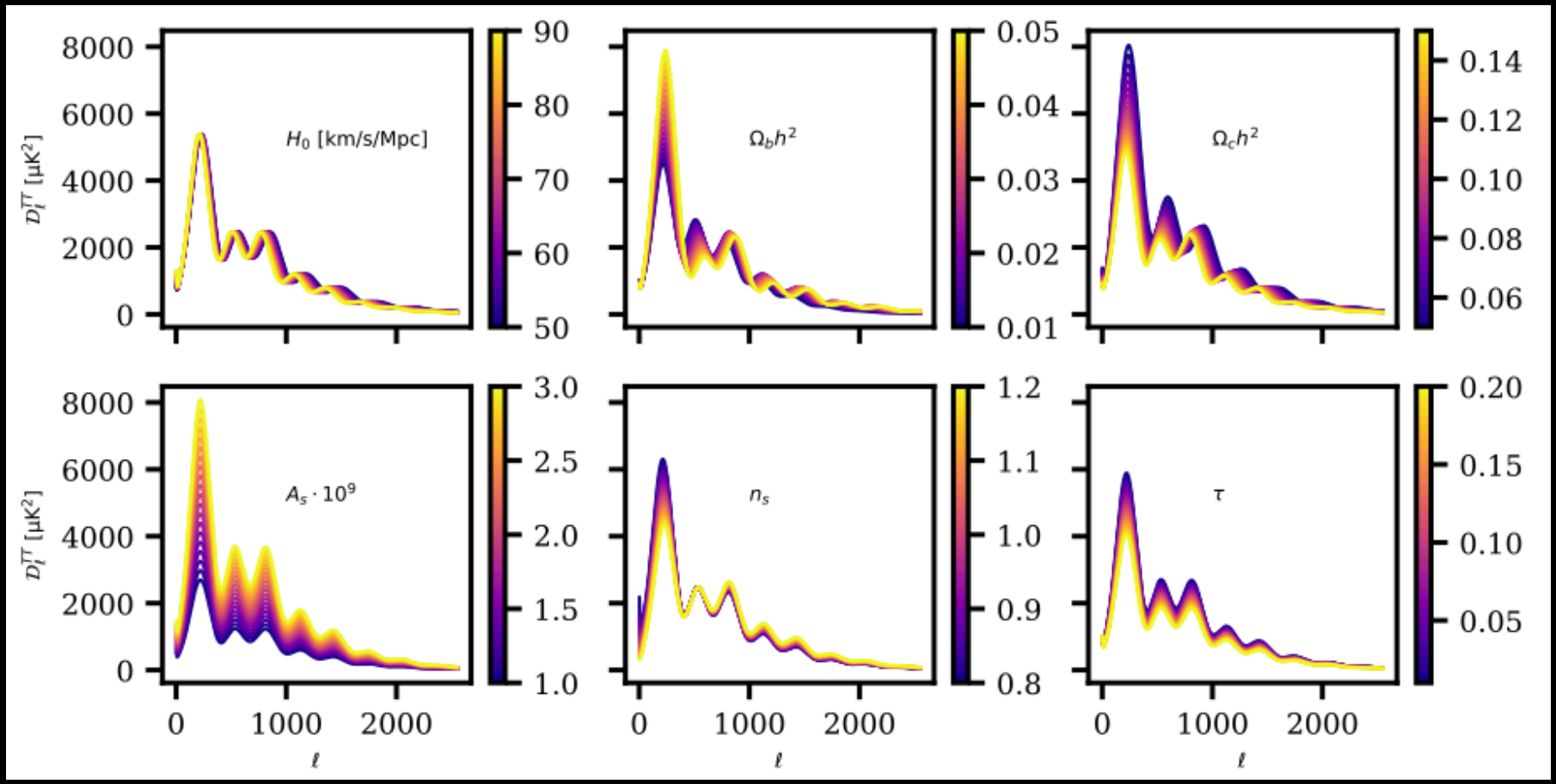

Lemos & Shah, arXiv:2307.13083

Cosmological parameters:
($\Omega_b h^2$, $\Omega_m h^2$, H0 , n_s , τ, As)

Theoretical model

We compare the angular power spectra we computed with the data and, using a bayesian analysis, we get a combination of cosmological parameter values in agreement with these.

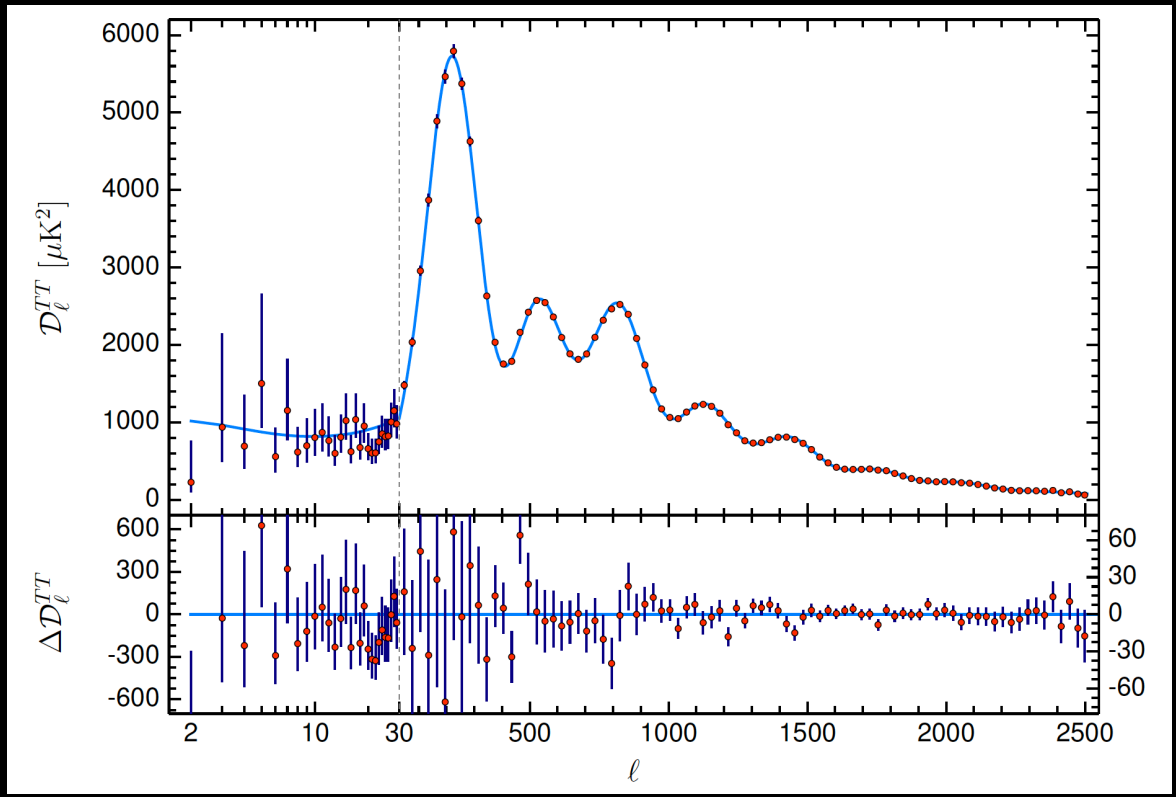

Planck 2018, Astron.Astrophys. 641 (2020) A6

Parameter constraints

We can extract 4 independent angular spectra from the CMB:

- Temperature
- Cross Temperature Polarization E
- Polarization type E (density fluctuations)
- Polarization type B (gravitational waves)

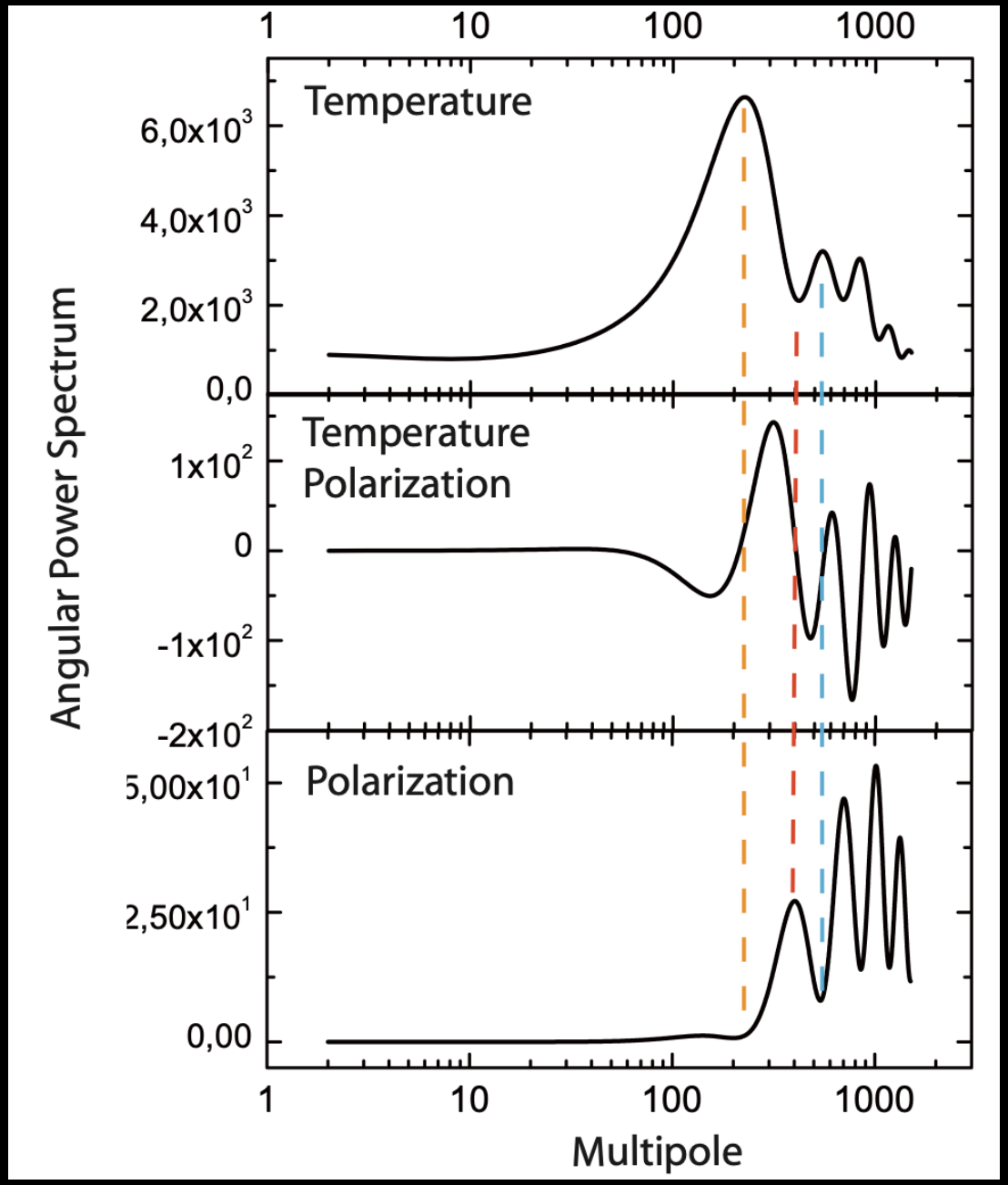

Borstnik et al., hep-ph/0401043

How to constrain parameters with the CMB

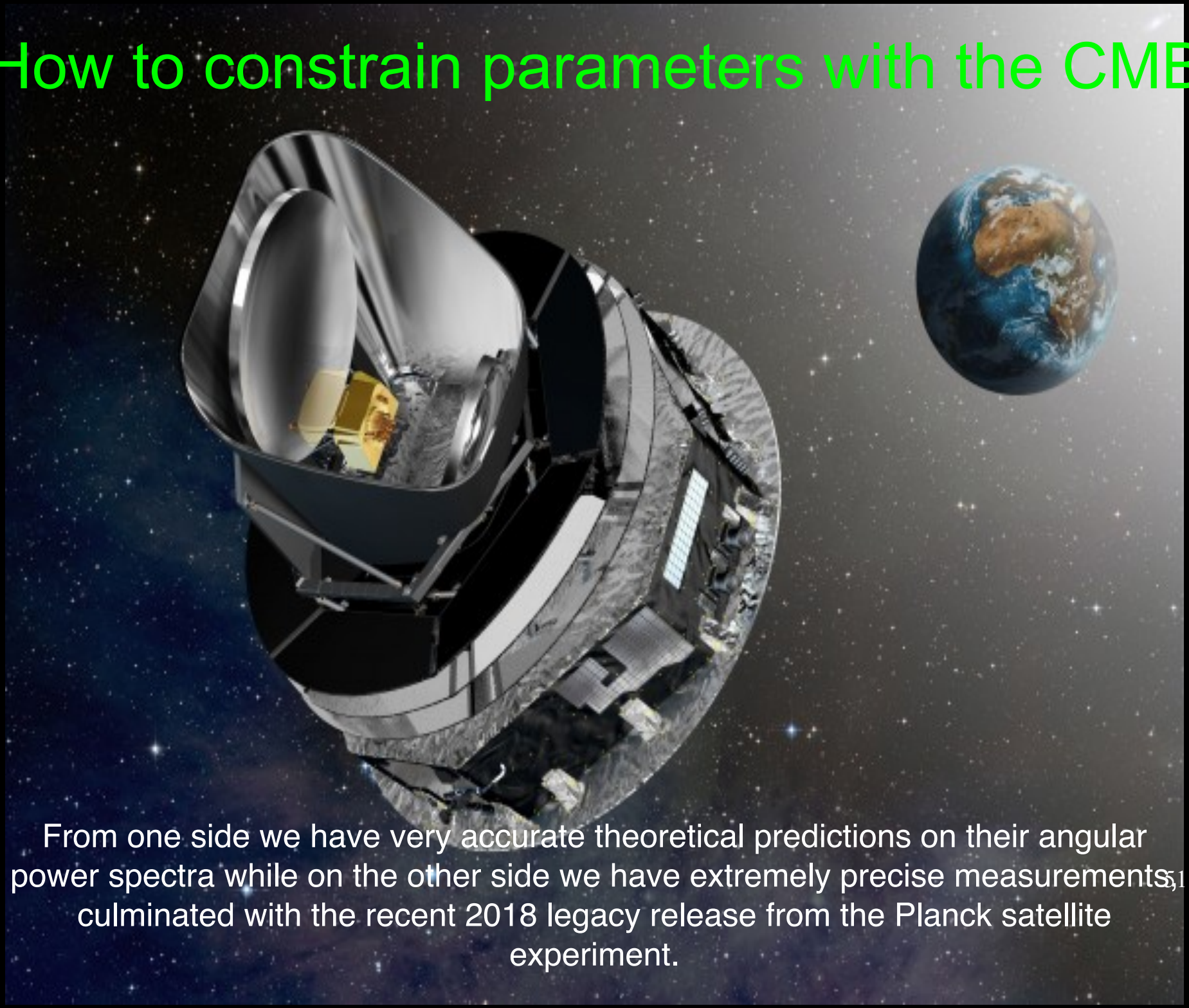

From one side we have very accurate theoretical predictions on their angular power spectra while on the other side we have extremely precise measurements, culminated with the recent 2018 legacy release from the Planck satellite experiment.

Planck satellite experiment

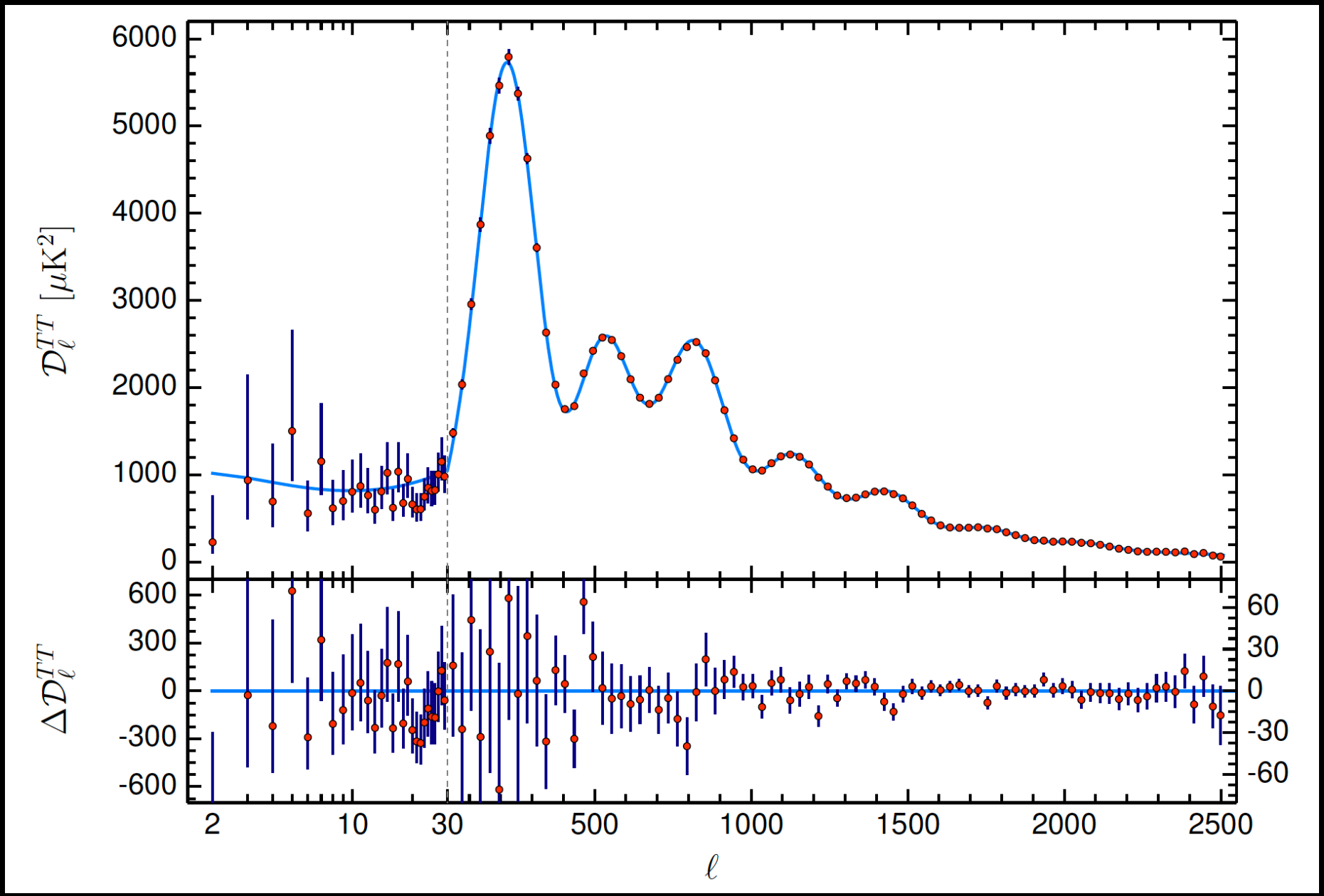

Planck 2018, Astron.Astrophys. 641 (2020) A6

Planck satellite experiment

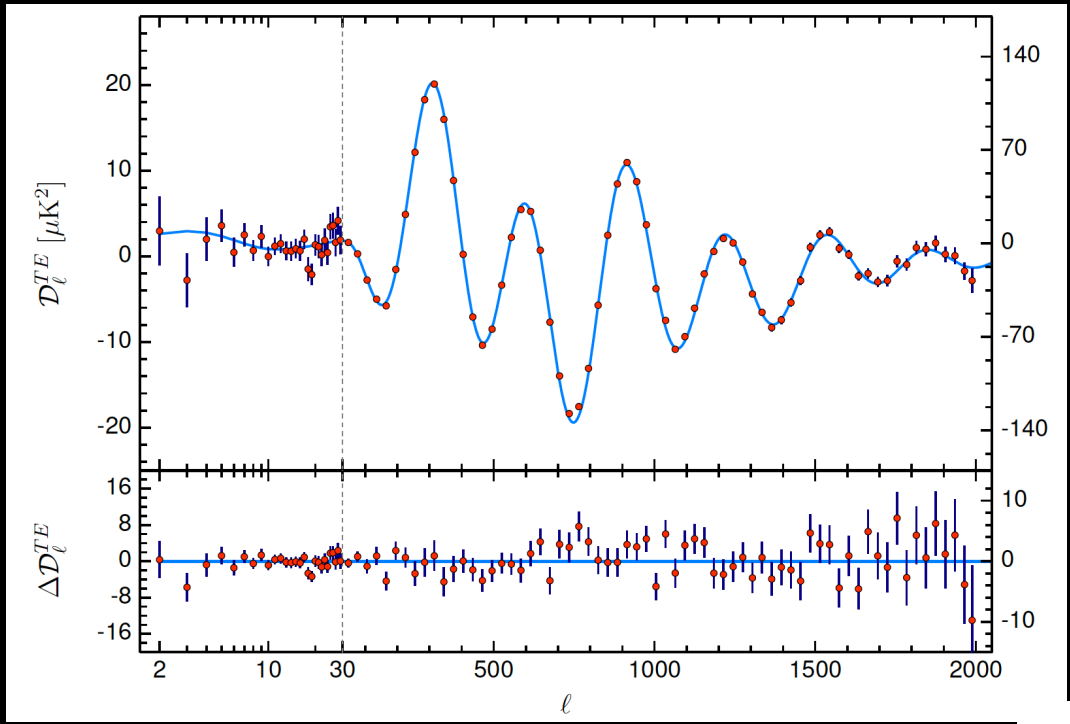

The theoretical spectra in light blues are computed from the best-fit base-LCDM theoretical spectrum fit to the Planck TT,TE,EE+lowE+lensing likelihood.

Residuals with respect to this theoretical model are shown in the lower panel in each plot.

Planck 2018, Astron.Astrophys. 641 (2020) A6

Polarization spectra

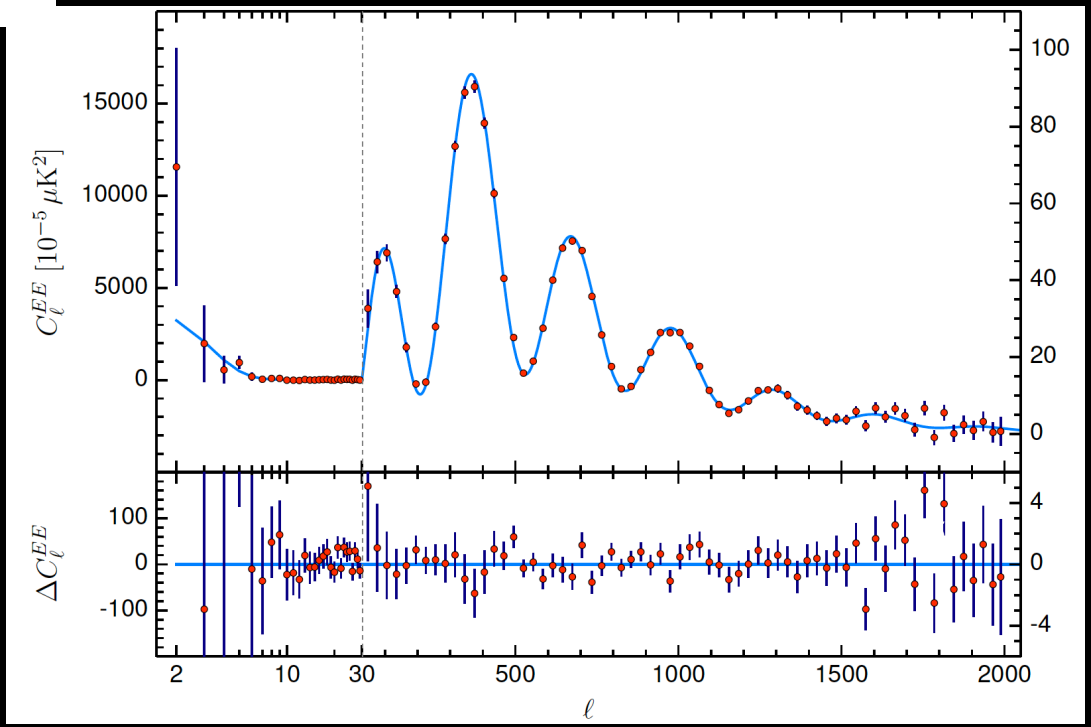

Planck satellite experiment

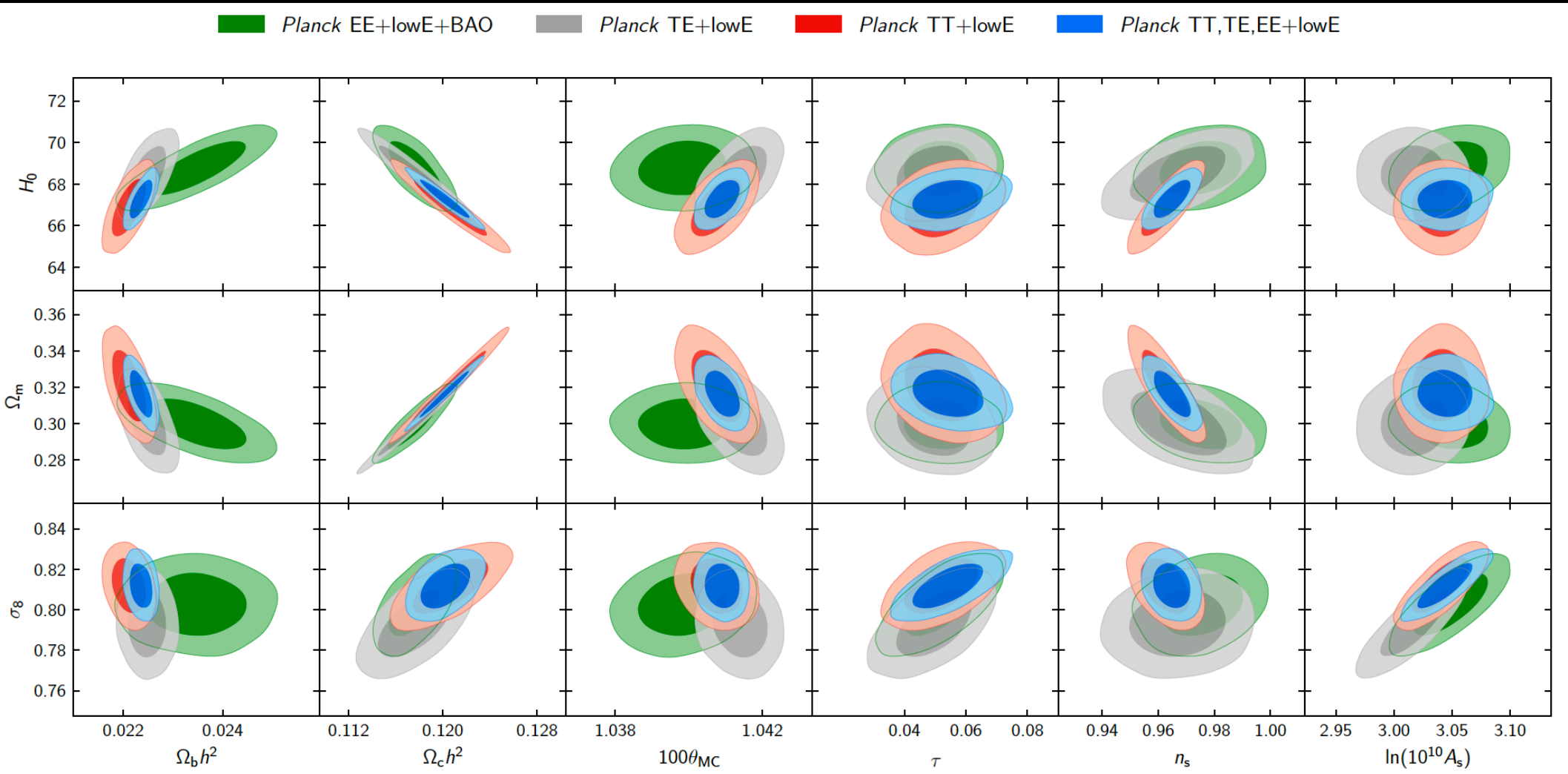

Planck 2018, Astron.Astrophys. 641 (2020) A6

Constraints on parameters of the LCDM model from the separate Planck EE, TE, and TT high-l spectra combined with low-l polarization (lowE), and, in the case of EE also with BAO, compared to the joint result using Planck TT,TE,EE+lowE.

How to constrain parameters with the CMB

Parameter	TT+lowE 68% limits	TE+lowE 68% limits	EE+lowE 68% limits	TT,TE,EE+lowE 68% limits	TT,TE,EE+lowE+lensing 68% limits	TT,TE,EE+lowE+lensing+BAO 68% limits
$\Omega_b h^2$	0.02212 ± 0.00022	0.02249 ± 0.00025	0.0240 ± 0.0012	0.02236 ± 0.00015	0.02237 ± 0.00015	0.02242 ± 0.00014
$\Omega_c h^2$	0.1206 ± 0.0021	0.1177 ± 0.0020	0.1158 ± 0.0046	0.1202 ± 0.0014	0.1200 ± 0.0012	0.11933 ± 0.00091
$100\theta_{MC}$	1.04077 ± 0.00047	1.04139 ± 0.00049	1.03999 ± 0.00089	1.04090 ± 0.00031	1.04092 ± 0.00031	1.04101 ± 0.00029
τ	0.0522 ± 0.0080	0.0496 ± 0.0085	0.0527 ± 0.0090	$0.0544^{+0.0070}_{-0.0081}$	0.0544 ± 0.0073	0.0561 ± 0.0071
$\ln(10^{10} A_s)$	3.040 ± 0.016	$3.018^{+0.020}_{-0.018}$	3.052 ± 0.022	3.045 ± 0.016	3.044 ± 0.014	3.047 ± 0.014
n_s	0.9626 ± 0.0057	0.967 ± 0.011	0.980 ± 0.015	0.9649 ± 0.0044	0.9649 ± 0.0042	0.9665 ± 0.0038
H_0 [km s^{-1} Mpc^{-1}]	66.88 ± 0.92	68.44 ± 0.91	69.9 ± 2.7	67.27 ± 0.60	67.36 ± 0.54	67.66 ± 0.42
Ω_Λ	0.679 ± 0.013	0.699 ± 0.012	$0.711^{+0.033}_{-0.026}$	0.6834 ± 0.0084	0.6847 ± 0.0073	0.6889 ± 0.0056
Ω_m	0.321 ± 0.013	0.301 ± 0.012	$0.289^{+0.026}_{-0.033}$	0.3166 ± 0.0084	0.3153 ± 0.0073	0.3111 ± 0.0056
$\Omega_m h^2$	0.1434 ± 0.0020	0.1408 ± 0.0019	$0.1404^{+0.0034}_{-0.0039}$	0.1432 ± 0.0013	0.1430 ± 0.0011	0.14240 ± 0.00087
$\Omega_m h^3$	0.09589 ± 0.00046	0.09635 ± 0.00051	$0.0981^{+0.0016}_{-0.0018}$	0.09633 ± 0.00029	0.09633 ± 0.00030	0.09635 ± 0.00030
σ_8	0.8118 ± 0.0089	0.793 ± 0.011	0.796 ± 0.018	0.8120 ± 0.0073	0.8111 ± 0.0060	0.8102 ± 0.0060
$S_8 \equiv \sigma_8(\Omega_m/0.3)^{0.5}$	0.840 ± 0.024	0.794 ± 0.024	$0.781^{+0.052}_{-0.060}$	0.834 ± 0.016	0.832 ± 0.013	0.825 ± 0.011

Planck 2018, Astron.Astrophys. 641 (2020) A6

2018 Planck results are a wonderful confirmation of the flat standard ΛCDM cosmological model, but are model dependent!
We can consider extensions to this model, adding parameters in the neutrino sector, and constraining these parameters in the same way.

The Neutrino effective number

The expected value is Neff = 3.044, if we assume standard electroweak interactions and three active massless neutrinos.
If we measure a Neff > 3.044, we are in presence of extra radiation.
The neutrino effective number is now very well constrained with Planck 2018:

$$N_{\rm eff} = 2.92^{+0.36}_{-0.37} \quad (95\,\%,\ \textit{Planck}\ \text{TT,TE,EE+lowE}),$$

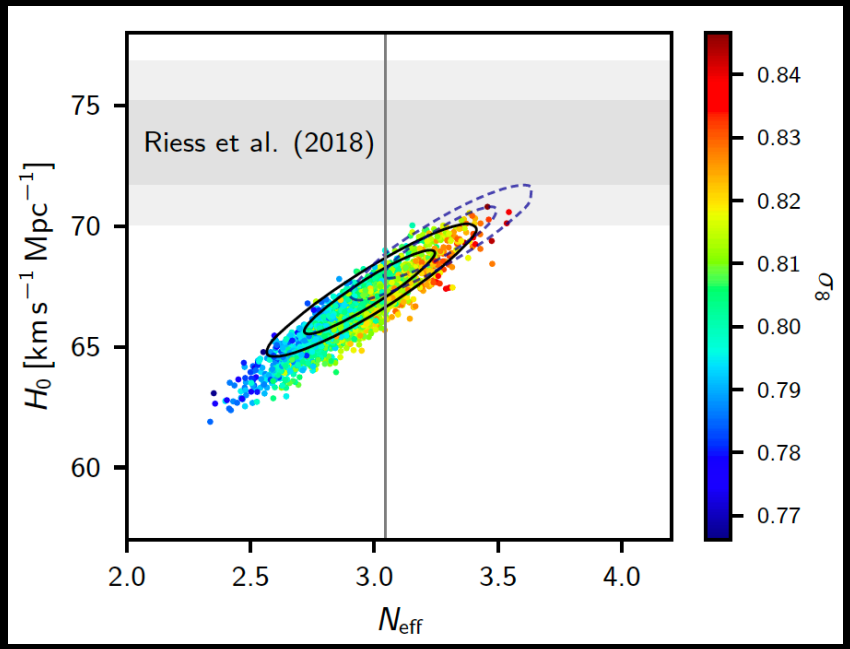

Planck 2018, Astron.Astrophys. 641 (2020) A6

The total neutrino mass and the CMB

Neutrinos are the only known particles behaving as
radiation at early times (during the CMB acoustic oscillations —> Neff)
and dark matter at late times (during structure formation),
which has consequences on the background evolution.
Actually, the neutrino temperature today is expected to be $T_\nu^0 \sim 1.7 \times 10^{-4}$ eV,
that is smaller than the two squared-mass differences,
so at least two of the neutrinos are not relativistic today.
We can compute the redshift at which neutrinos become non-relativistic,

$$1 + z_{\rm NR} = \frac{8}{21}\left(\frac{11}{4}\right)^{4/3} \frac{\rho^{\rm NR}_{\nu,0}}{N^\nu_{\rm eff}\rho_{\gamma,0}} \approx 1890\left(\tfrac{1}{3}\sum m_\nu/1\,{\rm eV}\right)$$

occurring when the average neutrino momentum drops below its mass
(see Alvey et al. arXiv:2111.12726 for the derivation of the formula).
The transition from the radiation to the matter regime depends on the ratio between the energy density of the non-relativistic neutrinos today and relativistic ones through Neff.
Therefore, we will have that neutrino eigenstates with a mass $m_i \ll 0.6$ eV
will become non - relativistic after photon decoupling ($z \approx 1090$).

Because the shape of the CMB spectrum is primarily influenced by the physical evolution
before recombination, the effect of the total neutrino mass
(not individual masses, Archidiacono et al. arXiv:2003.03354) appear through
a modified background evolution and some secondary anisotropy corrections.

The total neutrino mass and the CMB

Varying the total neutrino mass we vary the amount of matter density today.

Once neutrinos become non-relativistic,
their energy density is given by $\rho_\nu \simeq \sum m_i n_i$.
Since the number density is the same for every neutrino flavour,
the total neutrino mass can be factorized out.

The total neutrino density today will be:

$$\Omega_\nu = \frac{\rho_\nu^0}{\rho_{\rm crit}^0} = \frac{\sum m_\nu}{93.14 h^2 \ {\rm eV}}$$

increasing the total non-relativistic matter density at late time

$$H^2 = \left(\frac{\dot{a}}{a}\right)^2 = H_0^2 \left(\frac{\Omega_r}{a^4} + \frac{\Omega_m}{a^3} + \frac{\Omega_k}{a^2} + \Omega_\Lambda\right)$$

The total neutrino mass and the CMB

If we are varying the total non-relativistic matter density at late time,
increasing the total neutrino mass we will change
the redshift of the matter-to-radiation equality,
and the redshift of the matter-to-Λ equality.

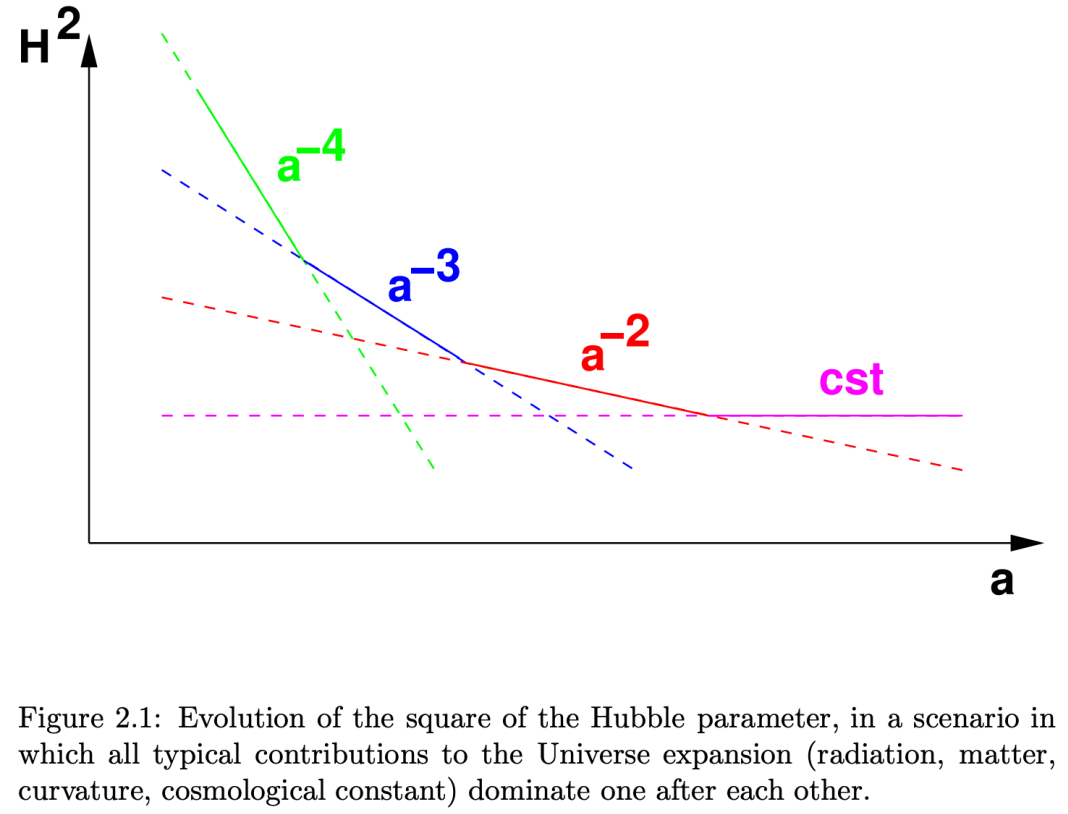

Figure 2.1: Evolution of the square of the Hubble parameter, in a scenario in which all typical contributions to the Universe expansion (radiation, matter, curvature, cosmological constant) dominate one after each other.

Lesgourgues, arxiv:astro-ph/0409426

The total neutrino mass and the CMB

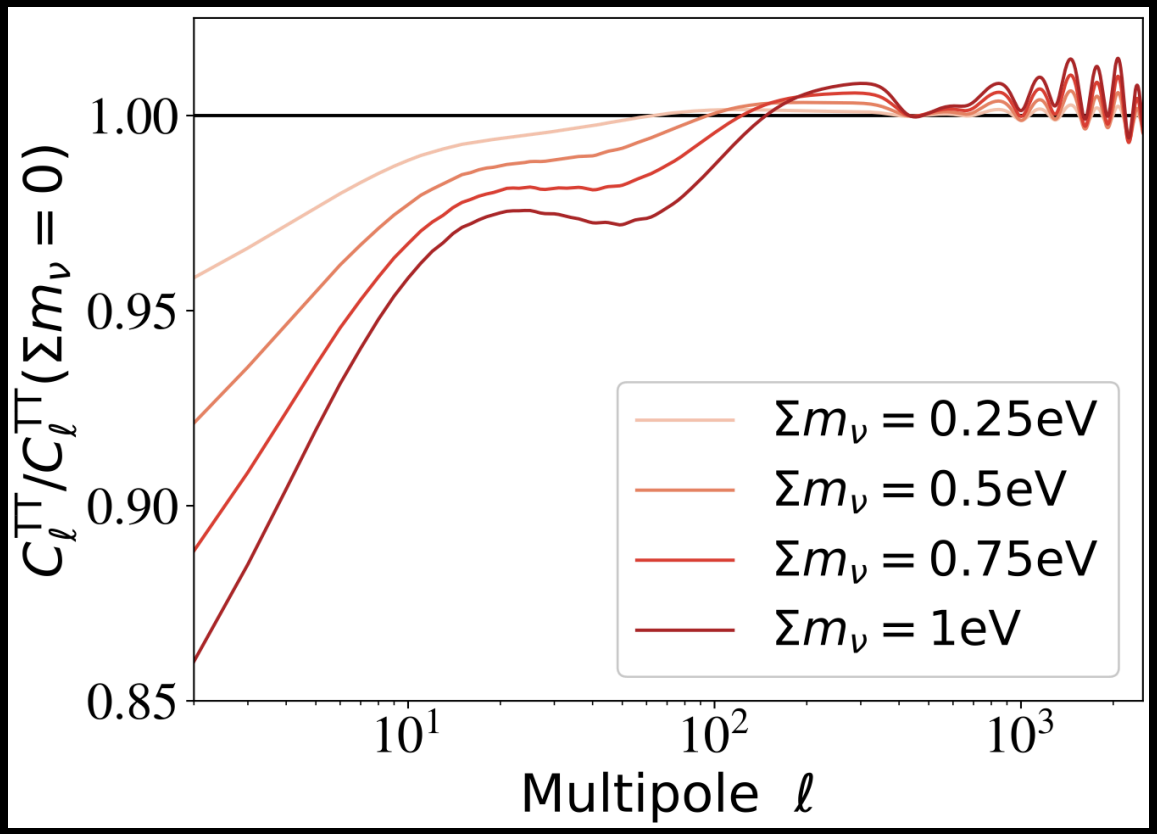

Lesgourgues & Verde, Review of Particle Physics, PTEP 2022 (2022) 083C01

Therefore, a higher total neutrino mass will show up as a suppression of the ISW effect.

If we fix all the parameters, we can see that an increase in neutrino mass comes together with a decrease in the late ISW effect explaining the depletion of the CMB spectrum for $l \leq 20$, while the early ISW effect is responsible for the dip present for $20 \leq l \leq 200$.

The total neutrino mass and the CMB

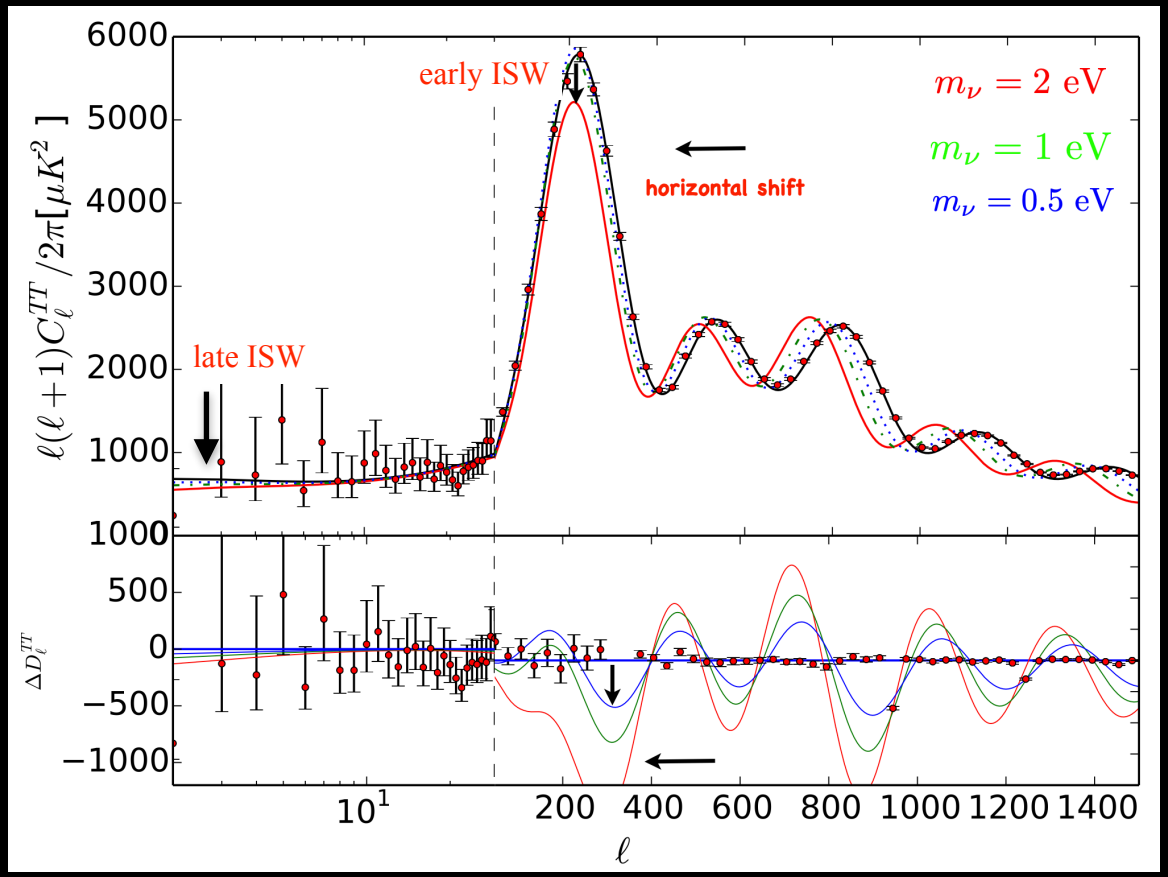

Credit figure: Olga Mena

This means a decrease in the height of the first CMB acoustic peak for the early ISW, and a decrease of the plateau at low multipoles for the late ISW. However, the CMB is only marginally sensitive to the late ISW effect due to cosmic variance.

Moreover, a change in the non-relativistic matter density at late times can impact the angular diameter distance to the last scattering surface $d_A(z_{dec})$, that controls the overall position of CMB peaks.

$$d_{\rm A}(z) = \frac{c}{H_0}\frac{1}{(1+z)}\int_0^z \frac{dz}{\left[\Omega_{\rm m,0}\,(1+z)^3 + \Omega_{\Lambda,0}\right]^{1/2}}$$

The total neutrino mass and the CMB

However, these effects are strongly degenerate with other cosmological parameters, so how can the CMB set strong constraints on Σm_ν?

This happens because of another secondary source of anisotropies: the CMB lensing.

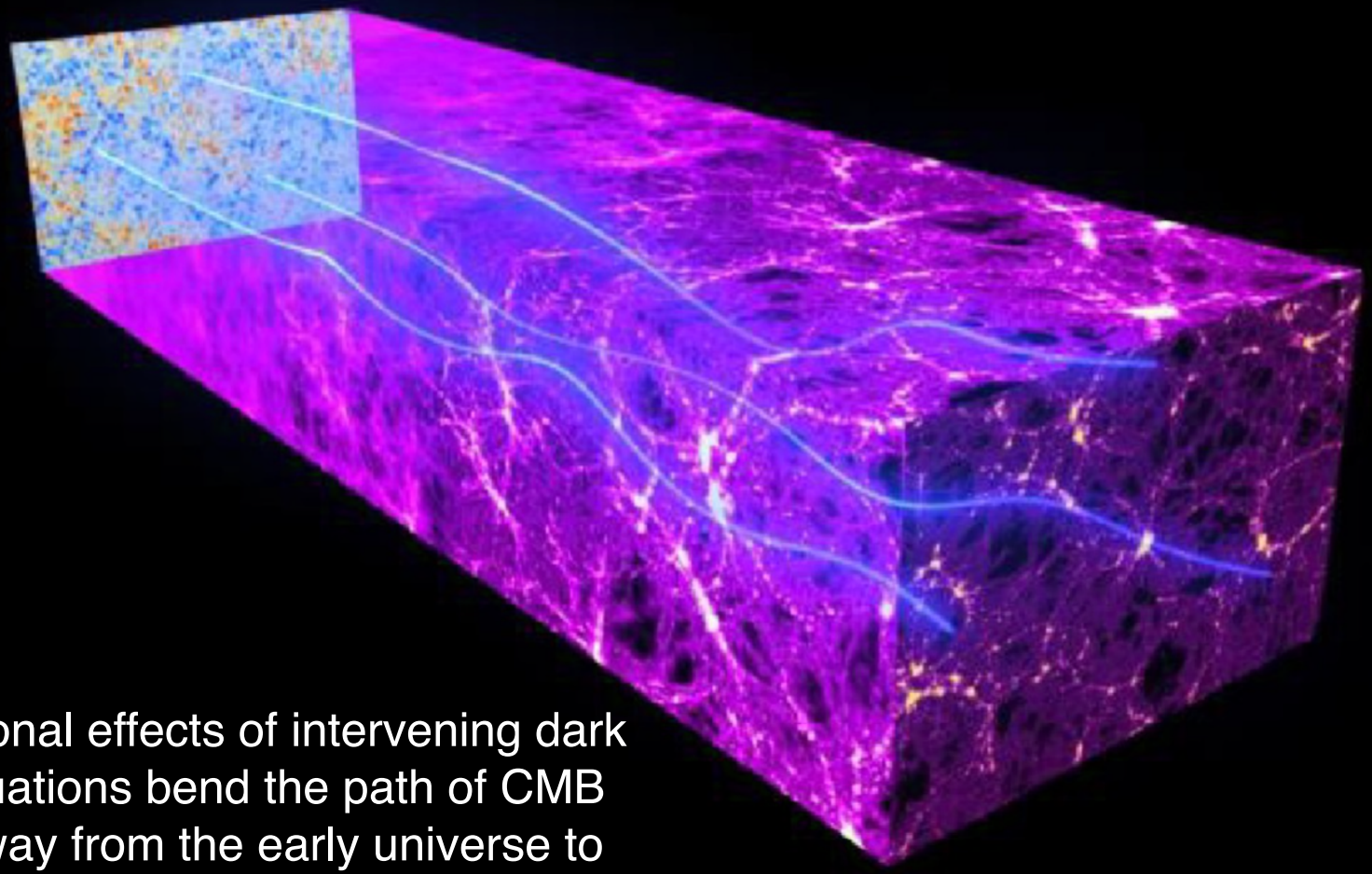

The gravitational effects of intervening dark matter fluctuations bend the path of CMB light on its way from the early universe to the telescope.

This “gravitational lensing” distorts our image of the CMB.

The CMB lensing

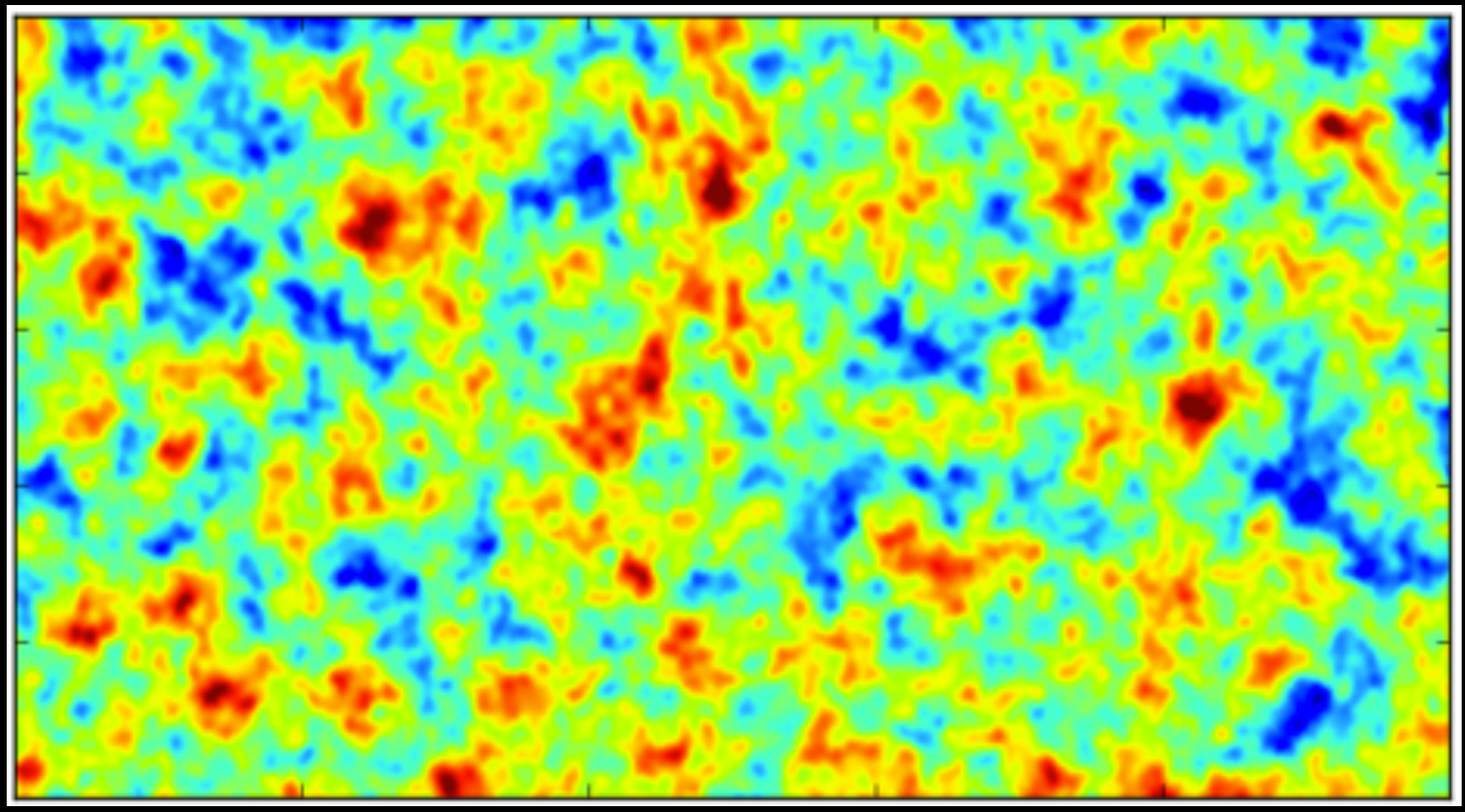

A simulated patch of CMB sky – **before dark matter lensing**

The CMB lensing

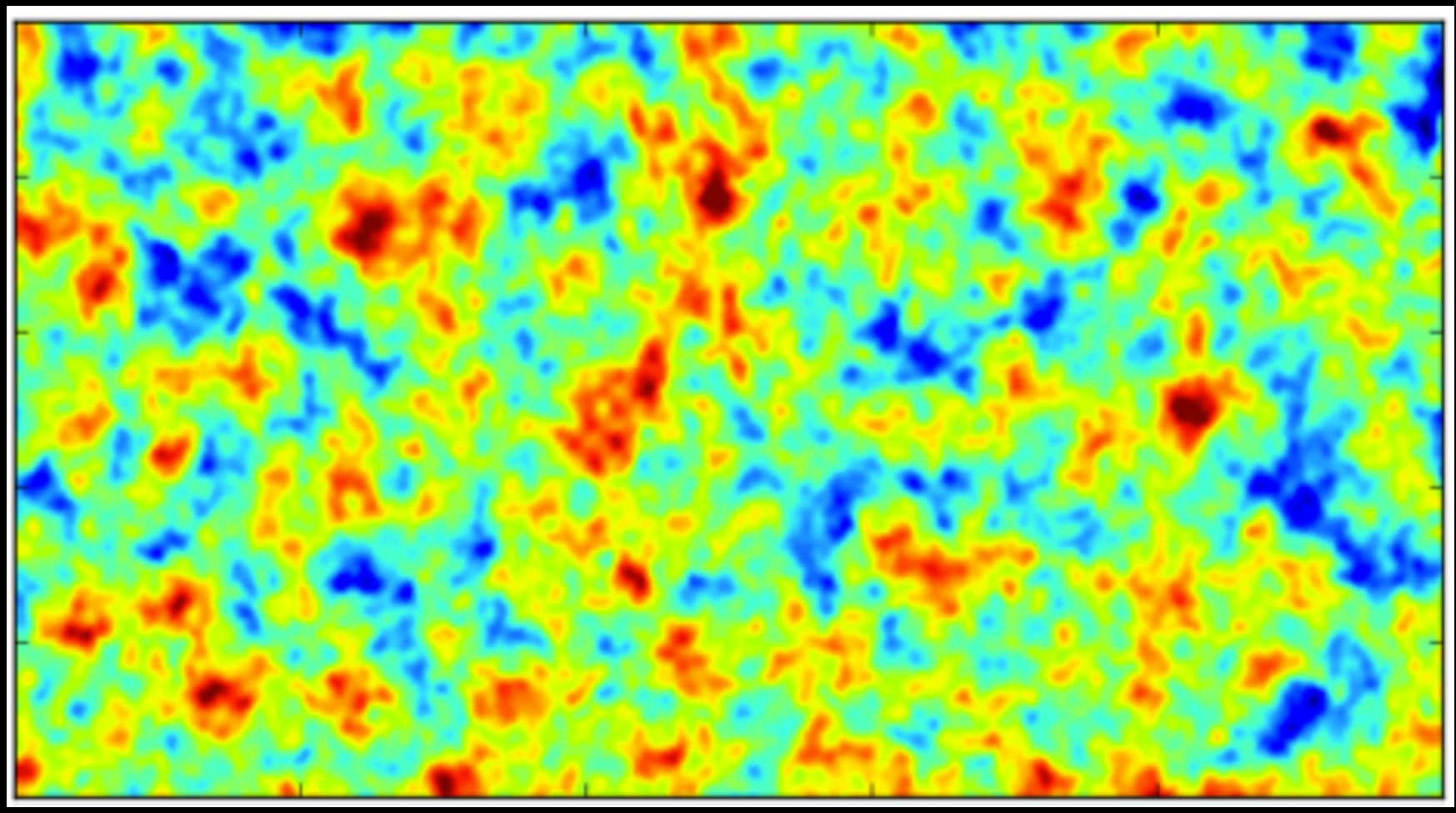

A simulated patch of CMB sky – **after dark matter lensing**

The total neutrino mass and the CMB

However, these effects are strongly degenerate with other cosmological parameters, so how can the CMB set strong constraints on Σm_ν?

This happens because of another secondary source of anisotropies: the CMB lensing.

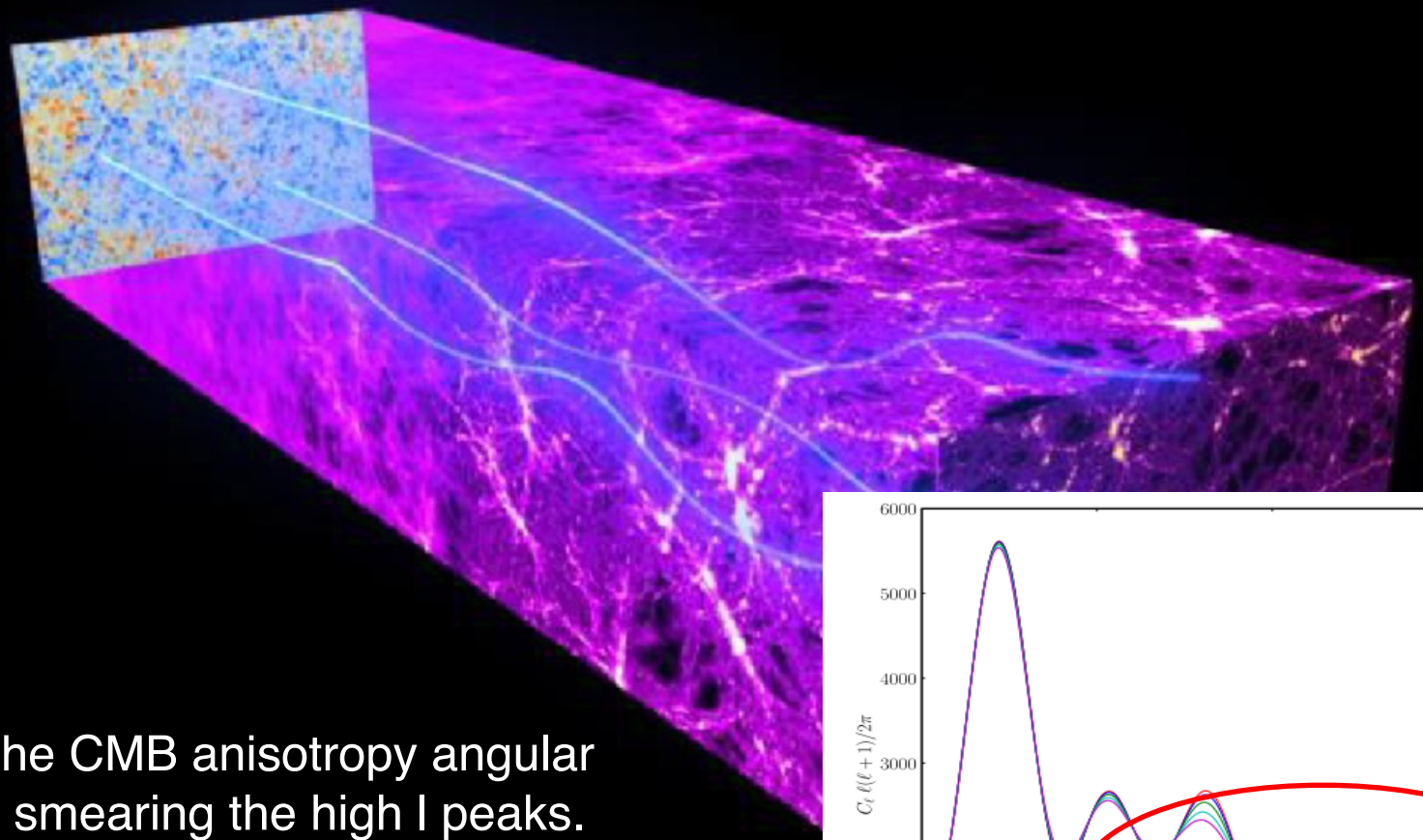

This affects the CMB anisotropy angular spectrum by smearing the high l peaks.

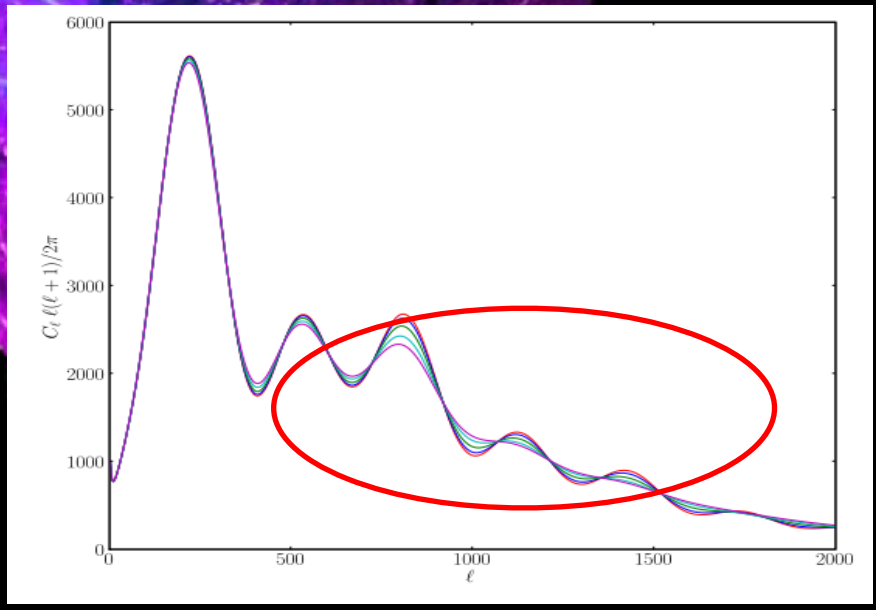

The total neutrino mass and the CMB

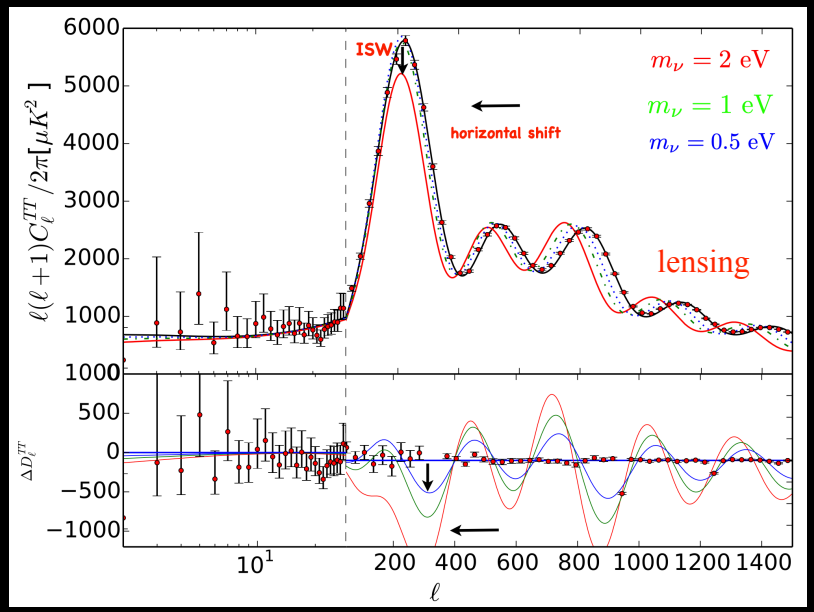

Credit figure: Olga Mena

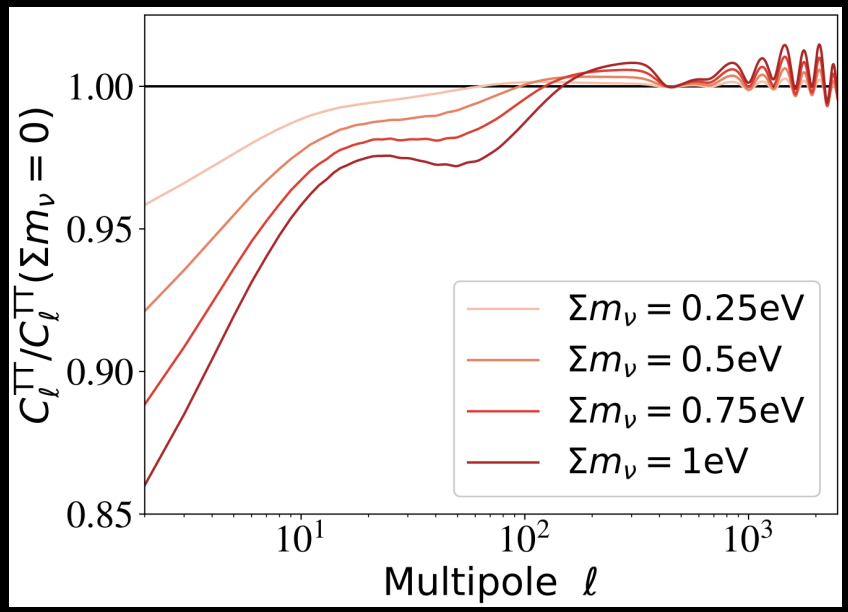

Lesgourgues & Verde, RPP, PTEP 2022 (2022) 083C01

Therefore, a higher total neutrino mass will have an effect also in the damping tail of the CMB power spectrum.

The total neutrino mass and the CMB

Planck 2018, Aghanim et al., arXiv:1807.06209 [astro-ph.CO]

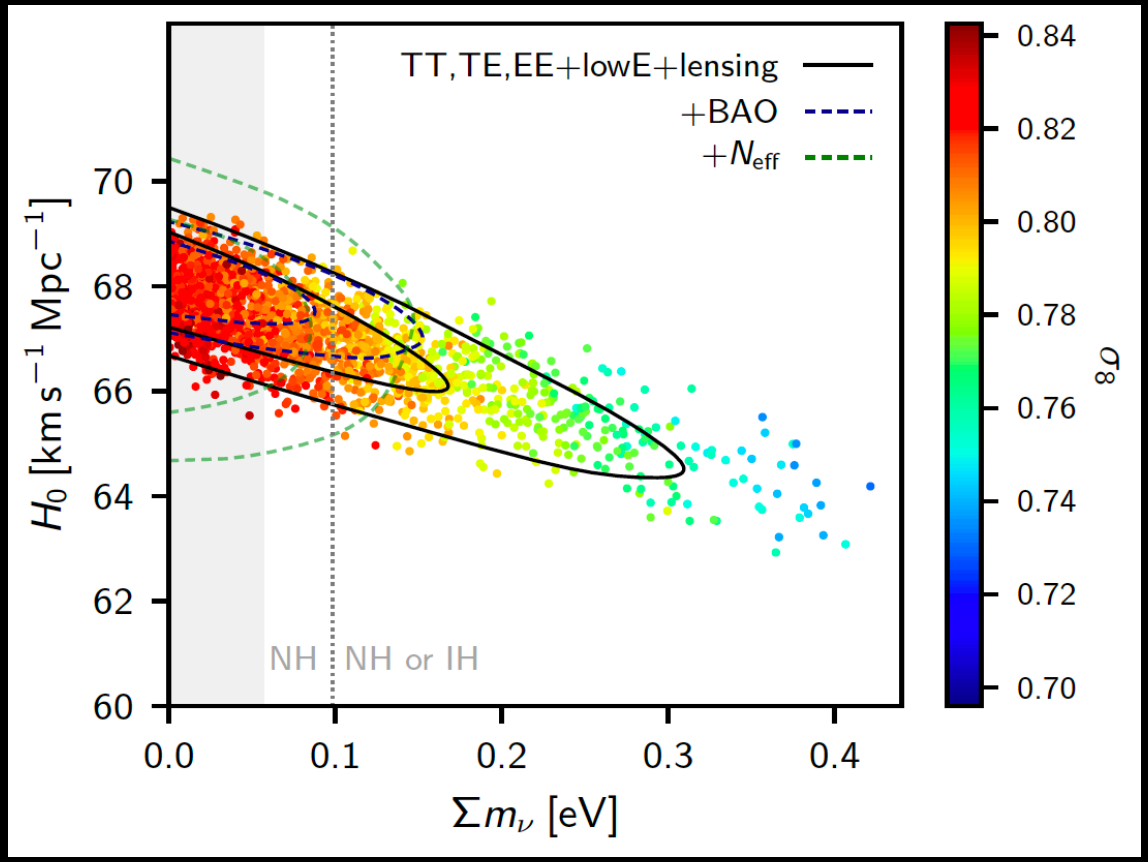

$$\sum m_\nu < 0.26 \text{ eV} \quad (95\,\%,\ \textit{Planck}\ \text{TT,TE,EE+lowE})$$

From Planck 2018 we have a very important upper limit on the total neutrino mass.

The total neutrino mass and the LSS

The main large scale structures (LSS) observables are
the power spectrum of the matter fluctuations in Fourier space

$$\left\langle \delta_m(\boldsymbol{k})\, \delta_m(\boldsymbol{k}') \right\rangle = (2\pi)^3\, P(k)\, \delta_D^{(3)}(\boldsymbol{k} - \boldsymbol{k}')$$

Or the two-point correlation function in the configuration space

$$\xi(r) = \int \frac{d^3k}{(2\pi)^3} P(k) e^{i\mathbf{k}\cdot(\mathbf{x}-\mathbf{x}')} \equiv \xi_m(r)$$

The total neutrino mass and the LSS

The shape of the matter power spectrum is the key observable for constraining the neutrino masses with cosmological methods.

This is defined as the two-point correlation function of the total non-relativistic matter fluctuation in Fourier space:

$$P(k,z) = \langle |\delta_{\rm m}(k,z)|^2 \rangle \quad \Rightarrow \quad \delta_{\rm m} = \frac{\sum_i \bar{\rho}_i \, \delta_i}{\sum_i \bar{\rho}_i}$$

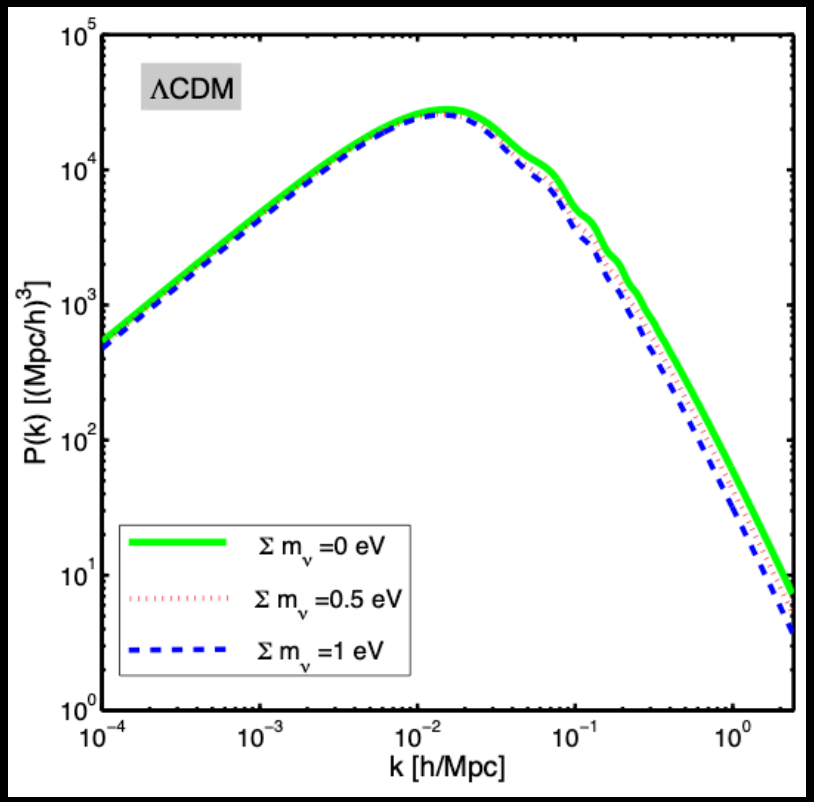

Chen & Xu, Phys.Lett.B 752

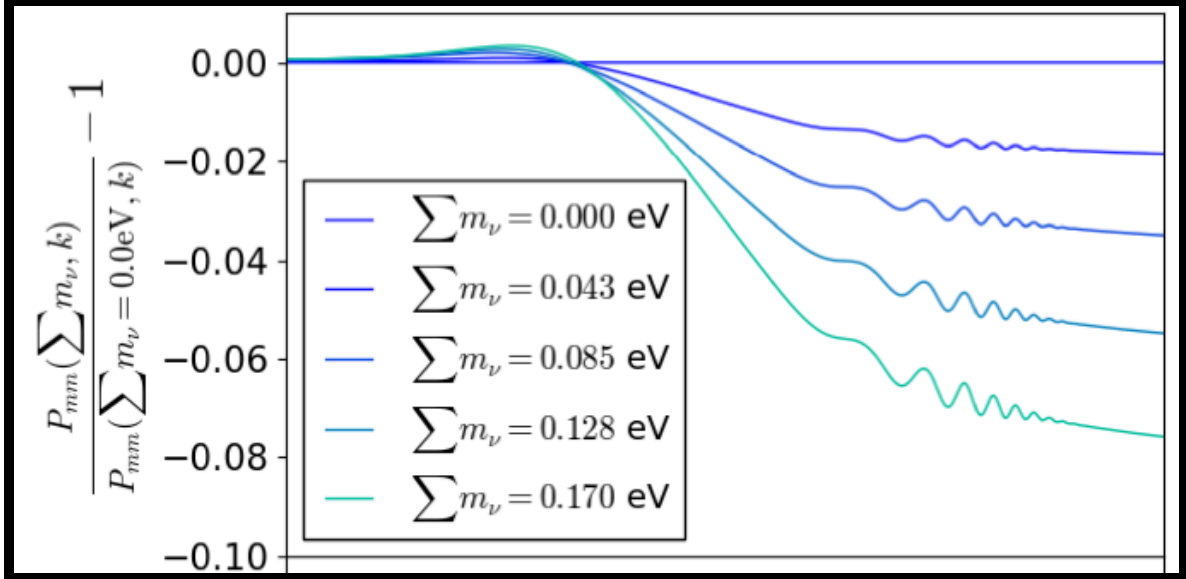

Whitford et al., arXiv:2112.10302

The total neutrino mass and the LSS

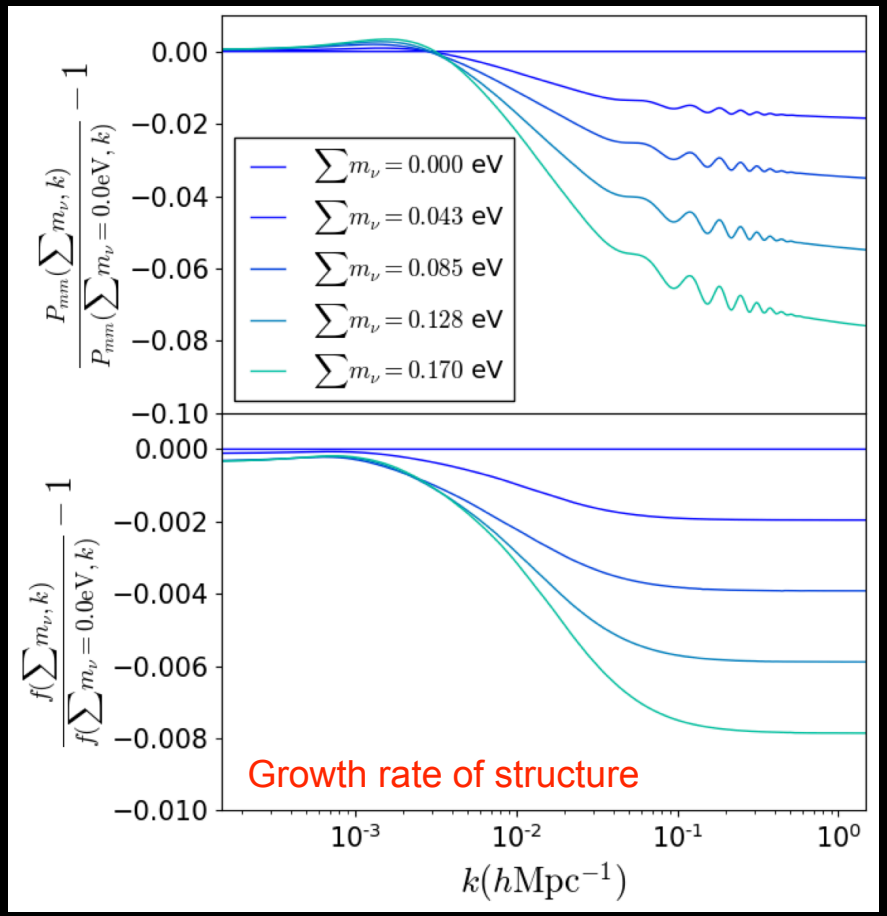

Whitford et al., arXiv:2112.10302

Neutrinos with sub-eV masses are hot thermal relics with very large thermal velocity exceeding the escape velocity of the gravitational potentials. Therefore they will only cluster at scales larger than their free streaming scale, defined as the distance traveled by neutrinos over a Hubble time scale

$$k_{\mathrm{fs},i}(z) \simeq \frac{0.677}{(1+z)^{1/2}} \left(\frac{m_{\nu,i}}{1\ \mathrm{eV}}\right) \Omega_{\mathrm{m}}^{1/2} h\ \mathrm{Mpc}^{-1}$$

Massive neutrinos will suppress the structure formation at small scales, affecting the large scale structures (LSS). On larger scales, they cluster in the same way as cold dark matter.

The net suppression of the power spectrum is scale dependent and the relevant length scale is the Jeans length for neutrinos which decreases with time as the neutrino thermal speed decreases.

$$k_J(t) = \left(\frac{4\pi G \bar{\rho}(t) a^2(t)}{c_s^2(t)}\right)^{1/2}$$

The total neutrino mass and the LSS

Abazajian et al., Astropart.Phys. 63 (2015) 66-80

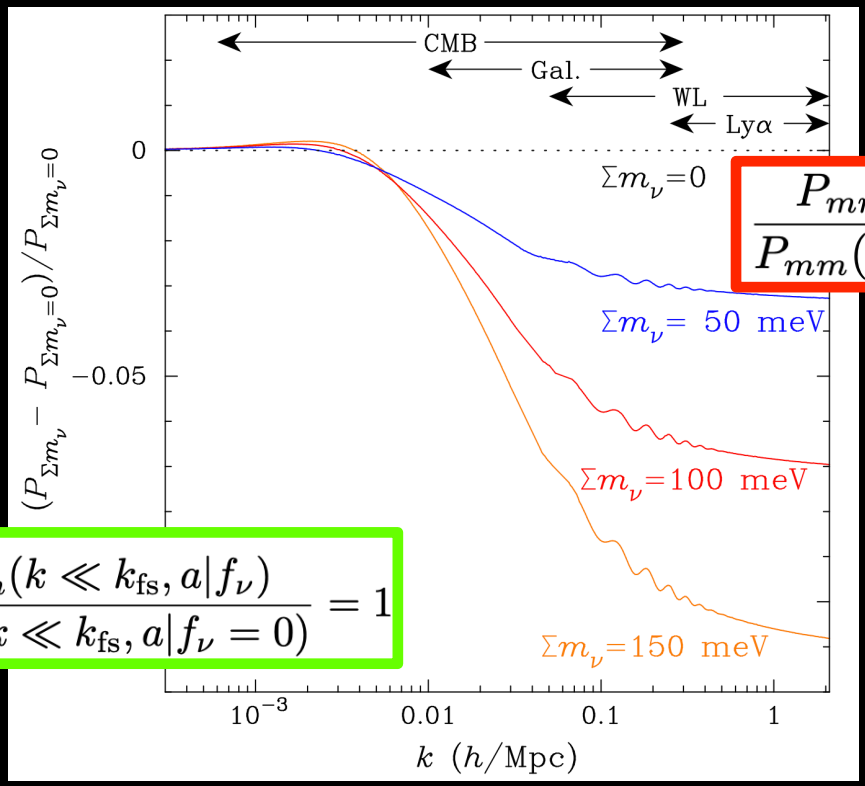

$$\frac{P_{mm}(k \gg k_{\rm fs}|f_\nu)}{P_{mm}(k \gg k_{\rm fs}|f_\nu=0)} \approx (1-8f_\nu)$$

$$f_\nu = \Omega_\nu/\Omega_m$$

$$\frac{P_{mm}(k \ll k_{\rm fs}, a|f_\nu)}{P_{mm}(k \ll k_{\rm fs}, a|f_\nu=0)} = 1$$

The power spectrum of total matter fluctuations has a negligible contribution from neutrinos on small scales, and is reduced by a factor $(1 - 2f_\nu)$.
Furthermore, on scales smaller than the free-streaming scale, the growth of cold dark matter and baryon fluctuations is reduced since neutrinos contribute to the background density, but not to the density fluctuations. This leads to an additional suppression of the small-scale linear matter power spectrum by about $(1 - 6f_\nu)$.
When combined, these effects result in an overall suppression factor of $(1 - 8f_\nu)$.

Lesgourgues & Verde, Review of Particle Physics, PTEP 2022 (2022) 083C01

The total neutrino mass and the LSS

The power spectrum of total matter fluctuations can be obtained with measurements of the gravitational lensing of the CMB, the clustering and the weak lensing of galaxies, and the number density of galaxy clusters.

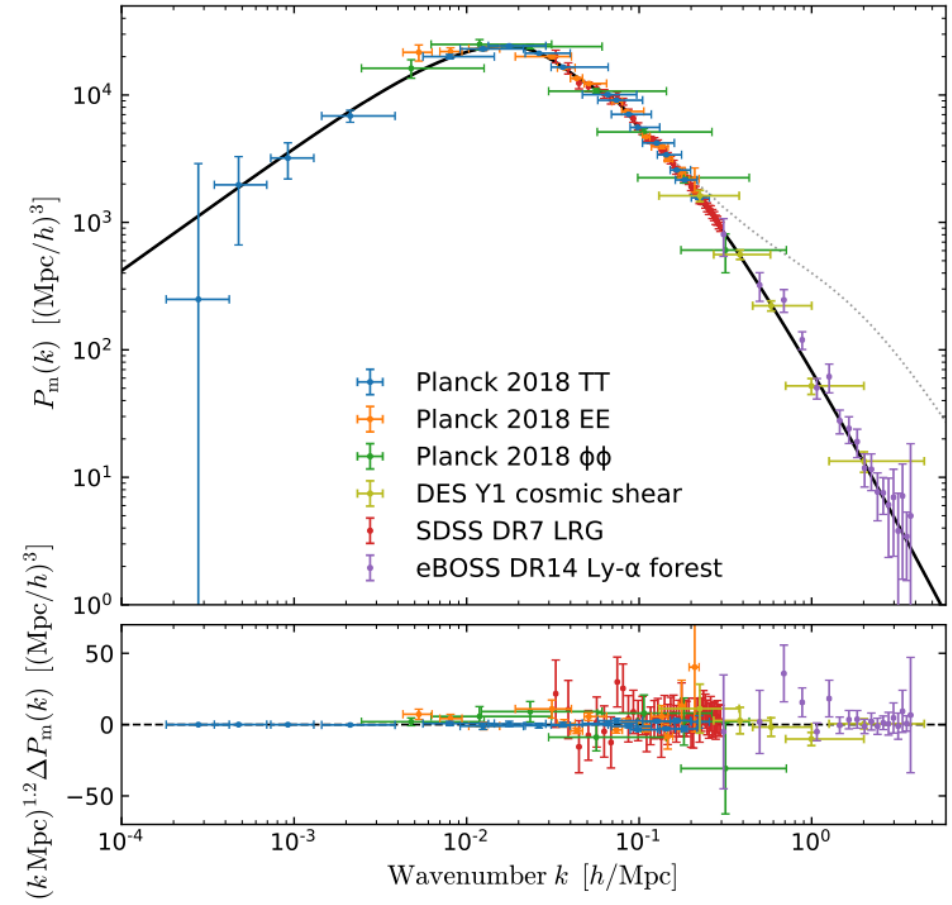

Chabanier et al, arXiv:1905.08103

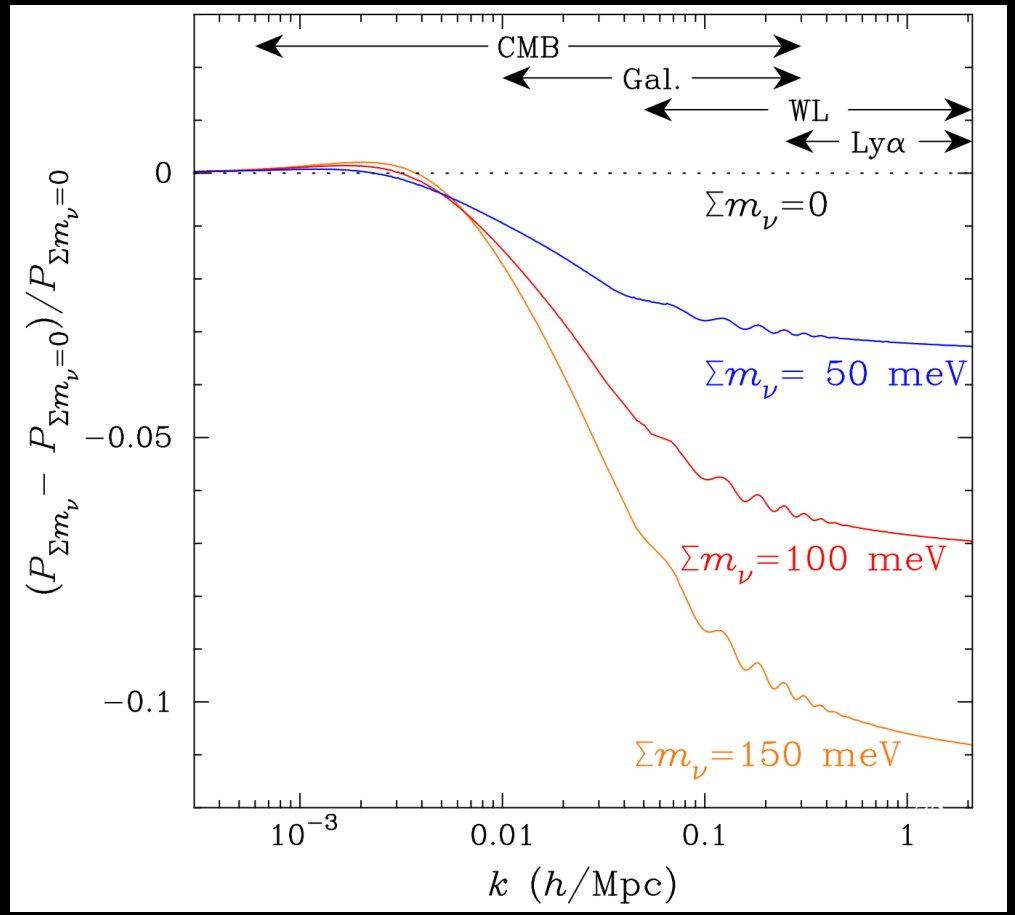

Abazajian et al., Astropart.Phys. 63 (2015) 66-80

The total neutrino mass and the LSS

At k > 0.1h/Mpc, we begin to see deviations from the linear evolution, so the perturbation theory breaks down and we need N-body simulations (Elbers et al. MNRAS 2021/2022) or beyond perturbative regime (Effective Field Theory of Large-Scale Structure) to analyse the data.

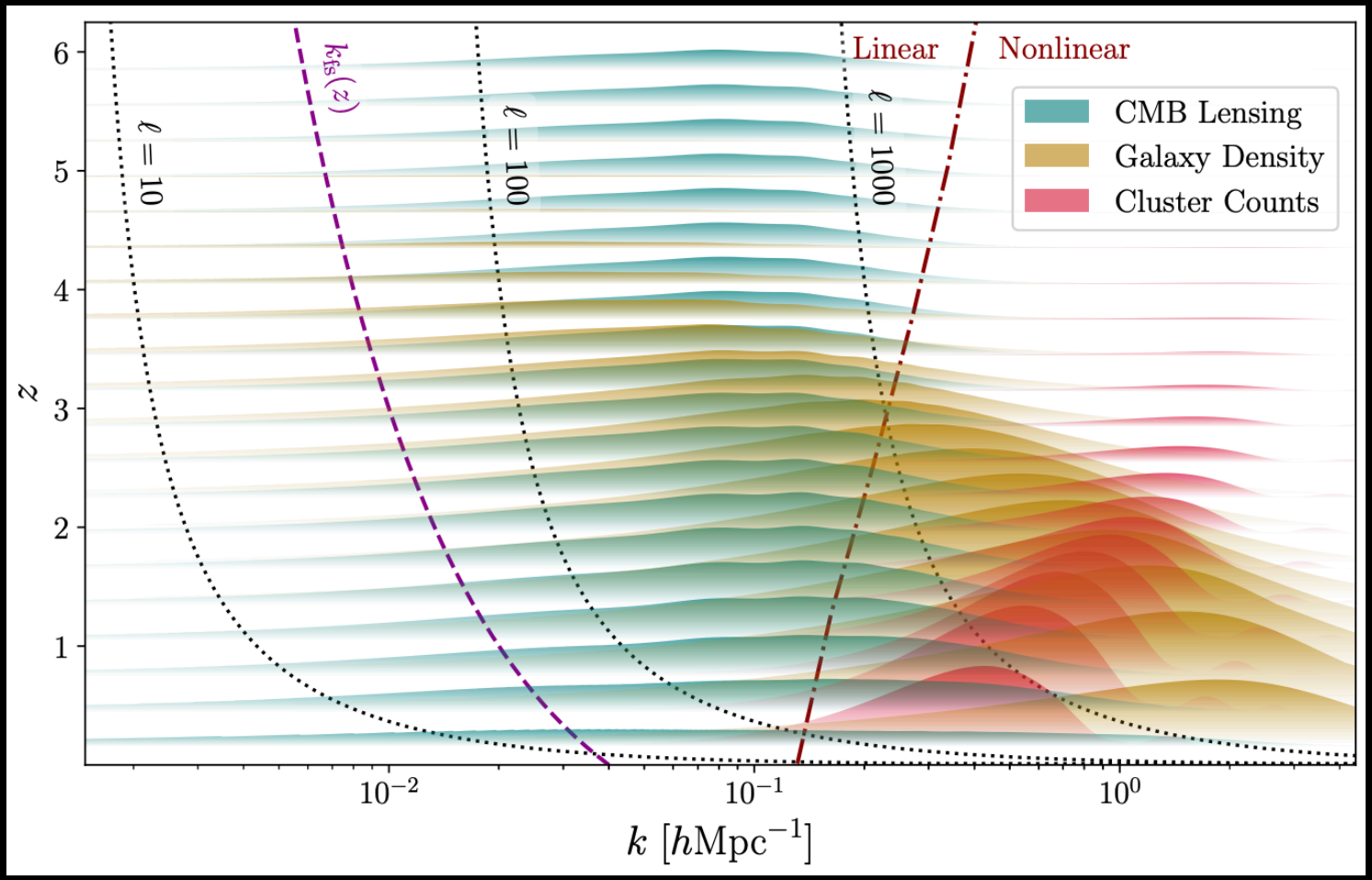

Green & Meyers, arXiv:2111.01096

The total neutrino mass and the LSS

CMB lensing reconstruction can be measured also in a different way,
i.e. using the trispectrum (or four-point correlation function) of the CMB maps,
resulting in a 40σ measurement of the lensing signal.
These data are complementary to the galaxy lensing data at lower redshift,
because they have a different degeneracy direction in the parameter space.

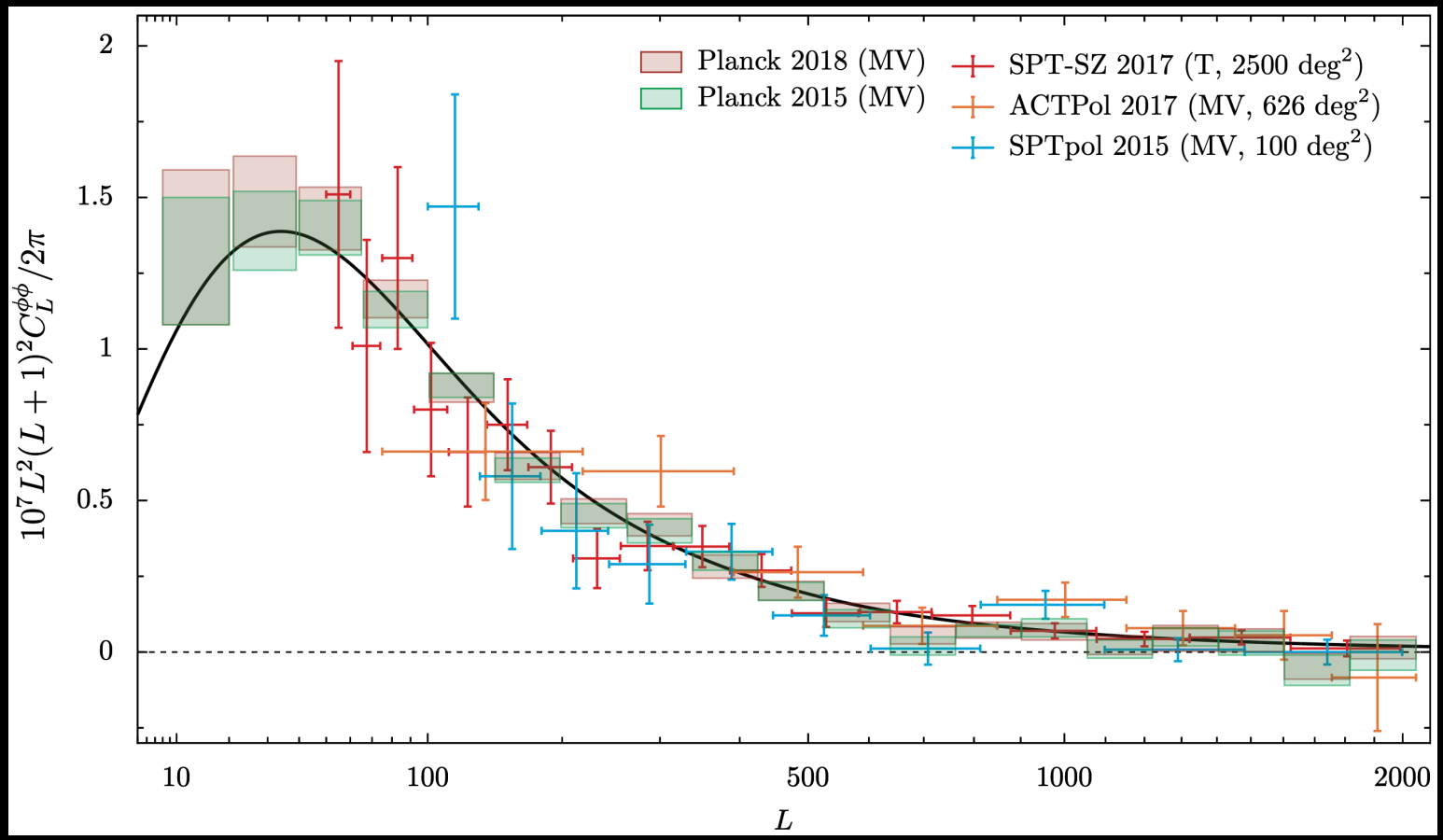

Planck collaboration, arXiv:1807.06210

The total neutrino mass and the LSS

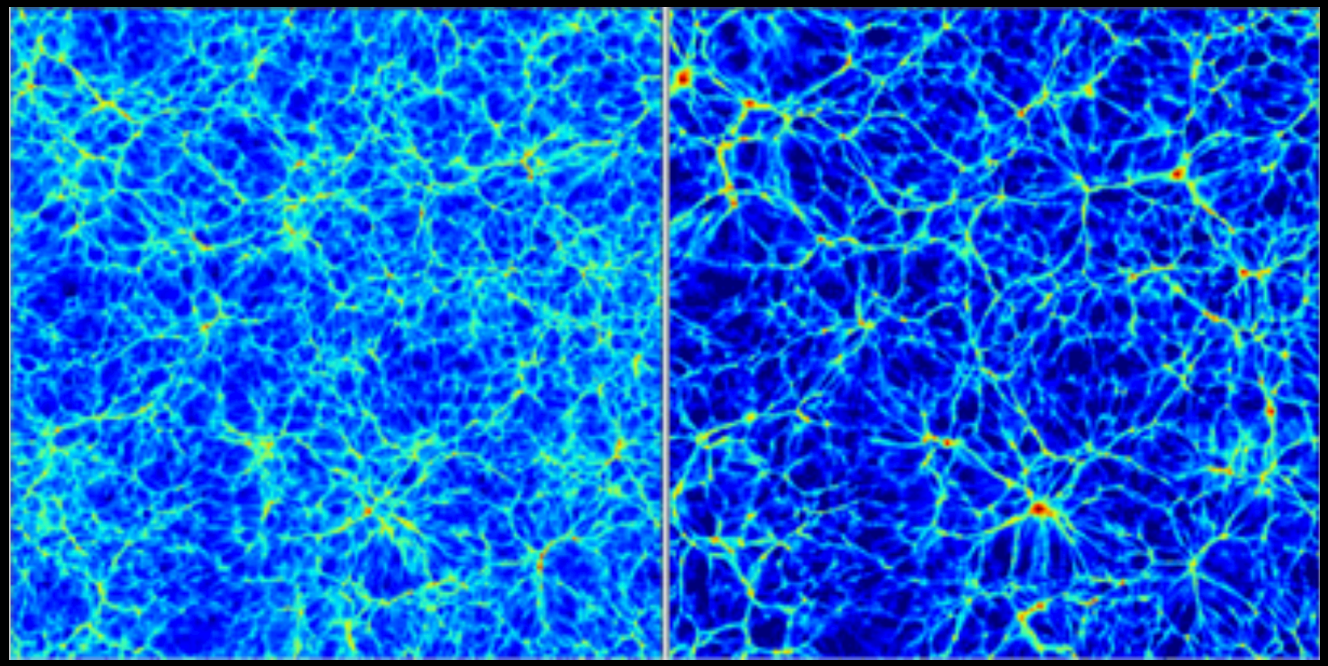

Given that massive neutrinos practically do not form structure,
more massive the neutrino is less structure we have, less the CMB lensing will be.
So a larger signal of lensing means a smaller neutrino mass.

$$\sum m_\nu < 0.24 \text{ eV} \quad (95\,\%,\ \text{TT,TE,EE+lowE+lensing})$$

Planck 2018, Aghanim et al., arXiv:1807.06209 [astro-ph.CO]

These strong limits indicate that we have a clear detection
of the lensing signal in the CMB spectra.

The total neutrino mass and BAO

The information contained in the matter clustering in the universe can be analyzed through measurements of the full-shape galaxy power spectrum or the Baryon Acoustic Oscillation (BAO) signal. Vagnozzi et al. arXiv:1701.08172 demonstrated that the BAO signal has greater constraining power compared to the extracted power spectrum, as it is less affected by factors such as non-linearities.

BAO form in the early universe, prior to recombination, when photons and baryons act as a strongly coupled fluid. This fluid's evolution is driven by the gravitational collapse into potential wells created by CDM, counterbalanced by the high pressure of the radiation component. The pressure waves generated by this interaction freeze at recombination, leaving a characteristic scale on the late-time matter clustering.
This scale appears as a localized peak in the two-point correlation function or a series of smeared peaks in the matter power spectrum.

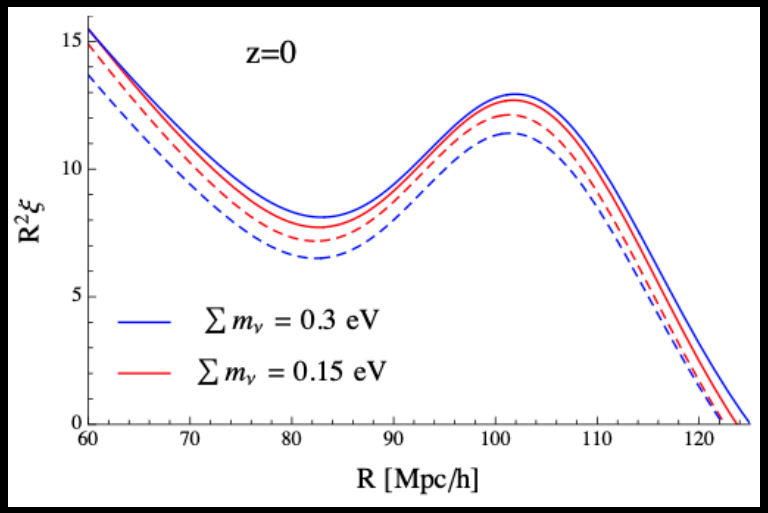

Peloso et al., *JCAP* 07 (2015) 001

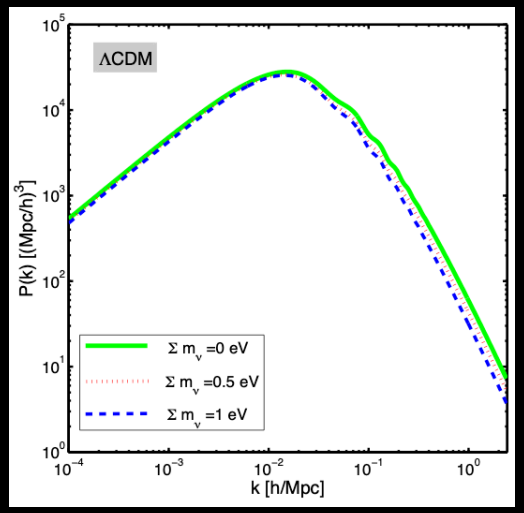

Chen & Xu, Phys.Lett.B 752

The total neutrino mass and BAO

This characteristic scale corresponds to distance that sound can travel between the Big Bang and the drag epoch, known as sound horizon at the drag epoch $r_s(z_{drag})$.

$$r_s(z_{\rm drag}) = \int_{z_{\rm drag}}^{\infty} dz \, \frac{c_s(z)}{H(z)}$$

The drag epoch is defined as the time when baryons and photons decouple (baryons are released from the drag of photons), occurring slightly later (z~1060) than photon decoupling (z~1090) because there are so few baryons relative to the number of photons.

Since the scale of these oscillations can be measured at recombination, BAO is considered a "standard ruler", meaning it has a known length that can be used to determine the angular diameter distance D_A. These fluctuations have evolved, and we can observe BAO at low redshifts in the distribution of galaxies.

The total neutrino mass and BAO

The BAO peak of the galaxy correlation function,
is one of the prominent observables in present day cosmology,
and is very sensitive to massive neutrinos.

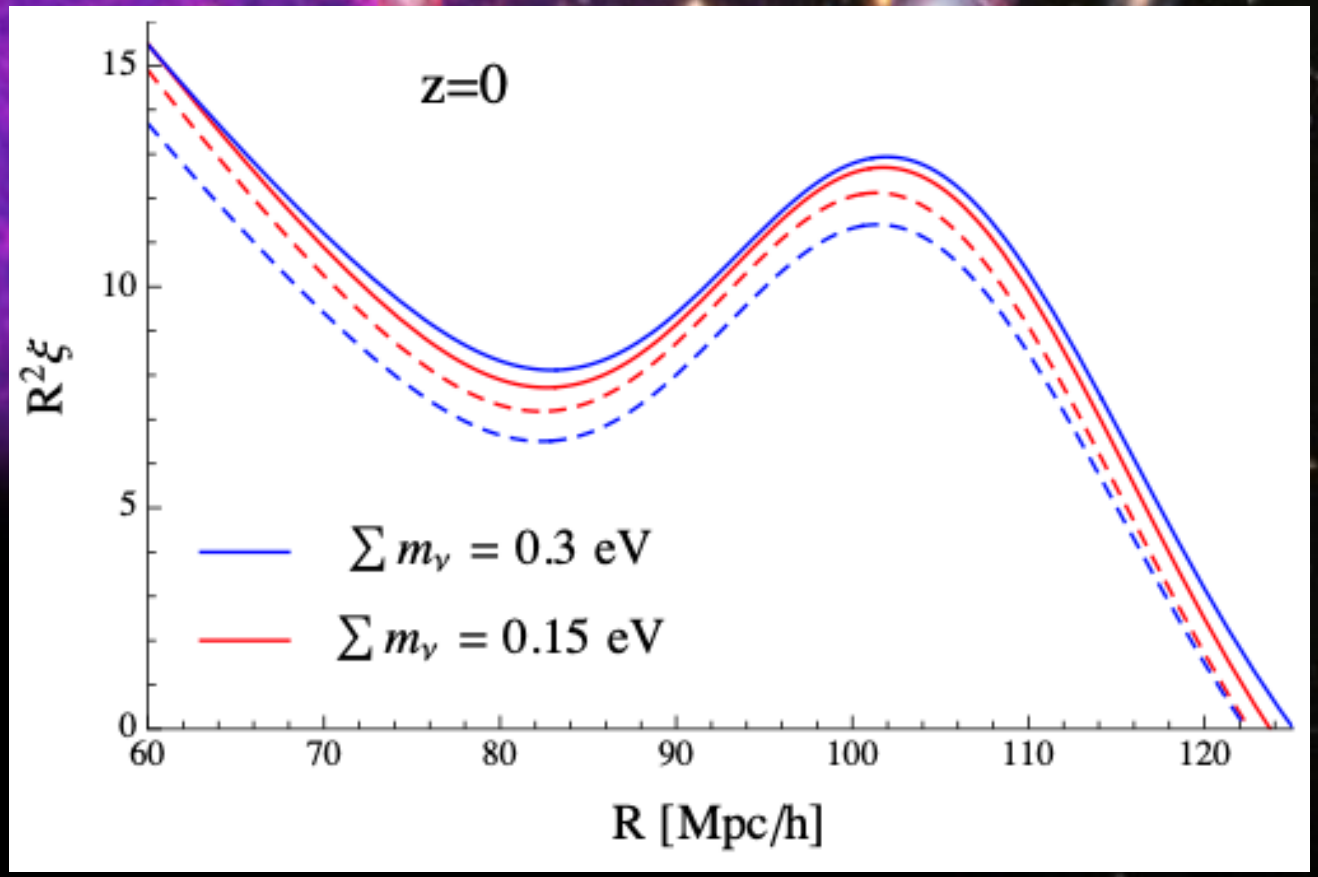

Peloso et al., *JCAP* 07 (2015) 001

The total neutrino mass and BAO

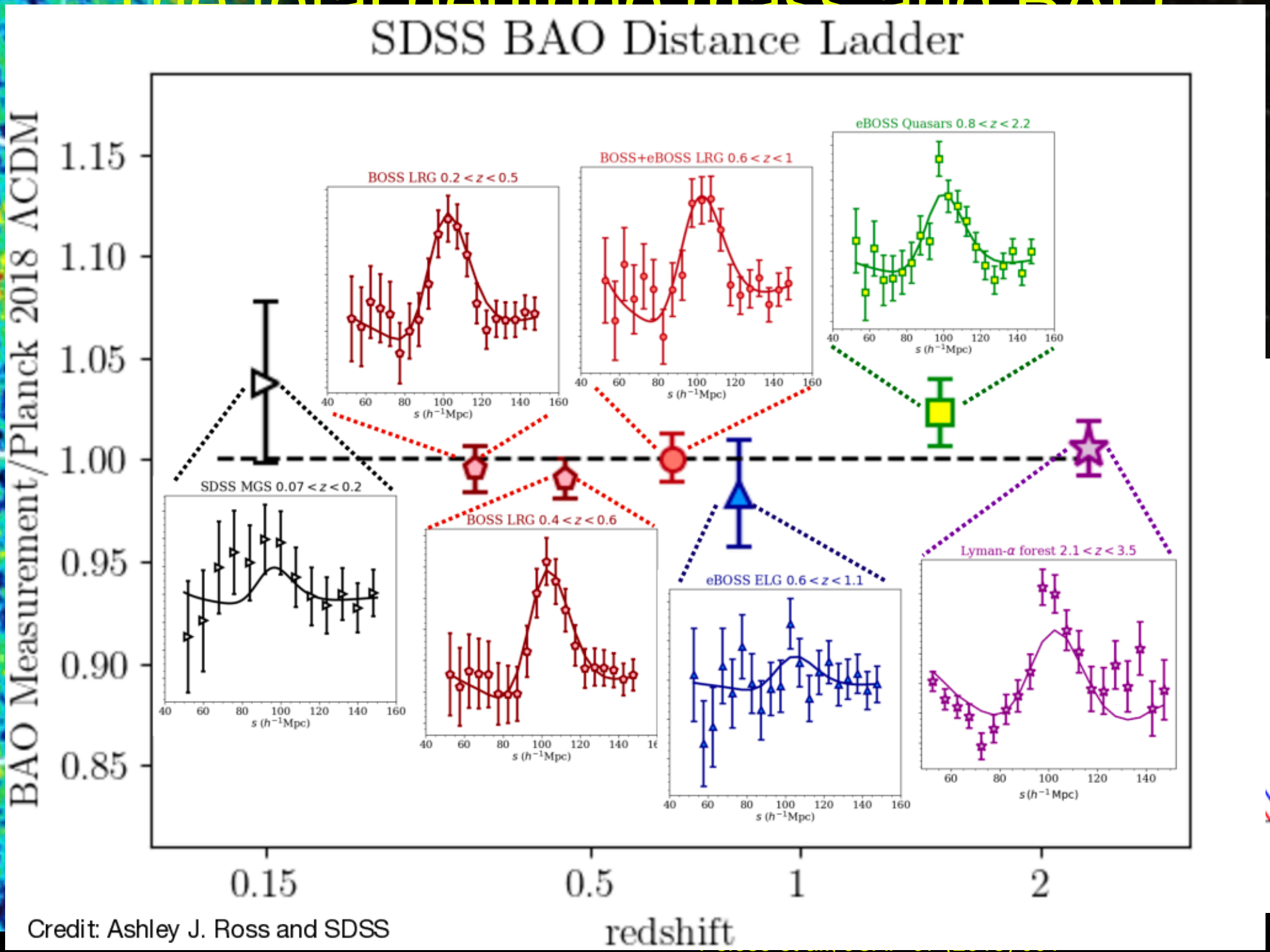

The total neutrino mass and BAO

Planck 2018, Aghanim et al., arXiv:1807.06209 [astro-ph.CO]

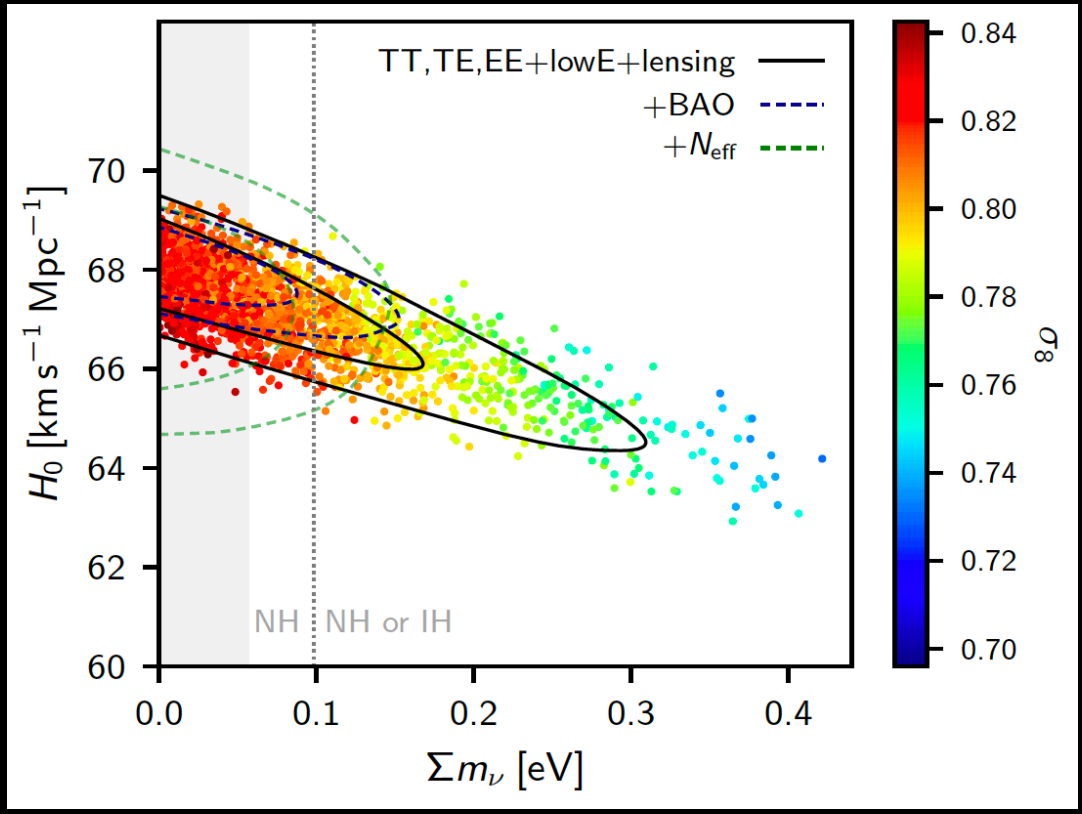

$\sum m_\nu < 0.13$ eV (95 %, *Planck* TT,TE,EE+lowE +BAO),

The inclusion of additional low redshift probes is mandatory in order to sharpen the CMB neutrino bounds. The most stringent bound is obtained when adding the BAO data that are directly sensitive to the free-streaming nature of neutrinos. Actually, the geometrical information they provide helps in breaking the degeneracies among cosmological parameters.

CMB constraints on the neutrino effective number and the total neutrino mass

$$\left.\begin{aligned} N_{\rm eff} &= 2.96^{+0.34}_{-0.33}, \\ \sum m_\nu &< 0.12 \text{ eV}, \end{aligned}\right\} \quad 95\,\%,\ \textit{Planck}\ \text{TT,TE,EE+lowE +lensing+BAO.}$$

Planck 2018, Aghanim et al., arXiv:1807.06209 [astro-ph.CO]

When varying Neff, the bound on the total neutrino mass remains unchanged, and the neutrino effective number is entirely consistent with its standard value of 3.044. These constraints remain very close to those found in 7-parameter models, indicating that the data clearly distinguish between the physical effects resulting from the inclusion of these two parameters.

The total neutrino mass and RSD

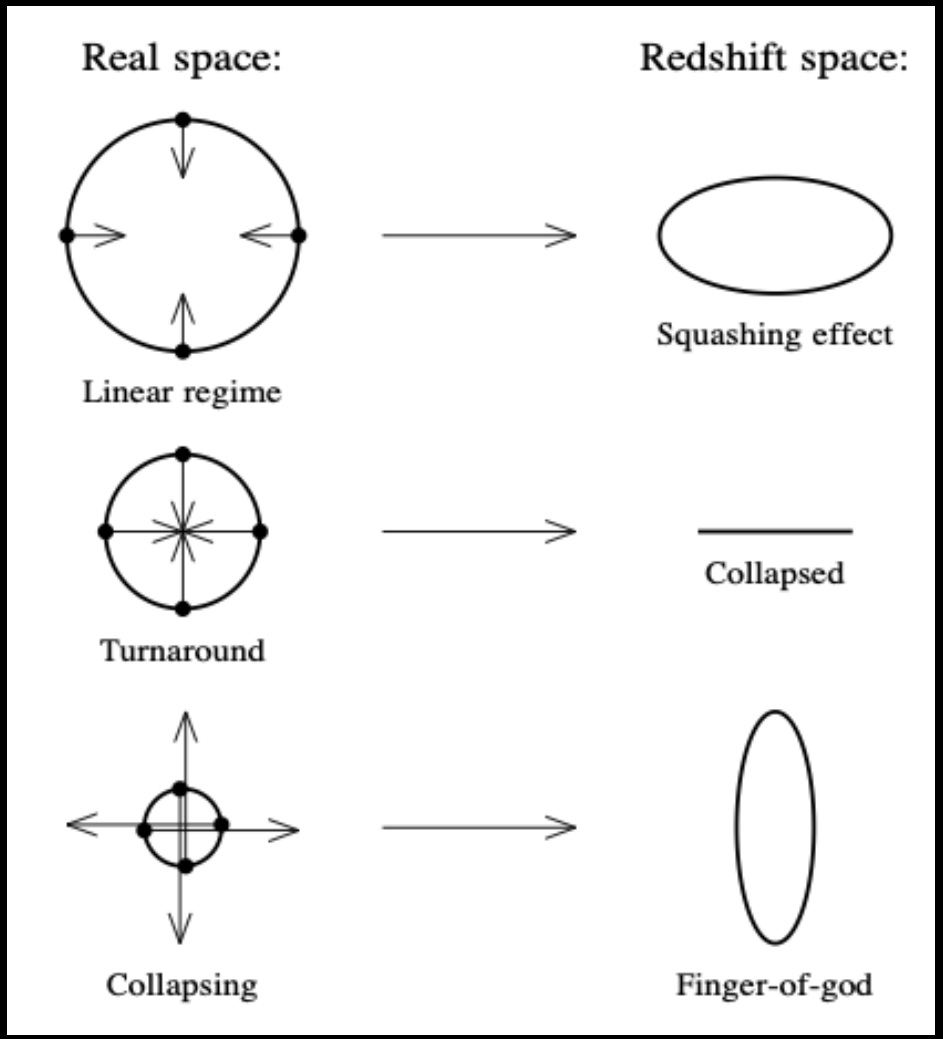

Hamilton, astro-ph/9708102 [astro-ph]

Analysing the clustering in the redshift space, we can study the Redshift Space Distortions (RSD). We will have a reduction or increase of the growth of structure along the radial direction, because of the peculiar velocities (anisotropic clustering).

Although the BAO shells are spherical in real space, distances obtained in redshift space contain contributions from peculiar velocities of the galaxies, and therefore the reconstructed distances suffer from distortions along the radial direction.

At large scales, the peculiar velocity of an infalling shell is small compared to its radius, and the shell appears squashed.

At smaller scales, the spatial distribution of galaxies appears to be elongated due to their velocity dispersion along the line of sight, producing the fingers-of-god.

Redshift Space Distortions

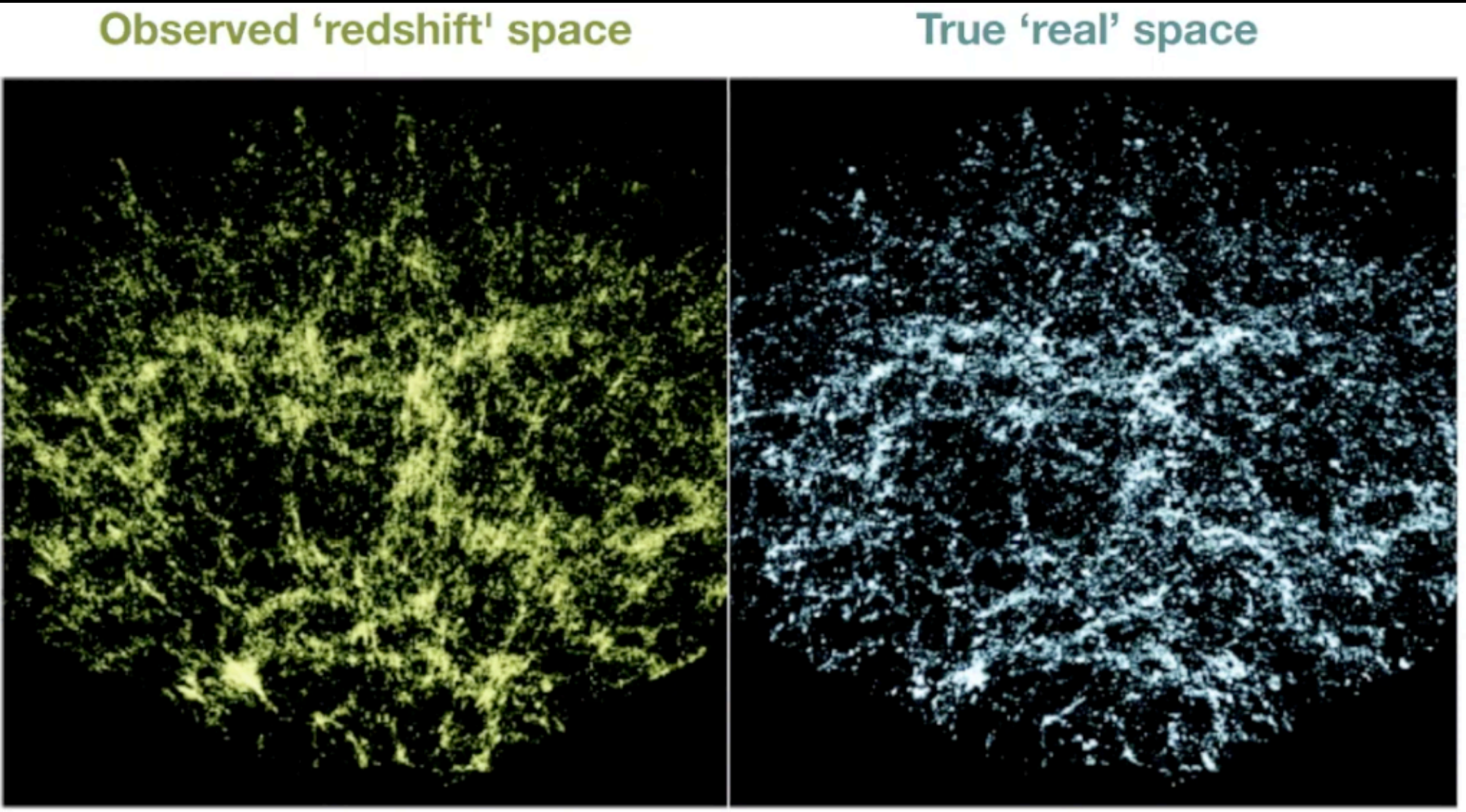

slide from Héctor Gil-Marín

The total neutrino mass and RSD

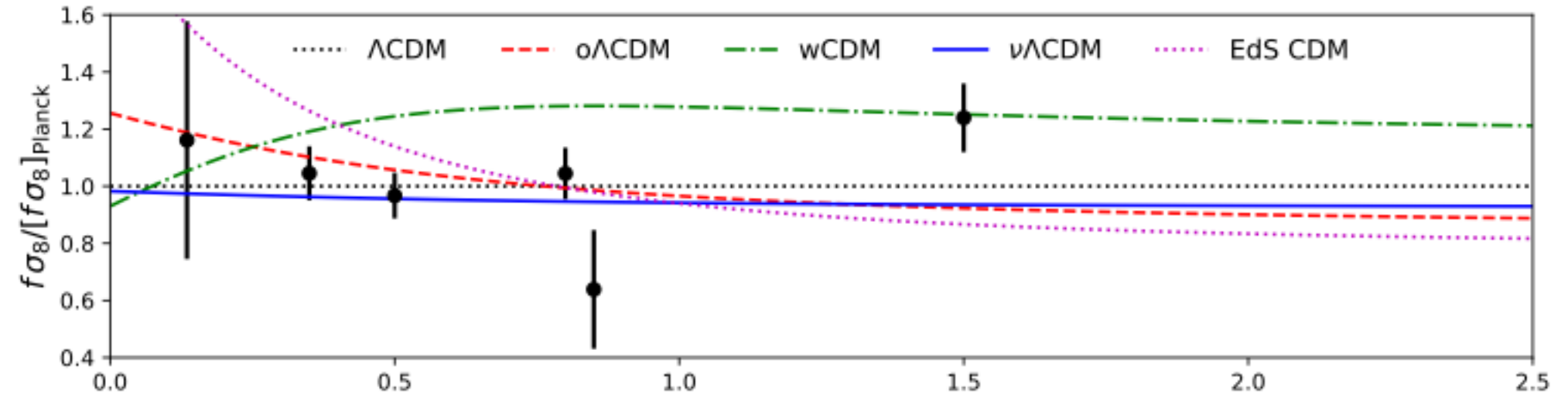

eBOSS collaboration, Alam et al., *Phys.Rev.D* 103 (2021) 8, 083533

This RSD effect modifies the galaxy power spectrum
and allows for an extraction of the product of the growth rate of structure (f) times
the clustering amplitude of the matter power spectrum (σ_8), the well-known $f\sigma_8$ observable.

We can see in the figure that massive neutrinos prefer a lower value for the $f\sigma_8$ data.

The total neutrino mass and RSD

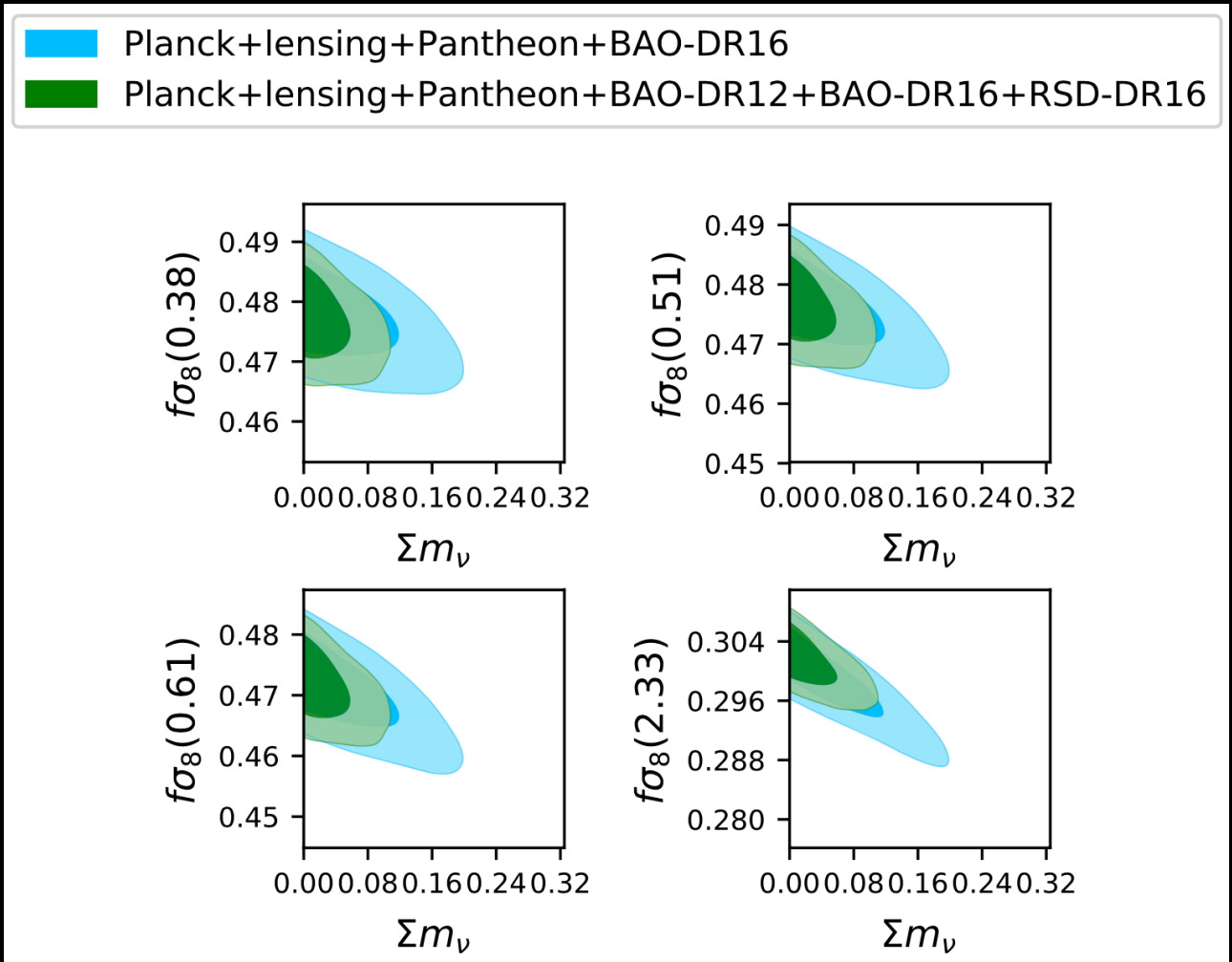

We can see in the figure that massive neutrinos prefer a lower value for the $f\sigma_8$ data.

Di Valentino et al., *Phys.Rev.D* 104 (2021) 8, 083504

The total neutrino mass and RSD

Constraints at 95% CL

Planck+lensing +Pantheon	Σm_ν [eV]
+ DR12 *BAO only*	< 0.116
+ DR12 *BAO+RSD*	< 0.118
+ DR16 *BAO only*	< 0.158
+DR16 *BAO+RSD*	< 0.101
+DR12 *BAO only* + DR16 *BAO only*	< 0.121
+DR12 *BAO only* + DR16 *BAO+RSD*	< 0.0866
+DR12 *BAO+RSD* + DR16 *BAO only*	< 0.125
+DR12 *BAO+RSD* + DR16 *BAO+RSD*	< 0.0934

When we add the latest RSD from eBOSS DR16 LRGs and QSOs samples to Planck+lensing+SNIa data obtain stronger constraints on the total neutrino mass.

Di Valentino et al., *Phys.Rev.D* 104 (2021) 8, 083504

The total neutrino mass and RSD

Constraints at 95% CL

Planck+lensing +Pantheon	Σm_ν [eV]
+ DR12 *BAO only*	< 0.116
+ DR12 *BAO+RSD*	< 0.118
+ DR16 *BAO only*	< 0.158
+DR16 *BAO+RSD*	< 0.101
+DR12 *BAO only* + DR16 *BAO only*	< 0.121
+DR12 *BAO only* + DR16 *BAO+RSD*	< 0.0866
+DR12 *BAO+RSD* + DR16 *BAO only*	< 0.125
+DR12 *BAO+RSD* + DR16 *BAO+RSD*	< 0.0934

When we add the latest RSD from eBOSS DR16 LRGs and QSOs samples to Planck+lensing+SNIa data obtain stronger constraints on the total neutrino mass.

The most constraining upper bounds $\Sigma m_\nu < 0.087$ eV at 95% CL is obtained when this dataset is combined with the BAO BOSS DR12 LRG measurements.
In other words, cosmological measurements prefer values of Σm_ν as close to zero as possible, disfavouring the minimal allowed value for IO at more than 2σ, but also the NO at more than 68% CL ($\Sigma m_\nu < 0.037$ eV).

Di Valentino et al., *Phys.Rev.D* 104 (2021) 8, 083504

New DESI BAO measurements

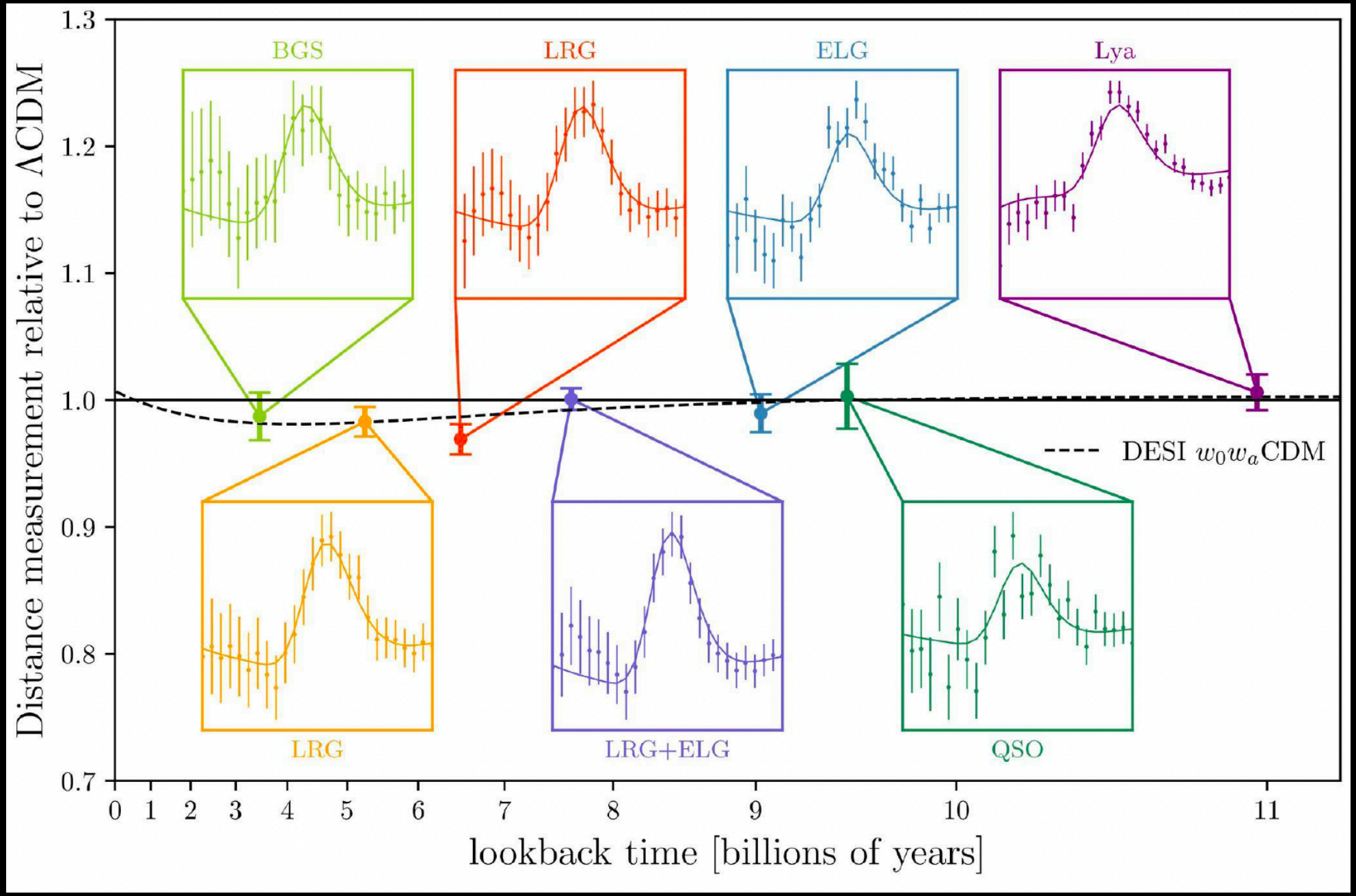

Credit: Arnaud de Mattia, CEA Saclay

New DESI BAO measurements

DESI collaboration, arXiv:2404.03002

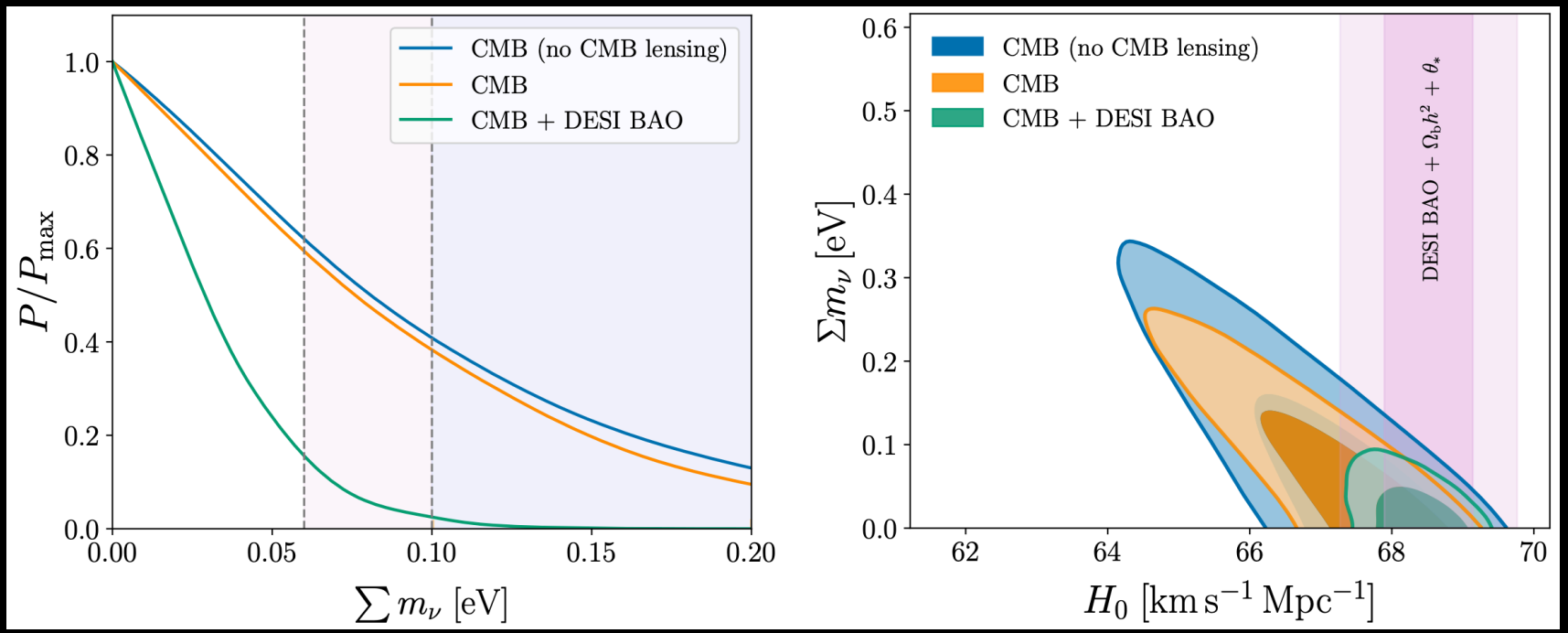

$$\sum m_\nu < 0.072\,\mathrm{eV} \quad (95\,\%,\ \mathrm{DESI\ BAO{+}CMB})$$

The improvement relative to CMB-only constraints is driven primarily by the tighter constraints on H0 obtained from BAO.

Tightest neutrino mass constraints

Wang, Mena, Di Valentino and Gariazzo, arXiv:2405.03368

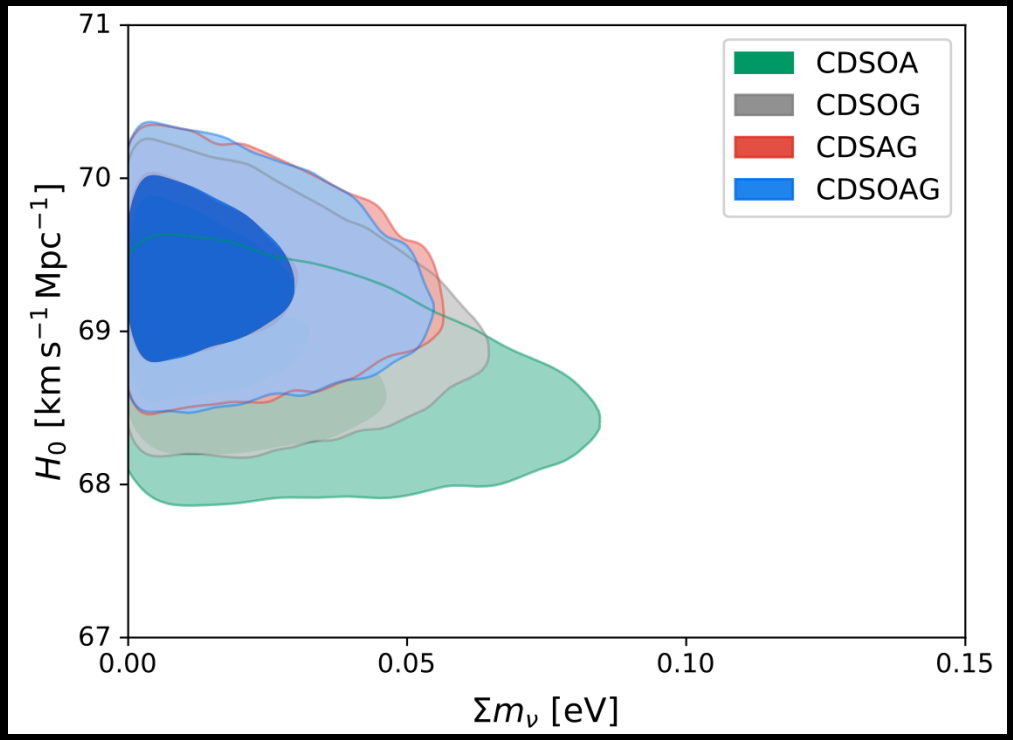

The tightest bound we find here is $\Sigma m_\nu < 0.043$ eV at 95% CL after combining Planck CMB with DESI BAO, Type Ia Supernovae, Gamma Ray Bursts, cosmic chronometers, and galaxy clusters, showing a clear tension between neutrino oscillation results and cosmological analyses.

Neutrino mass ordering

At this point, we should discuss mass ordering.

Even though the absolute masses of neutrinos ν are unknown, lower bounds on the total neutrino mass are established through global analyses of oscillation data. These analyses provide the best-fit values for the standard model mass splitting.

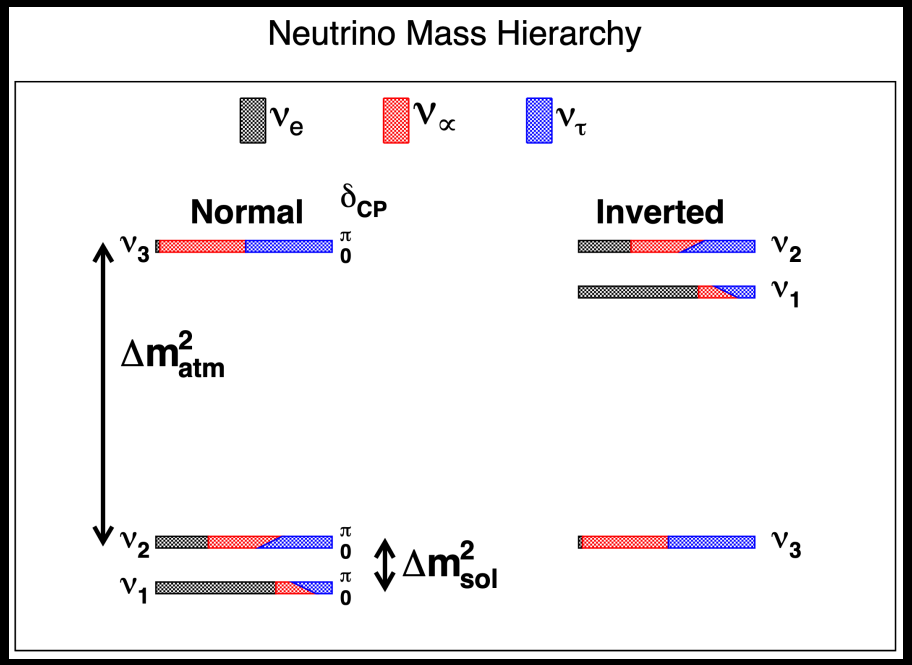

Qian and Vogel, arXiv:1505.01891

By setting the lightest neutrino mass to zero, we can determine the lower bounds on the total neutrino mass for the normal or inverted ordering:

$$\sum m_\nu > \begin{cases} (0.0591 \pm 0.00027)\,\text{eV} & (\text{NO}) \\ (0.0997 \pm 0.00051)\,\text{eV} & (\text{IO}) \end{cases}$$

Neutrino mass ordering

However, cosmological probes are sensitive to the total neutrino mass, but not to individual masses.

Typically, the neutrino masses are assumed to be degenerate ($m_\nu = m \geq 0$) and the lower bound of the total neutrino mass ($\Sigma m_\nu = m_1 + m_2 + m_3$) is set to 0, which is in the unphysical region.

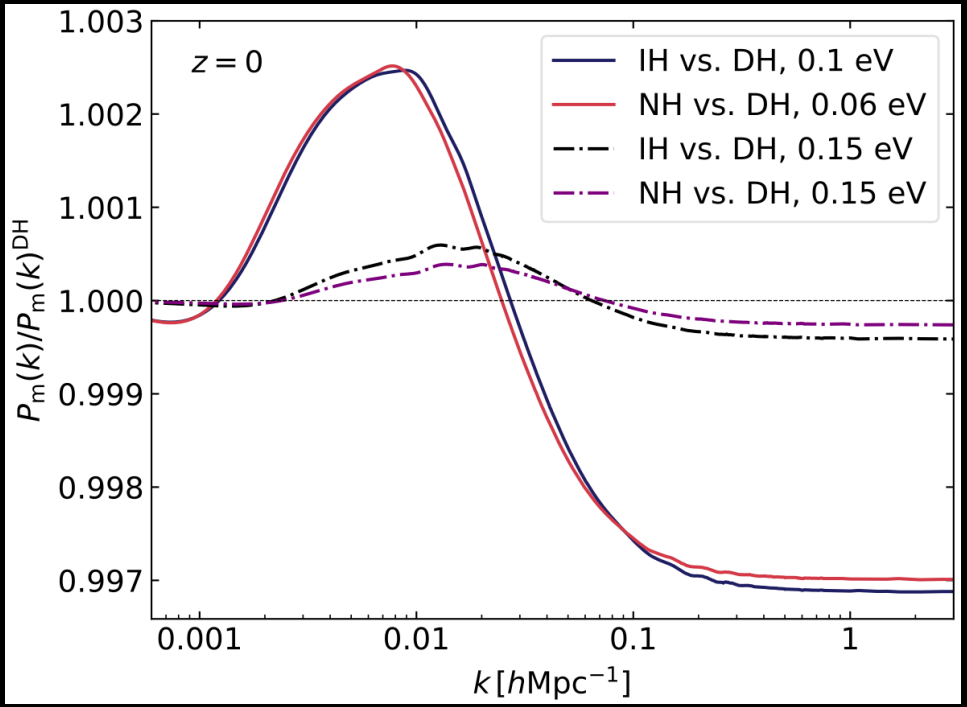

Archidiacono et al. arXiv:2003.03354

Although the assumption of degenerate neutrino ordering is incorrect and causes changes in cosmological observables compared to the actual normal or inverted neutrino ordering, the induced changes are so small that they will remain undetectable, even with extremely optimistic assumptions about future data.

Neutrino mass ordering

However, the upper bounds obtained are strongly dependent on the choice of the prior for Σm_ν used in the cosmological analysis.

$$\sum m_\nu < 0.072\,\mathrm{eV} \quad (95\,\%,\ \mathrm{DESI\ BAO{+}CMB})$$

DESI collaboration, arXiv:2404.03002

$$\sum m_\nu < 0.113\,\mathrm{eV} \quad (95\,\%,\ \mathrm{DESI\ BAO{+}CMB};\ \textstyle\sum m_\nu > 0.059\,\mathrm{eV}),$$

$$\sum m_\nu < 0.145\,\mathrm{eV} \quad (95\,\%,\ \mathrm{DESI\ BAO{+}CMB};\ \textstyle\sum m_\nu > 0.10\ \mathrm{eV}).$$

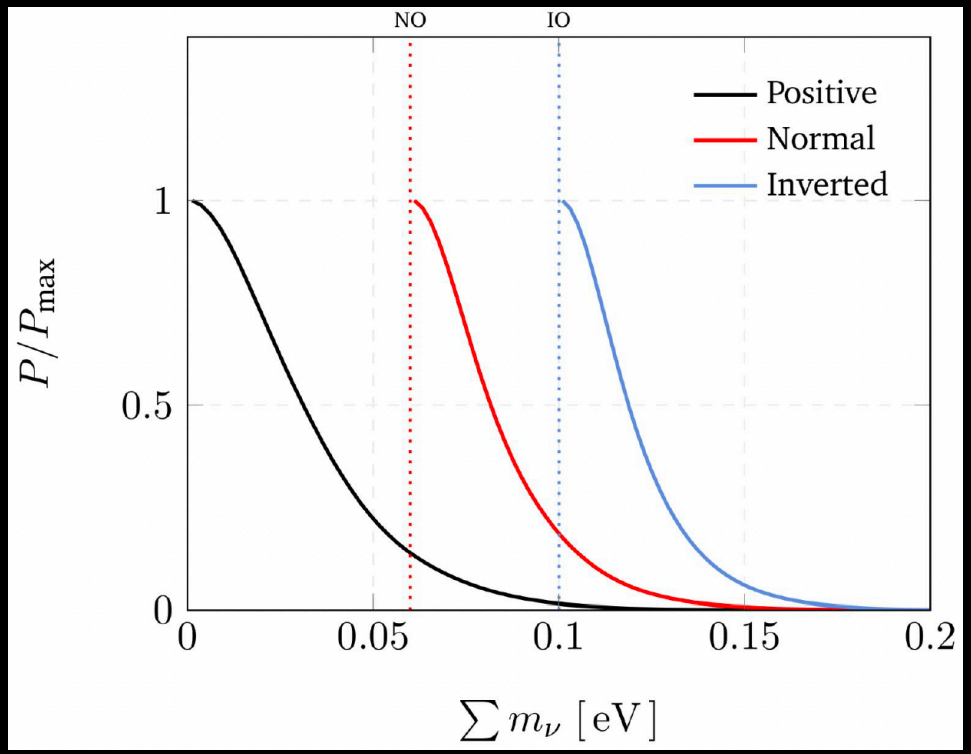

Credit Figure: Willem Elbers

Neutrino mass ordering

Dataset combination	ΛCDM+$\sum m_\nu$	
	$\sum m_\nu$ (eV)	$B_{\rm NO,IO}$
baseline (CMB + DESI)	< 0.072	8.1
baseline + SNeIa	< 0.081	7.0
baseline + CC	< 0.073	7.3
baseline + SDSS	< 0.083	6.8
baseline + SH0ES	< 0.048	47.8
baseline + XSZ	< 0.050	46.5
baseline + GRB	< 0.072	8.7
aggressive combination (baseline + SH0ES + XSZ)	< 0.042 eV	72.6
CMB (with ACT "extended" likelihood)+DESI	< 0.072	8.0
CMB+DESI (with 2020 `HMCode`)	< 0.074	7.5
CMB (with `v1.2` ACT likelihood)+DESI	< 0.082	7.4

Jiang et al., arXiv:2407.18047

95% CL upper limits on the sum of the neutrino masses Σm_ν and Bayes factor for normal ordering versus inverted ordering $B_{NO,IO}$ (with values of $B_{NO,IO} > 1$ indicating a preference for the normal ordering) in light of different dataset combinations.

Constraints on the total neutrino mass

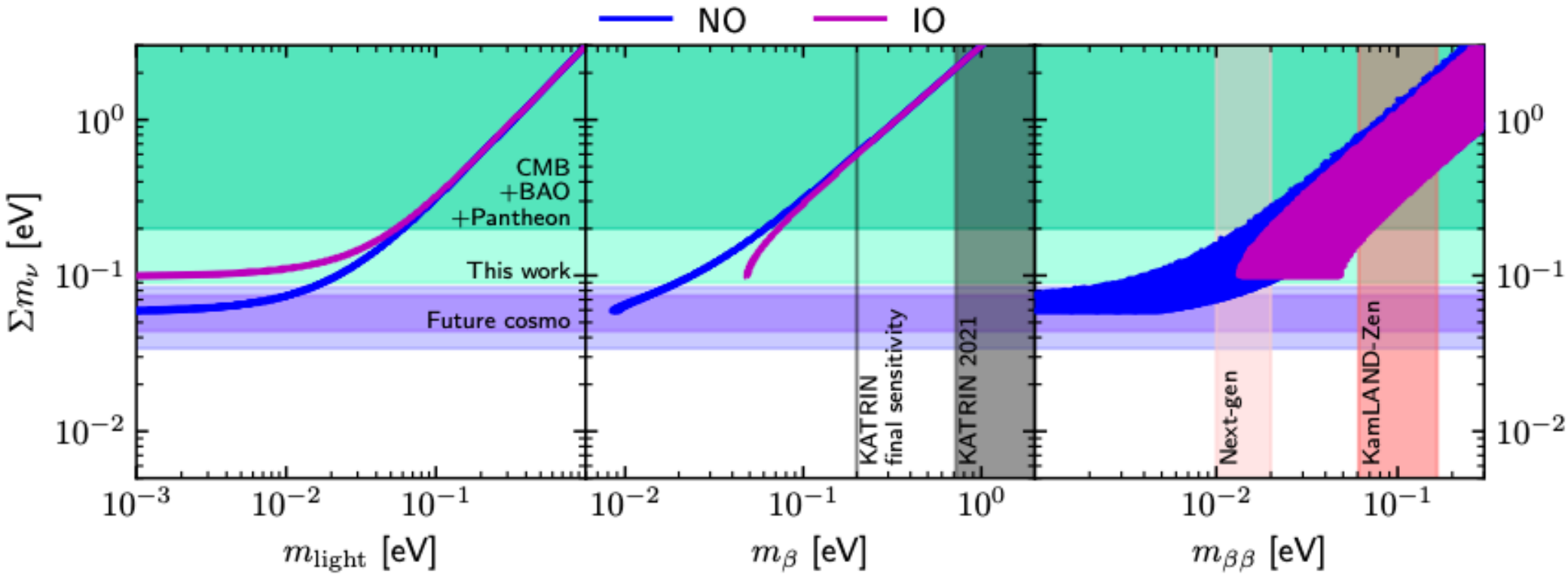

Here we illustrate the theoretical expectations within each mass ordering for the three observables of neutrino masses: beta-decay (mβ), neutrinoless double beta decay mββ and the cosmological measured quantity Σmν.
The light green horizontal band represents the most constraining bound before DESI, which is $\Sigma m_\nu < 0.087$ eV at 95% CL.
This very tight limit has crucial implications for direct neutrino mass laboratory searches, suggesting that they are not expected to detect any signal.

Di Valentino et al., *Phys.Rev.D* 104 (2021) 8, 083504

Constraints on the total neutrino mass

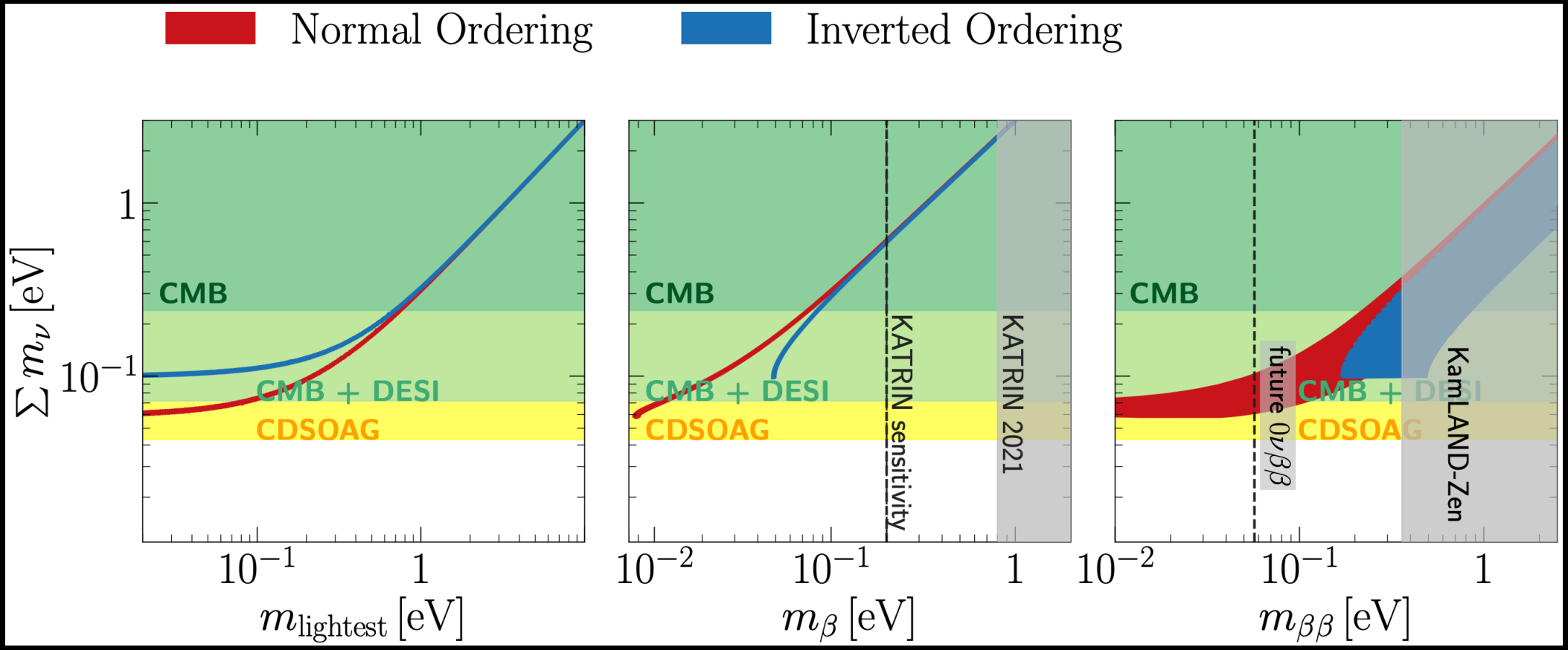

The light green horizontal band represents the most constraining bound after DESI, which is $\Sigma m_\nu < 0.072$ eV at 95% CL, while the yellow band indicates the tightest bound available in the literature after combining with other cosmological probes, which is $\Sigma m_\nu < 0.043$ eV at 95% CL, significantly below the minimal value allowed by oscillation data.

Wang, Mena, Di Valentino and Gariazzo, arXiv:2405.03368

Constraints on the total neutrino mass

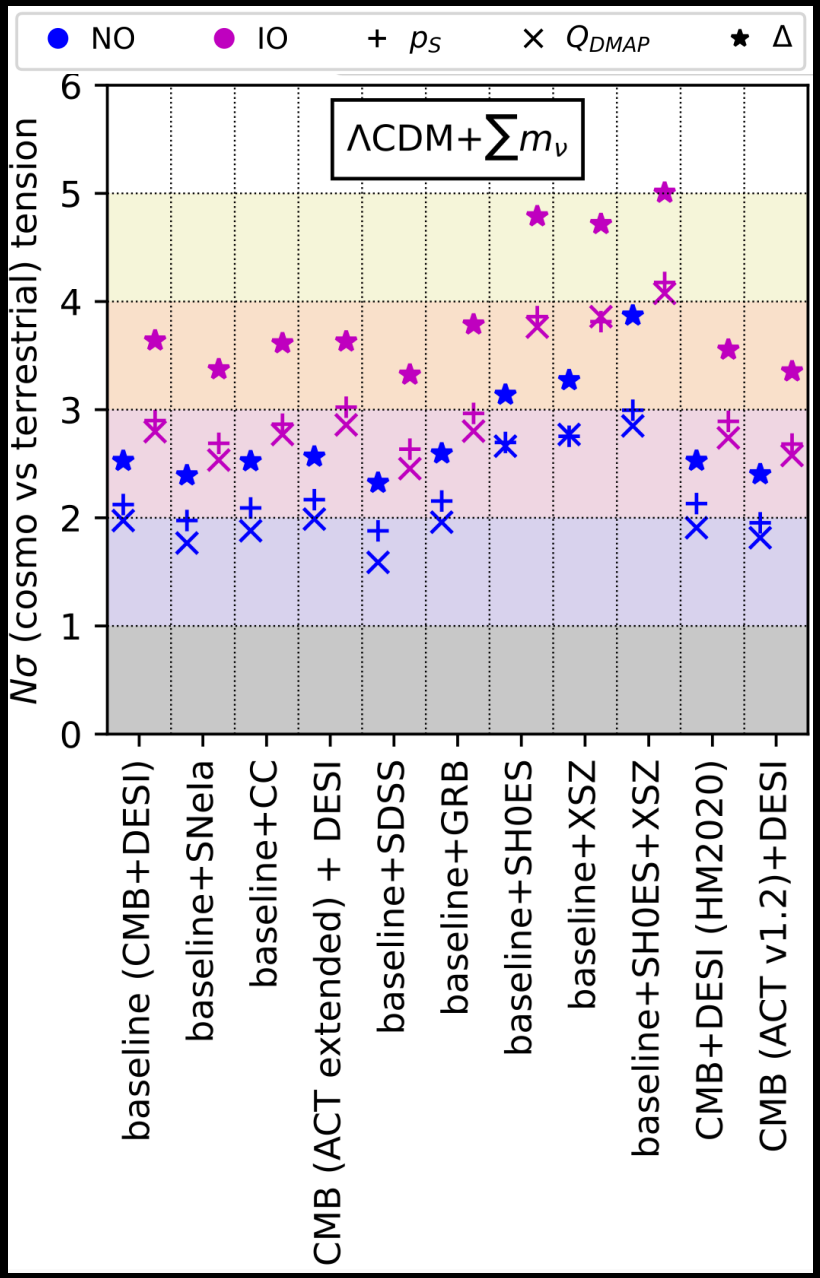

Jiang et al., arXiv:2407.18047

This is the quantification of the tension between cosmology and terrestrial constraints on the masses and mass splittings.
Here we display the tension in equivalent number of standard deviations for different dataset combinations, and for three different test statistics.
We can see that the level of tension between cosmological and terrestrial experiments for NO is around 2.5σ, while for IO increase to ≈ 3.5σ.

How much neutrinos constraints could be improved in the future?

Timeline of current and future ground-based CMB experiments

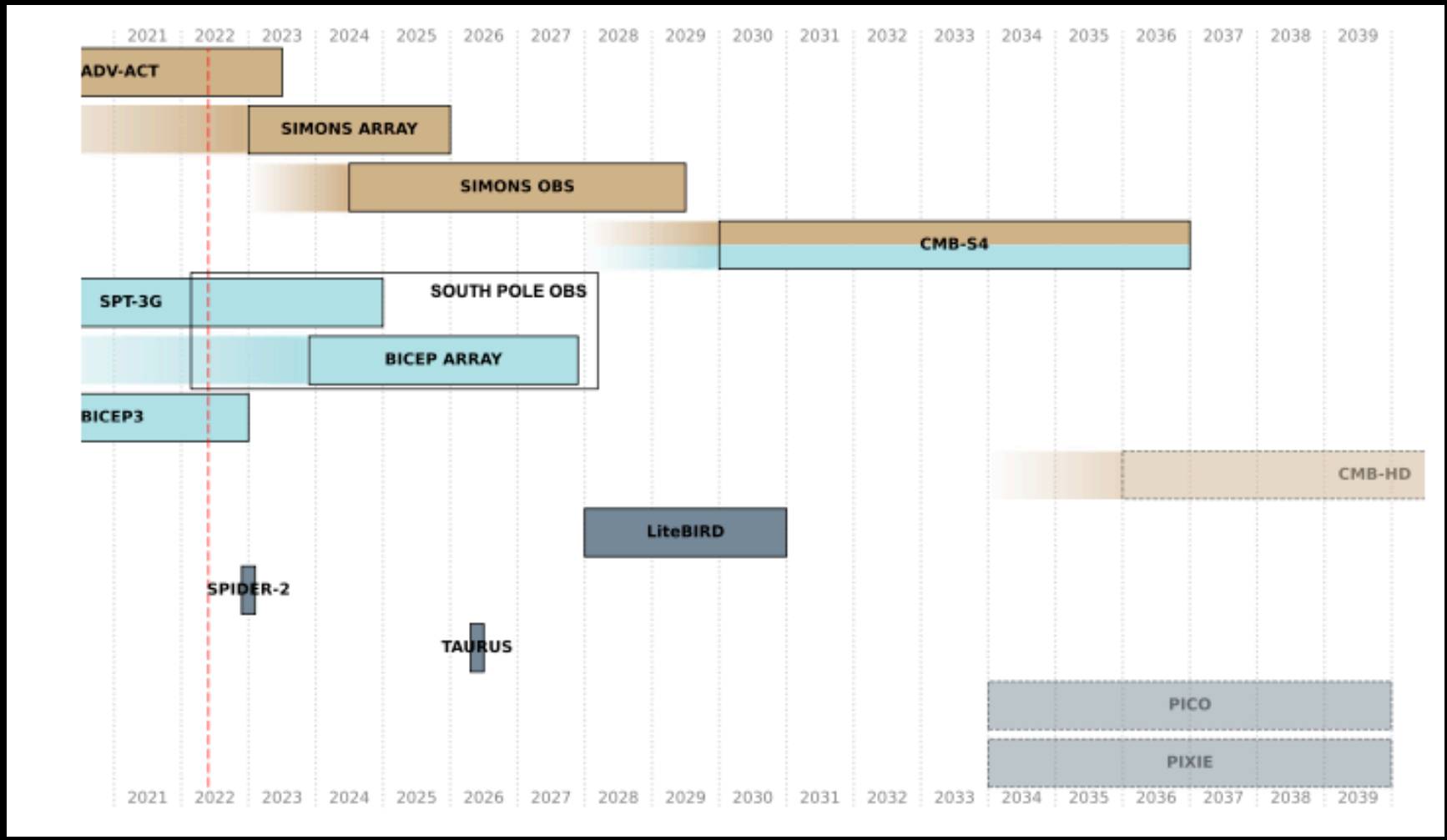

Chang et al. 2022, SNOWMASS, arXiv:2203.07638

Ground-based CMB telescopes are at the moment the proposals with the highest probability of being realised. However, they needs large angular scale measurements (as Planck or future experiments) and a perfect a priori knowledge of the foregrounds.

Importance of the optical depth

Large angular scale measurements of the CMB are crucial for accurately determining the optical depth, and, as a consequence, the total neutrino mass.

The first stars ended the dark ages of the Universe thanks to their UV emissions, which gradually ionized the neutral hydrogen, that made the Universe transparent after the epoch of recombination.
This process is known as reionization.
The exact timing of cosmic reionization remains uncertain.
However, cosmological measurements can constrain the optical depth to reionization τ, which can be related to the redshift of reionization (zre) under the assumption of instantaneous process.

During the cosmic reionization, CMB photons undergo Thomson scattering off free electrons at scales smaller than the horizon size.
As a result, they deviate from their original trajectories, reaching us from a direction different from the one set during recombination.
Similarly to recombination, this introduces a novel 'last scattering' surface at later times and produces distinctive imprints in the angular power spectra of temperature and polarization anisotropies.

Importance of the optical depth

A well-known effect of reionization is the enhancement of the CMB polarization spectrum at large angular scales,
along with a suppression of temperature anisotropies at smaller scales ($A_s e^{-2\tau}$).

The distinctive polarization bump produced by reionization on large scales dominates the signal in the EE spectrum, with its amplitude strongly dependent on the total integrated optical depth to reionization:

$$\tau = \sigma_{\rm T} \int_0^{z_{\rm rec}} dz\, \bar{n}_e(z)\, \frac{dr}{dz},$$

where σ_T is the Thomson scattering cross-section,
$\bar{n}_e(z)$ is the proper number density of free electrons at redshift z,
and dr/dz is the line-of-sight proper distance per unit redshift.
Therefore, precise observations of E-mode polarization on large scales are crucial.

Importance of the optical depth

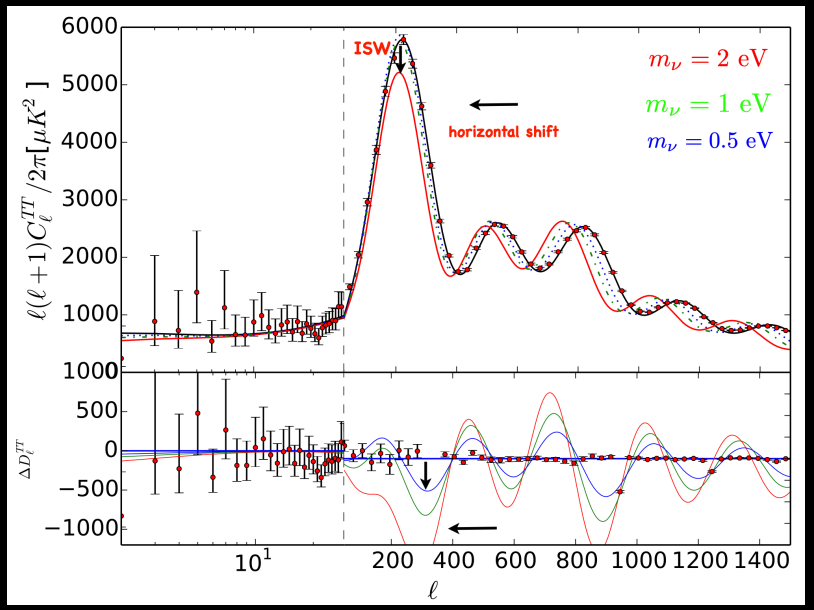

Credit figure: Olga Mena

There is a well-known degeneracy between τ and Σmν.
Considering CMB data only,
particularly focusing on the TT spectrum,
an increase in Σmν results in a suppression of
structure, reducing the smearing of the damping tail.
This suppression effect
can be compensated by an increase in τ.

Since the CMB TT spectrum measures $A_s e^{-2\tau}$,
the value of A_S should also be increased accordingly.
However, A_S determines the overall amplitude
of the matter power spectrum,
which is also affected by massive neutrinos
that reduce small-scale clustering.

By including low-l polarization measurements of τ,
the degeneracy between τ and Σmν will be broken,
allowing for more precise measurements of Σmν.

Simons Observatory

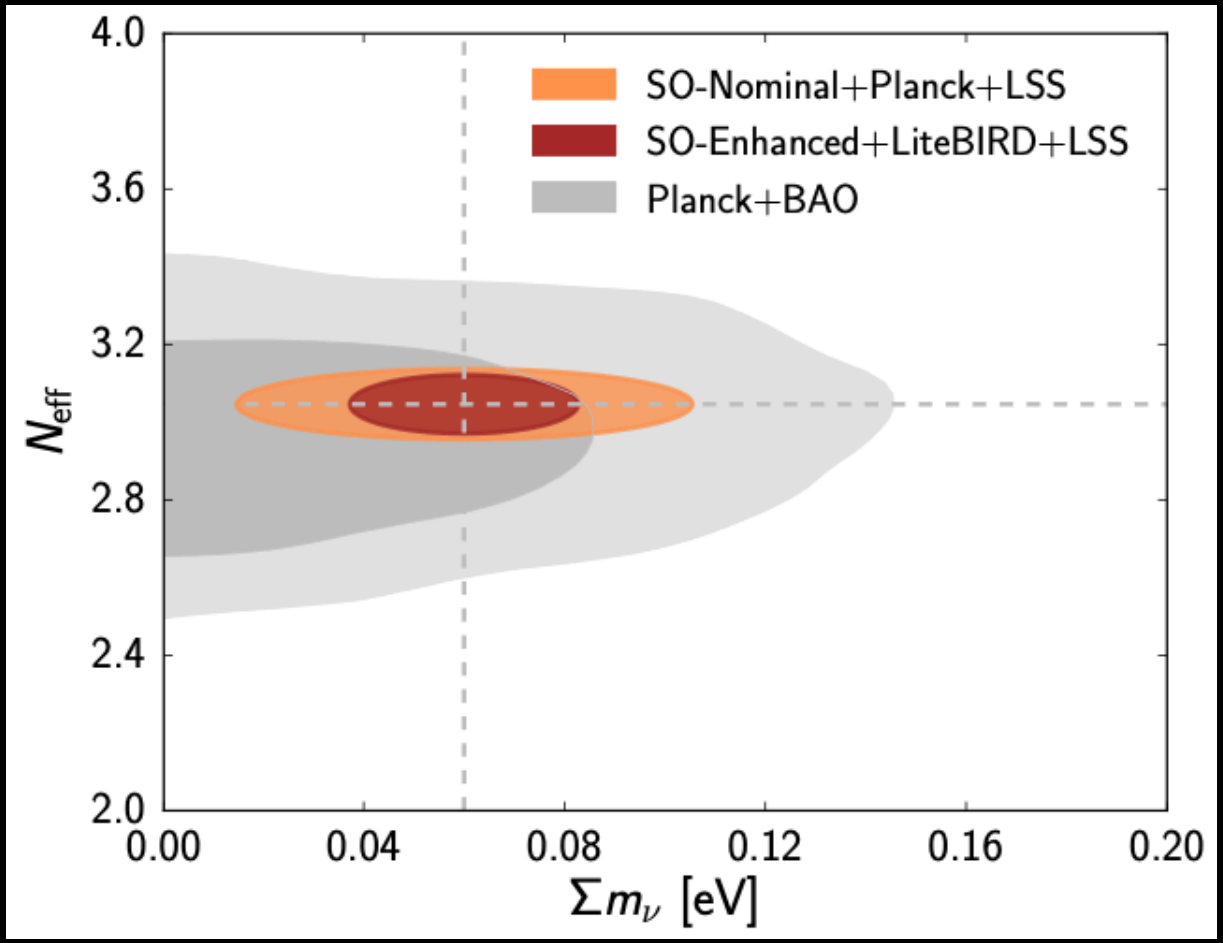

Abitbol et al. 2019, Astro2020, arXiv:1907.08284

The Simons Observatory aims to measure the total neutrino mass σ (∑m_V) = 0.04 eV when combined with DESI BAO and LSST weak lensing data.
When combined with LiteBIRD's future cosmic variance-limited measurements of the optical depth to reionization SO can instead reach σ (∑m_V) = 0.02 eV.
Moreover, SO aims to measure σ (Neff) = 0.07.

CMB-S4

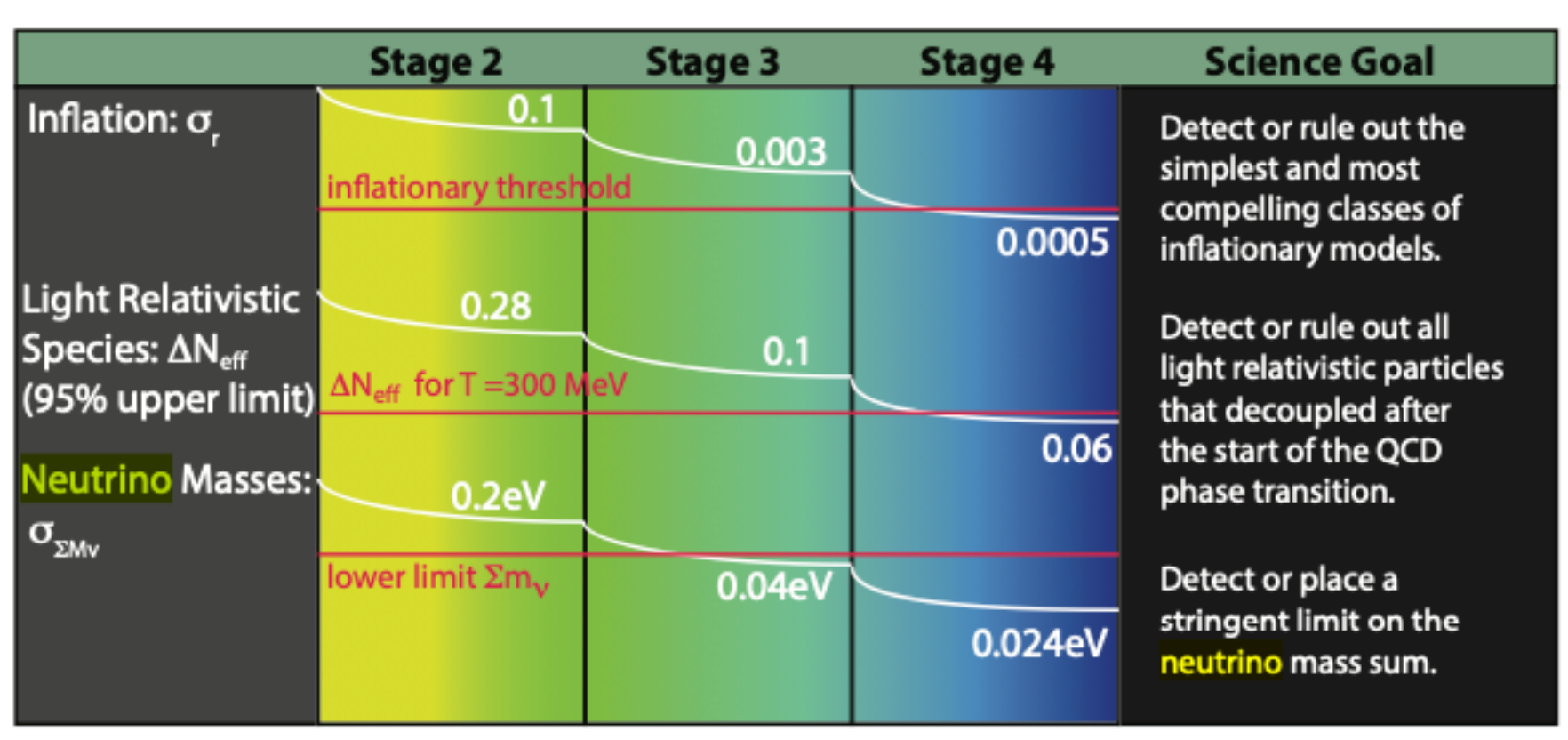

Chang et al. 2022, SNOWMASS, arXiv:2203.07638

CMB-S4 aims to determine N_{eff} with an uncertainty ≤ 0.06 at the 95% confidence level.

When combined with BAO from DESI, and the current measurement of the optical depth from Planck, CMB-S4 measurements of the lensing power spectrum (or cluster abundances) will provide a constraint on the sum of neutrino masses of $\sigma(\sum m_\nu) = 0.024$ eV, and this would improve to $\sigma(\sum m_\nu) = 0.014$ eV with better measurements of the optical depth.

PICO

Hanany et al., NASA PICO collaboration, arXiv:1902.10541.

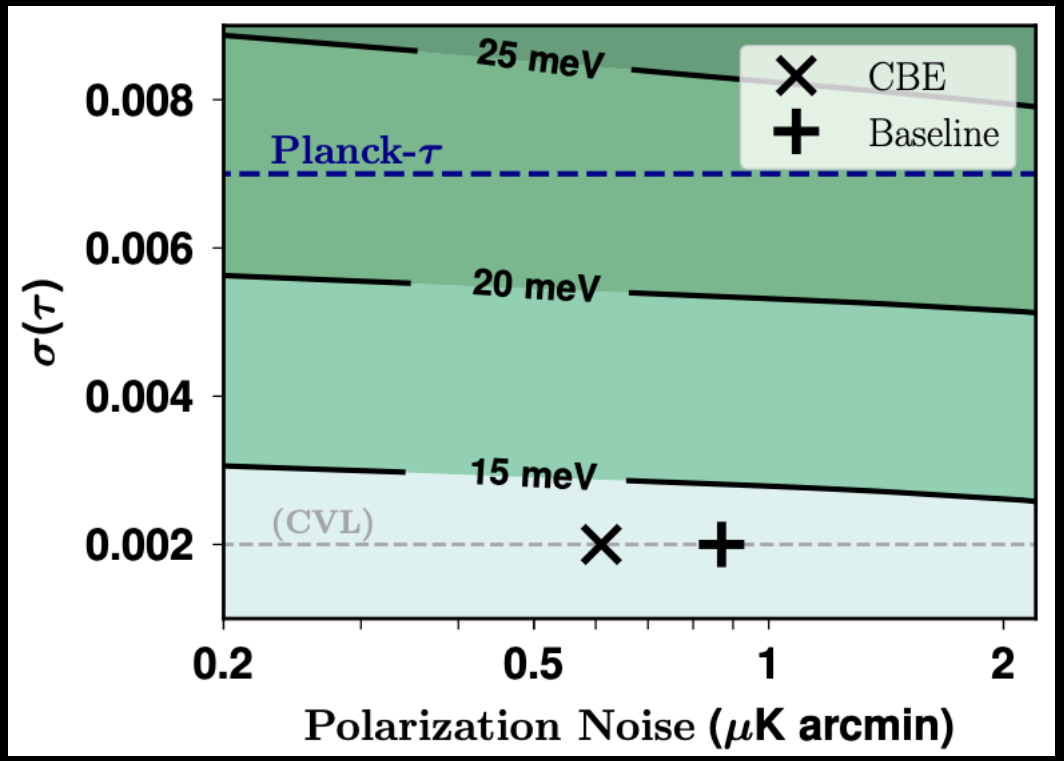

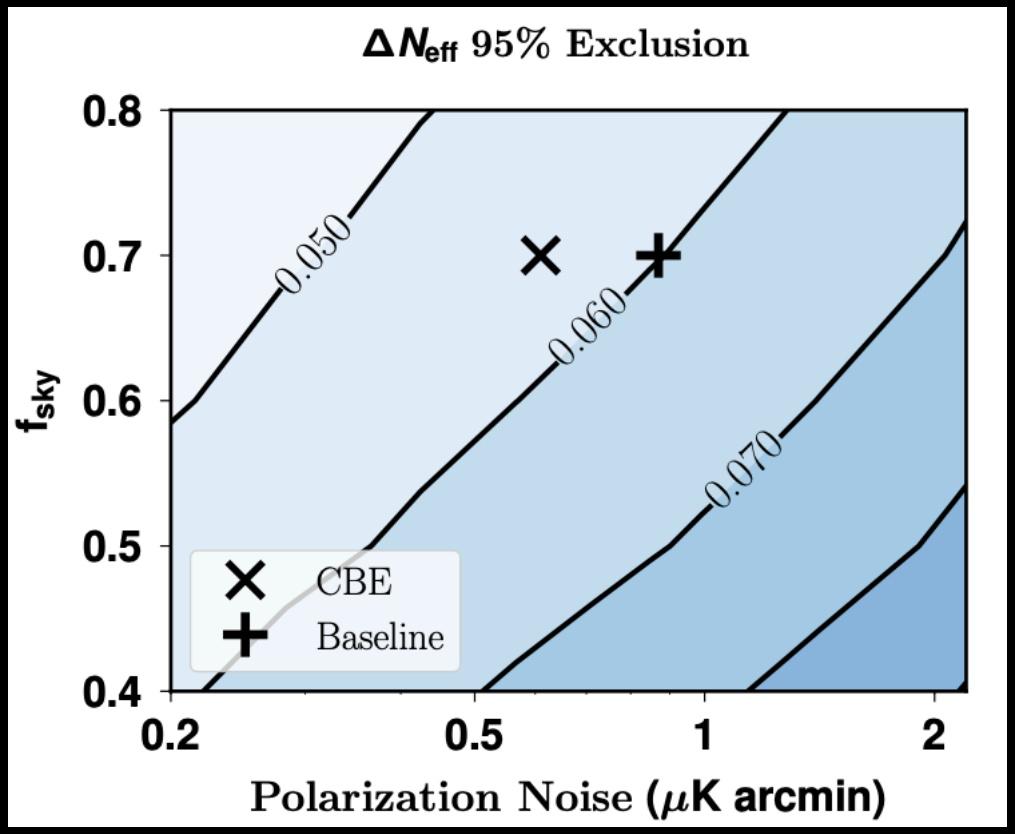

PICO + future BAO (DESI or Euclid) should reach σ ($\sum m_\nu$) = 14 meV, i.e. a 4σ detection of the minimum sum for the NO.

Moreover, it should constrain the constrain $\Delta N_{eff} < 0.06$ at 95% CL.

This is the only instrument that can measure very precisely all these neutrino properties (+ optical depth) with the same single dataset.

CMB-HD

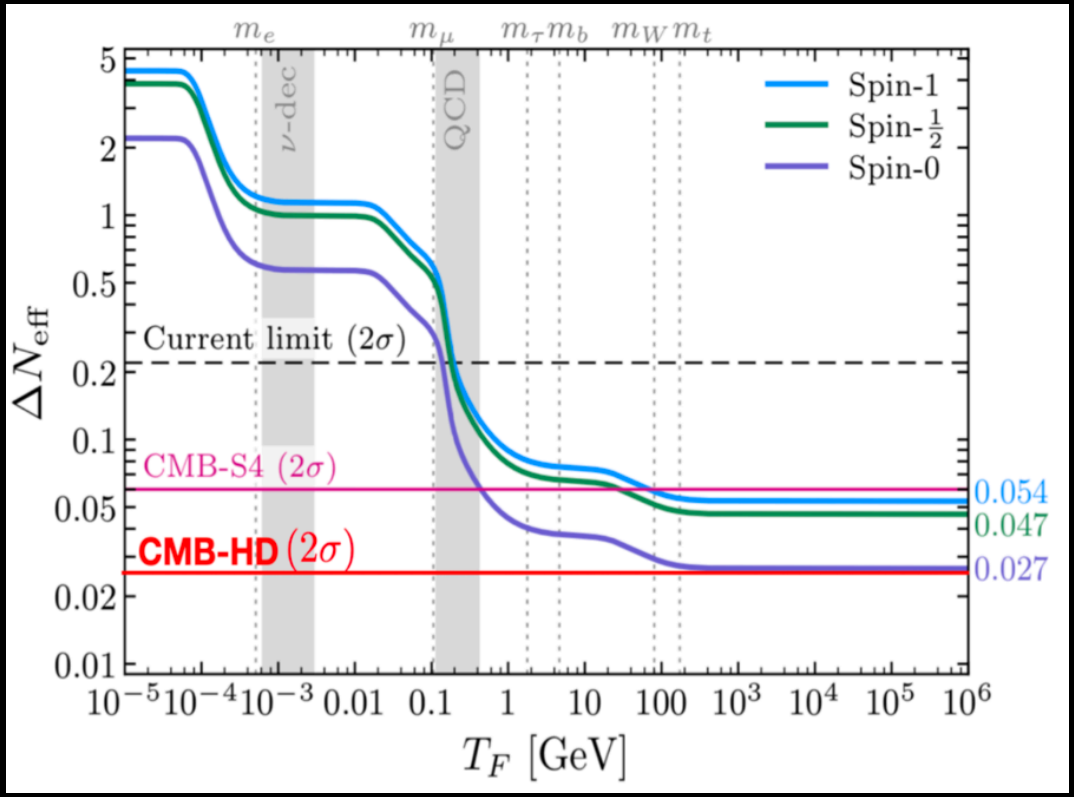

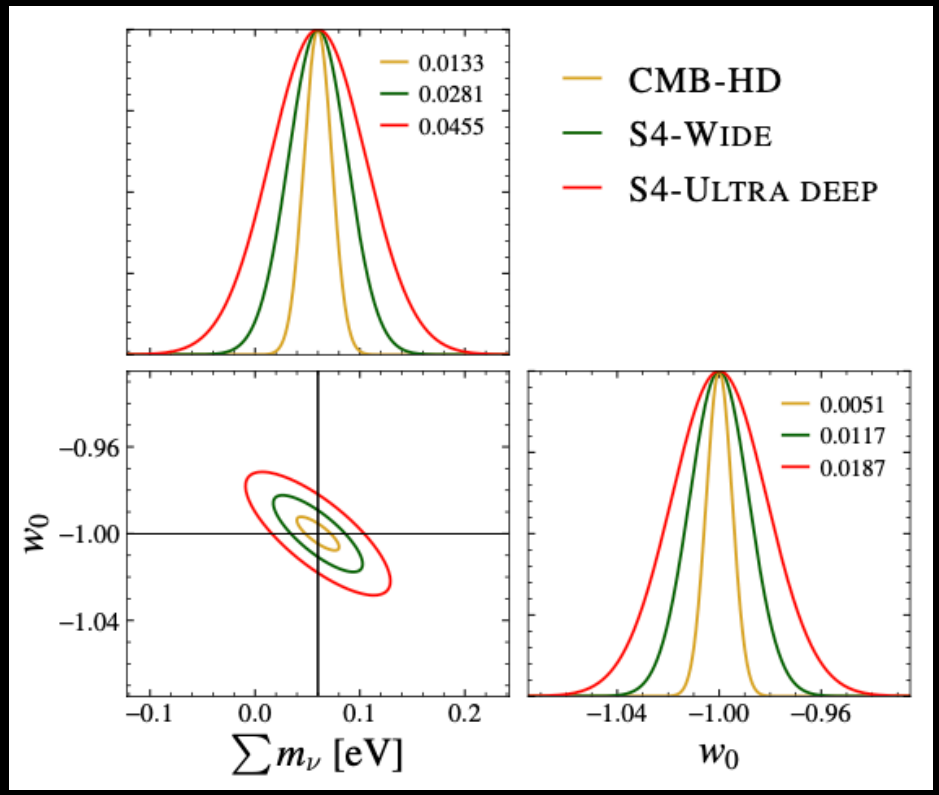

Aiola et al. 2022, SNOWMASS, arXiv:2203.05728

CMB-HD, a futuristic millimetre-wave survey, could achieve an uncertainty on $N_{eff} \sim 0.014$ at the 68% CL and $\sigma(\sum m_\nu) = 0.013$ eV (at least 5σ detection for the sum of the neutrino masses), by measuring the gravitational lensing of the CMB and the thermal and kinetic SZ effect on small scales.

The ΛCDM model

“Cosmologists are often in error but never in doubt”

Lev Landau

All the models are wrong, but some are useful

Out of various cosmological models proposed in literature,
the Lambda cold dark matter (ΛCDM) scenario has been chosen
as the "standard model" because it accurately describes
a wide range of astrophysical and cosmological observations.

However, despite its incredible success,
ΛCDM harbours large areas of phenomenology and ignorance.
For example, it still cannot explain key concepts in our understanding of the structure and evolution of the Universe, at the moment based on
unknown quantities, that are also its largest components.
In addition, their physical evidence comes from cosmological and astrophysical observations only, without strong theoretical motivations.

The ΛCDM model

Three unknown pillars:

- an early stage of accelerated expansion (Inflation) which produces the initial, tiny, density perturbations, needed for structure formation.

- a clustering matter component to facilitate structure formation (Dark Matter),

- an energy component to explain the current stage of accelerated expansion (Dark Energy).

The ΛCDM model

Three unknown pillars:

- an early stage of accelerated expansion (Inflation) which produces the initial, tiny, density perturbations, needed for structure formation.
- a clustering matter component to facilitate structure formation (Dark Matter),
- an energy component to explain the current stage of accelerated expansion (Dark Energy).

In addition, the ΛCDM model is based on the simplest form for these unknown quantities, mostly motivated by computational simplicity, i.e. the theoretical predictions under ΛCDM for several observables are, in general, easier to compute and include fewer free parameters than most other solutions.

The ΛCDM model

Three unknown pillars:

- an early stage of accelerated expansion (Inflation) which produces the initial, tiny, density perturbations, needed for structure formation.
- a clustering matter component to facilitate structure formation (Dark Matter),
- an energy component to explain the current stage of accelerated expansion (Dark Energy).

Specific solutions for ΛCDM:

- Inflation is given by a single, minimally coupled, slow-rolling scalar field;
- Dark Matter is a pressureless fluid made of cold, i.e., with low momentum, and collisionless particles;
- Dark Energy is a cosmological constant term.

The ΛCDM model

Despite its theoretical shortcomings, ΛCDM remains the preferred model
due to its ability to accurately describe observed phenomena.
However, the ΛCDM model with its six parameters is not based on deep-rooted physical principles and should be considered, at best,
an approximation of an underlying physical theory that remains undiscovered.

Hence, as observations become more numerous and accurate,
deviations from the ΛCDM model are expected to be detected.
And in fact, discrepancies in important cosmological parameters,
have already arisen in various observations
with different statistical significance.

While some of these tensions may have a systematic origin,
their recurrence across multiple probes suggests that there may be flaws in the standard cosmological scenario, and that new physics may be necessary
to explain these observational shortcomings.

Therefore, the persistence of these tensions could indicate
the failure of the canonical ΛCDM model.

1. Negative total neutrino mass

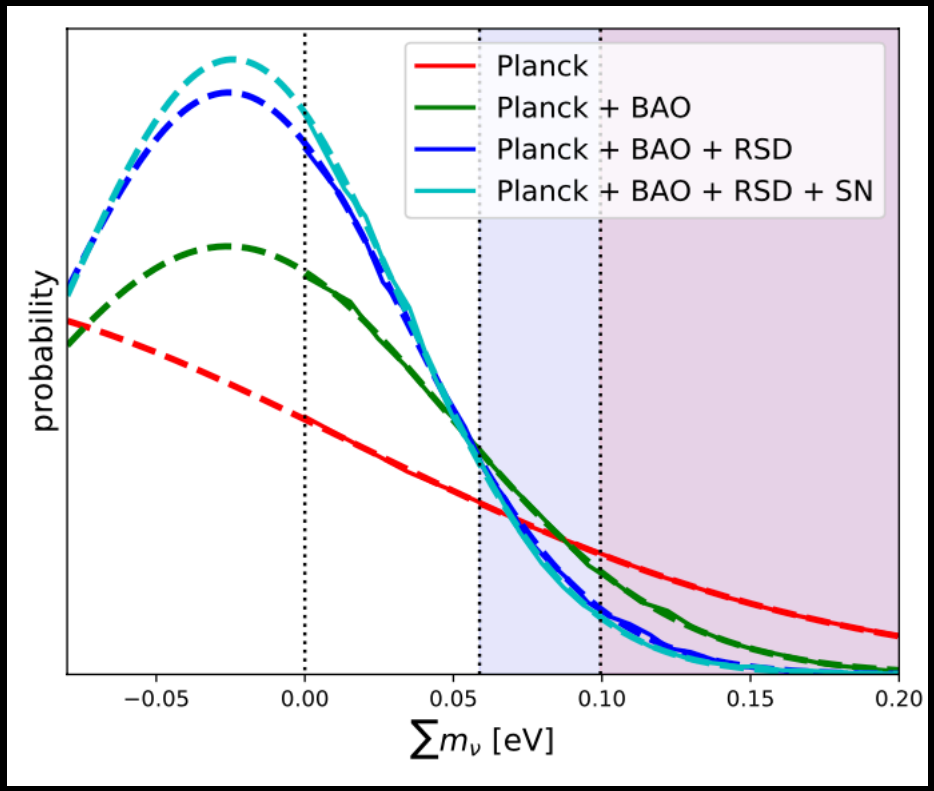

eBOSS collaboration, Alam et al., *Phys.Rev.D* 103 (2021) 8, 083533

Actually the total neutrino mass preferred by the cosmological data is null or negative!!
Although this was not statistically significant, it showed a first hint of a tension between cosmology and neutrino oscillation experiments.

1. Negative total neutrino mass

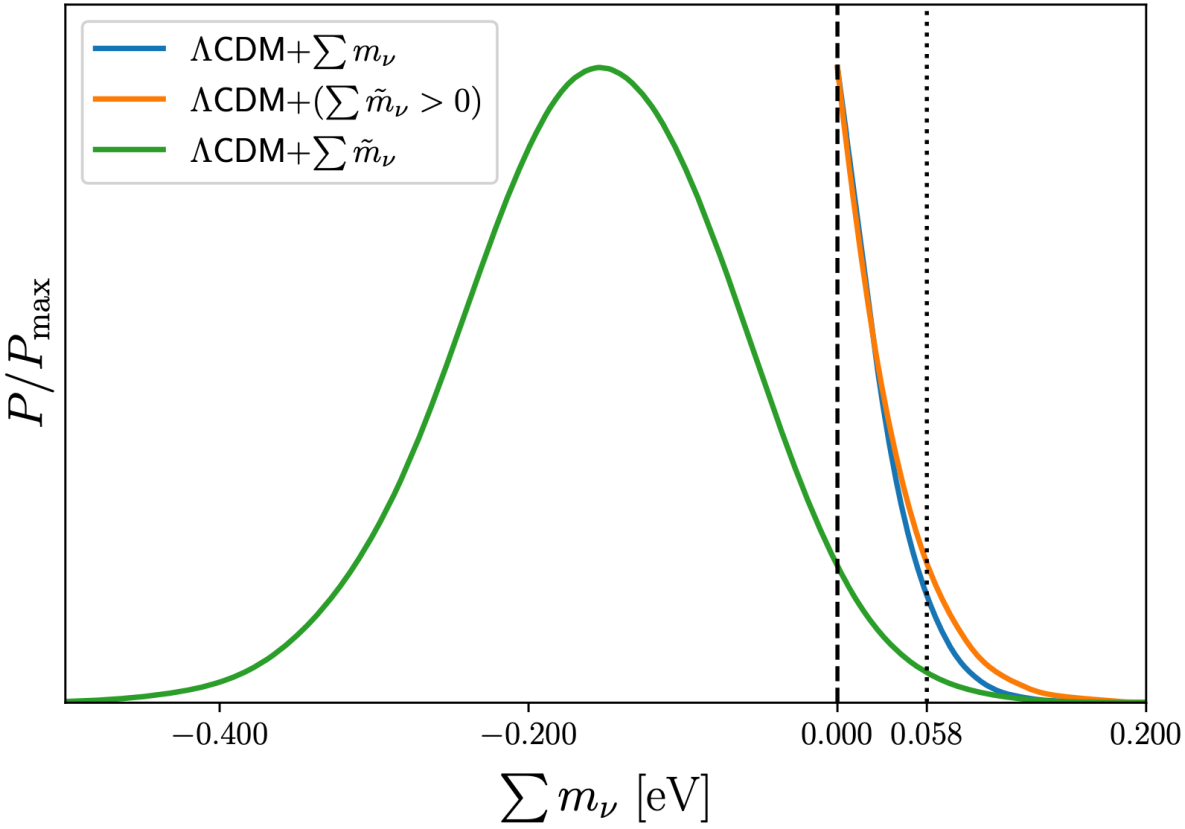

Figure 1: Posterior of neutrino mass in eV inferred from Planck + ACT Lensing + DESI data. The blue line shows constraints on a model with a physical neutrino mass, the orange line shows constraints where the neutrino mass is parametrized as an effect on the CMB lensing power spectrum and restricted to be positive, and the green line shows constraints on a parametrized neutrino mass that is allowed to be negative. The best fit for the parametrized neutrino mass is $\sum \tilde{m}_\nu = -160$ meV, and the minimal neutrino mass of 58 meV is disfavored at 3σ. For details about the parametrization of negative neutrino mass and the data sets used, see Section 2.2.

Craig et al., arXiv:2405.00836

1. Negative total neutrino mass

Elbers al., arXiv:2407.10965

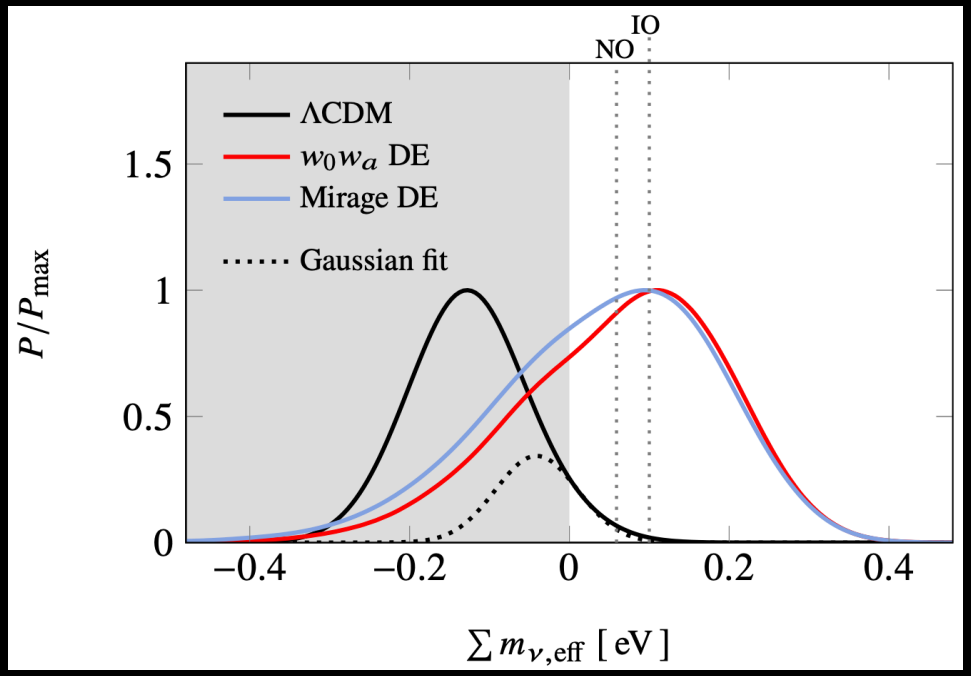

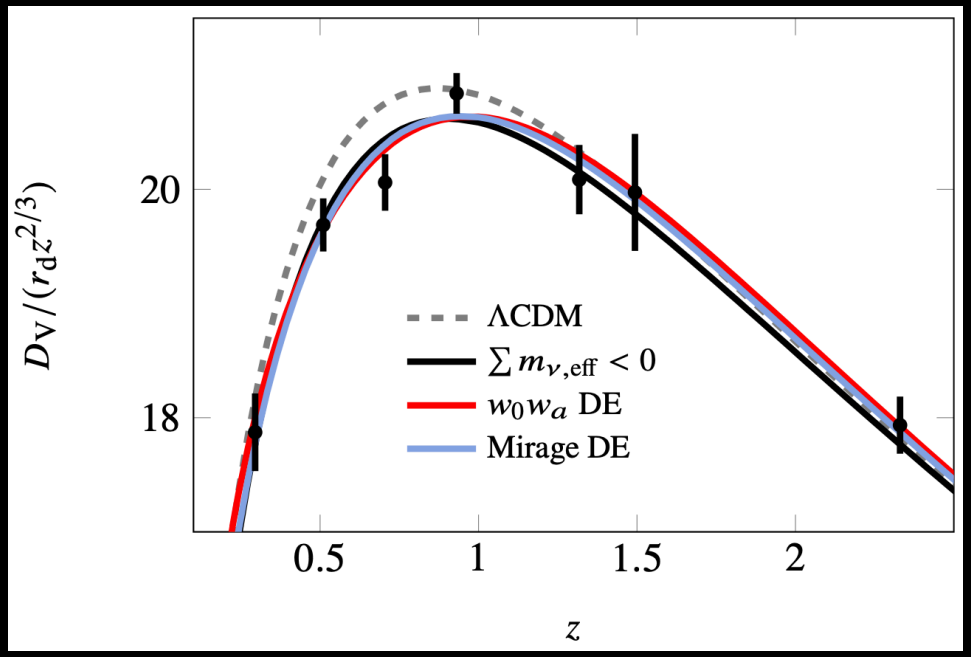

However, introducing more freedom in the DE sector, and in particular considering a dynamical DE as preferred by the BAO DESI data, we can restore larger neutrino masses, more in agreement with laboratory data.

2. The Hubble tension

The Hubble constant H0 describes the expansion rate of the Universe today.

This can be obtained in two ways:

1. measuring the luminosity distance and the recessional velocity of known galaxies, and computing the proportionality factor.

Hubble's Law

$$v = H_0 D$$

This approach is model independent and based on geometrical measurements.

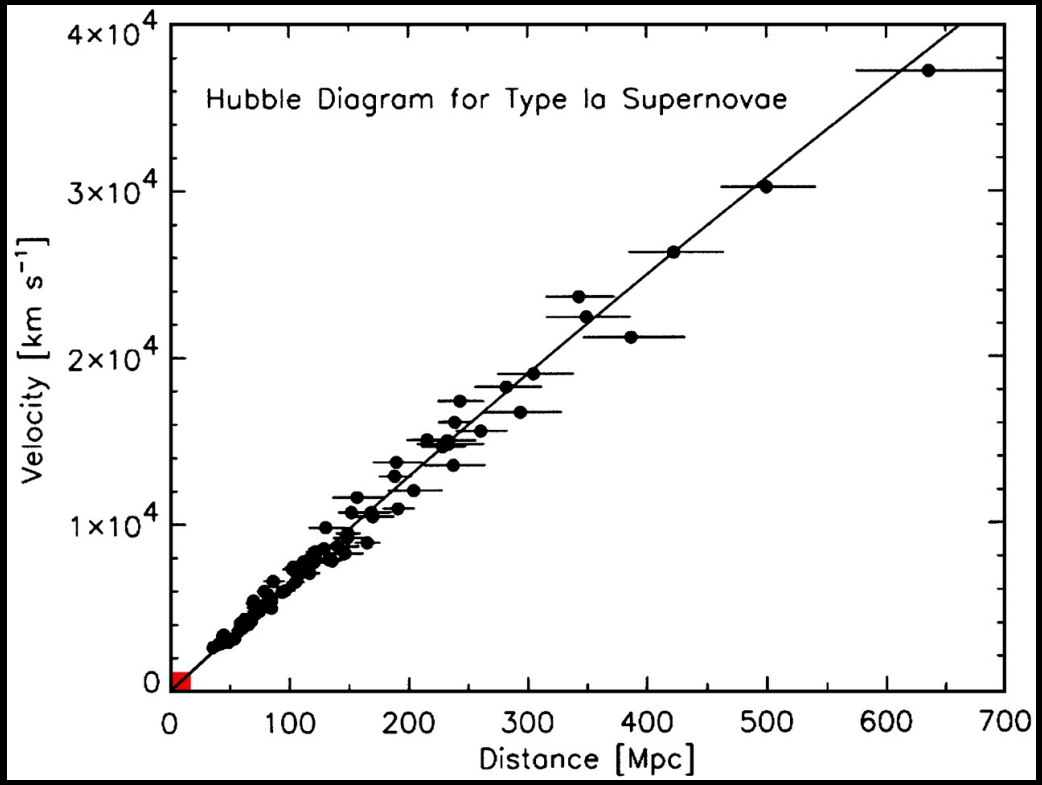

Jha, S. (2002) Ph.D. thesis (Harvard Univ., Cambridge, MA).

2. The Hubble tension

The Hubble constant H0 describes the expansion rate of the Universe today.

This can be obtained in two ways:

1. measuring the luminosity distance and the recessional velocity of known galaxies, and computing the proportionality factor.
2. considering early universe measurements, and assuming a model for the expansion history of the universe.

For example, we have CMB measurements and we assume the standard model of cosmology, i.e. the ΛCDM scenario.

1st Friedmann equations describes the expansion history of the universe:

$$H^2(z) = H_0^2 \left(\Omega_m (1+z)^3 + \Omega_k (1+z)^2 + \Omega_\Lambda\right).$$

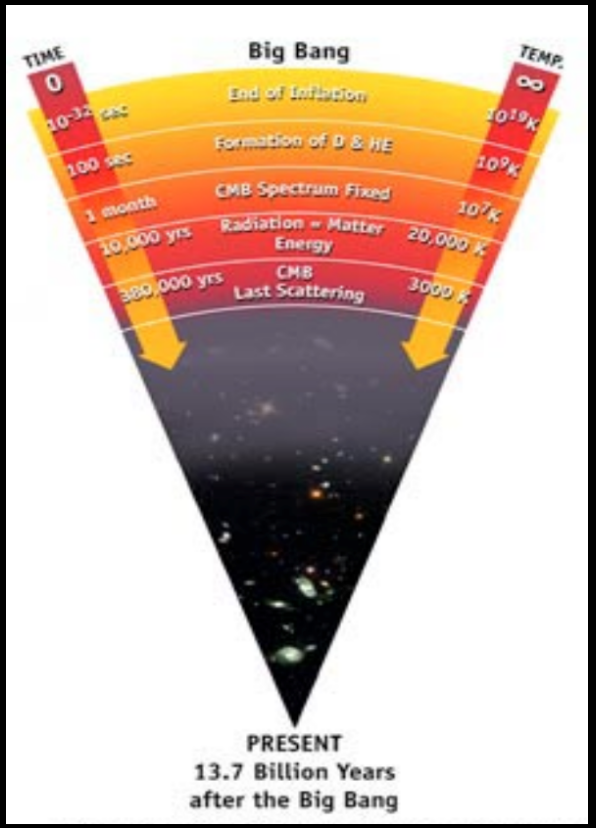

2. The Hubble tension

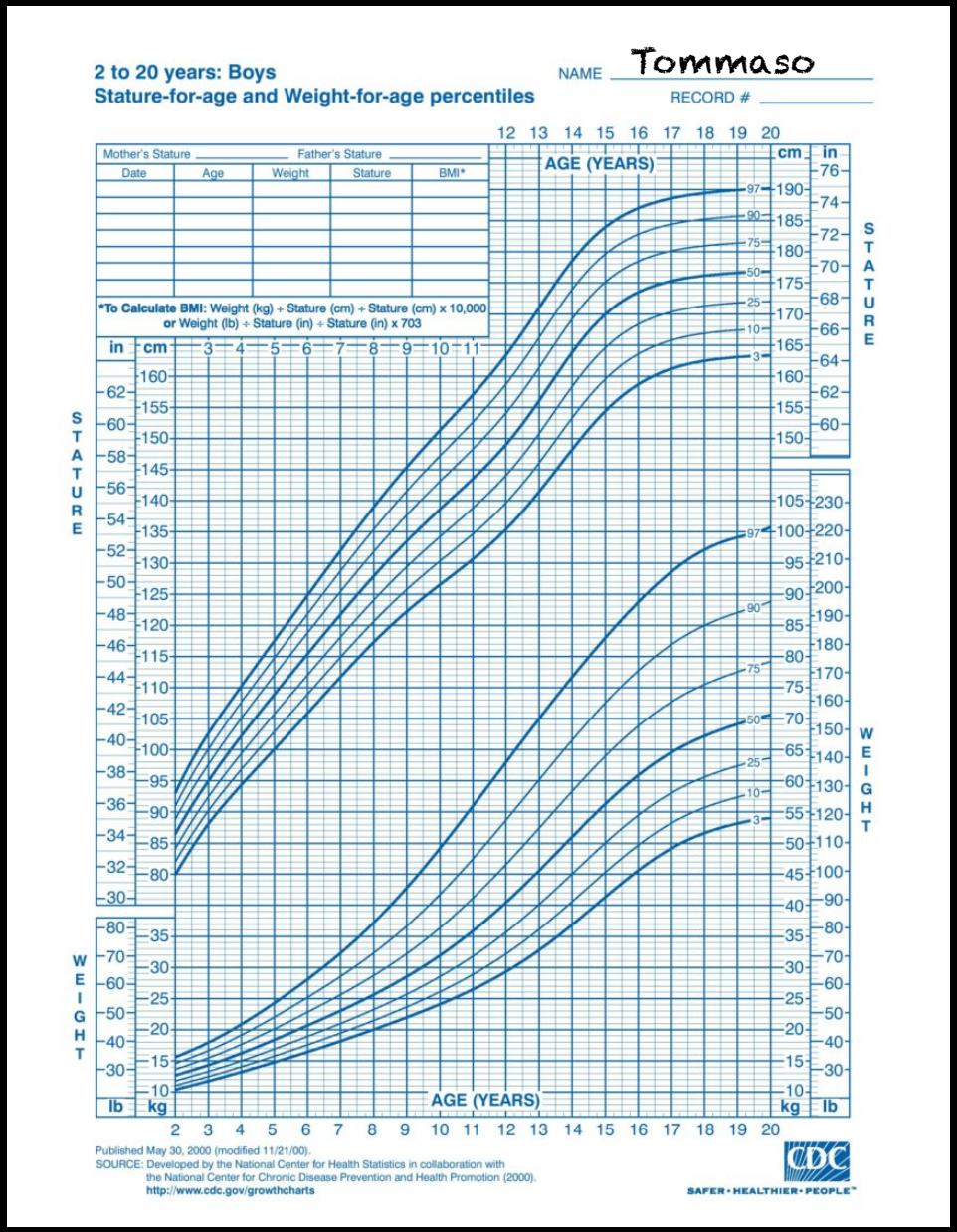

2. The Hubble tension

If we compare the H0 estimates using these 2 methods they disagree.

The Planck estimate assuming a “vanilla" ΛCDM cosmological model:
H0 = 67.36 ± 0.54 km/s/Mpc

Planck 2018, Astron.Astrophys. 641 (2020) A6

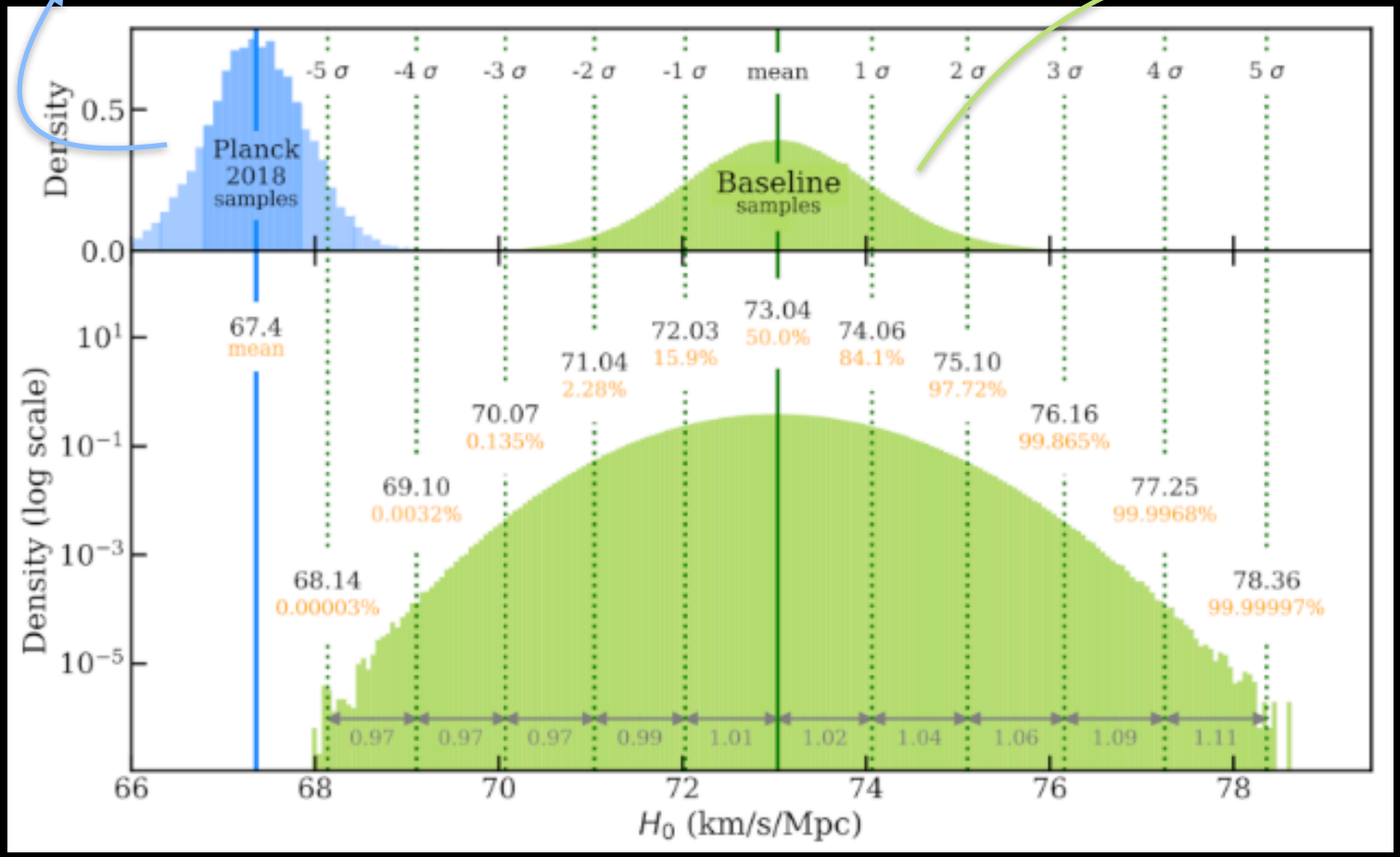

The latest local measurements obtained by the SH0ES collaboration

H0 = 73.04 ± 1.04 km/s/Mpc

Riess et al. arXiv:*2112.04510*

5σ = one in 3.5 million implausible to reconcile the two by chance

2. The Hubble Distance Ladder

If we compare the H0 estimates using these 2 methods they disagree.

The Planck estimate assuming a “vanilla" ΛCDM cosmological model:
H0 = 67.36 ± 0.54 km/s/Mpc

Planck 2018, Astron.Astrophys. 641 (2020) A6

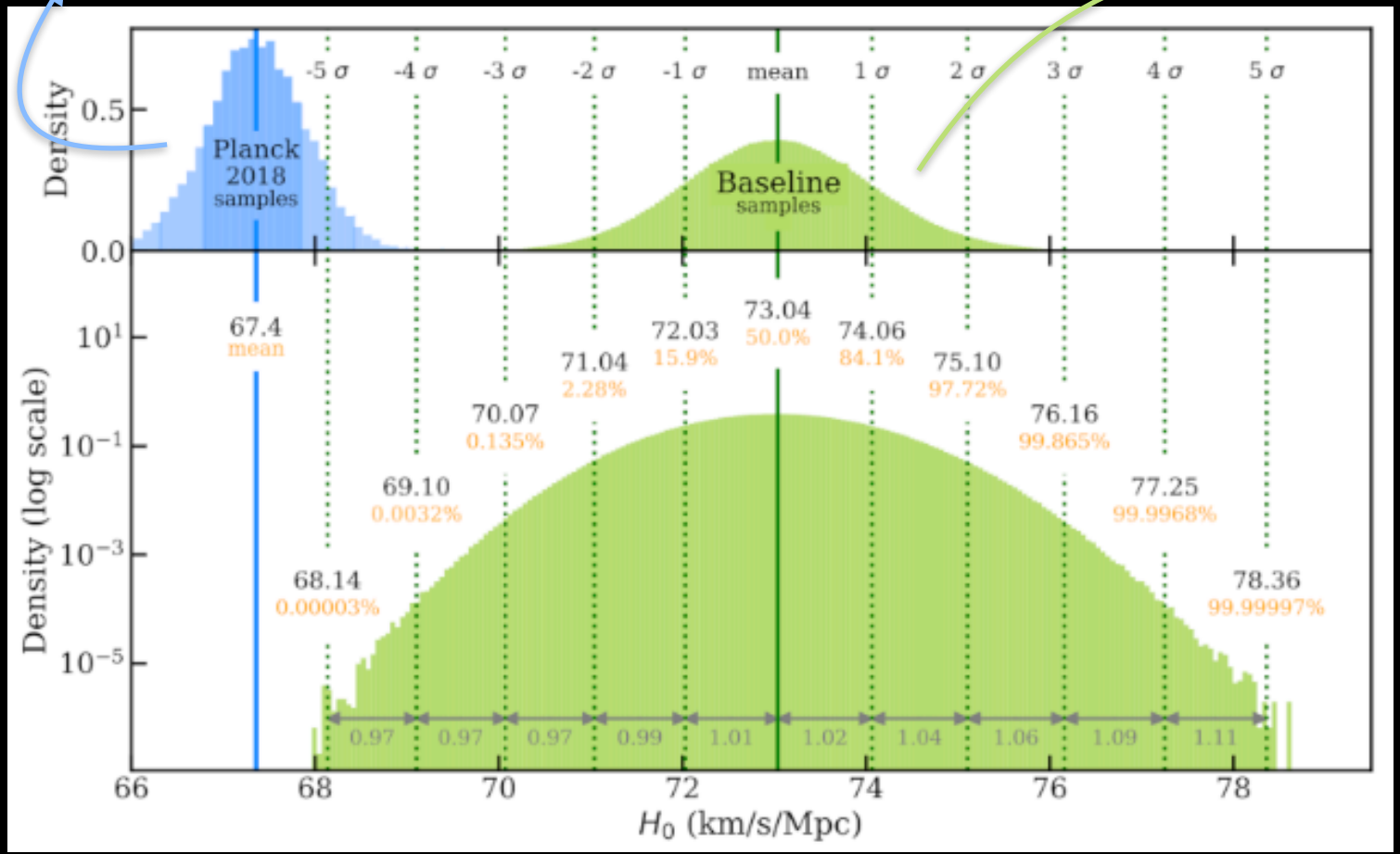

The latest local measurements obtained by the SH0ES collaboration

H0 = 73.04 ± 1.04 km/s/Mpc

Riess et al. arXiv:*2112.04510*

5σ = one in 3.5 million implausible to reconcile the two by chance

2. The Hubble Distance Ladder

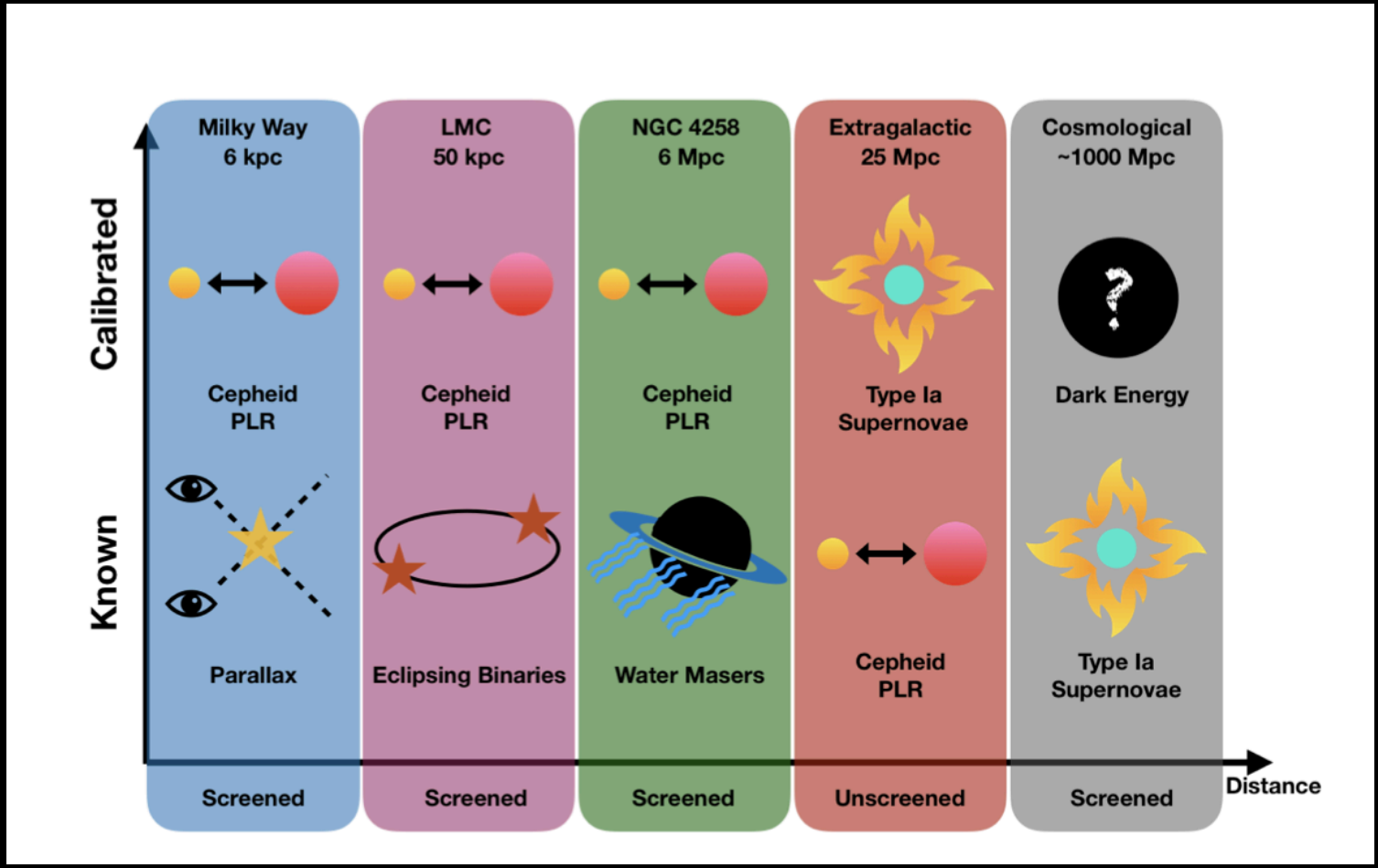

Riess et al. arXiv:*2112.04510*

2. The Hubble tension

The H0 value is very important for the determination of the total neutrino mass.
In fact, there exist a very important negative correlation between the Hubble constant and the sum of the neutrino masses.

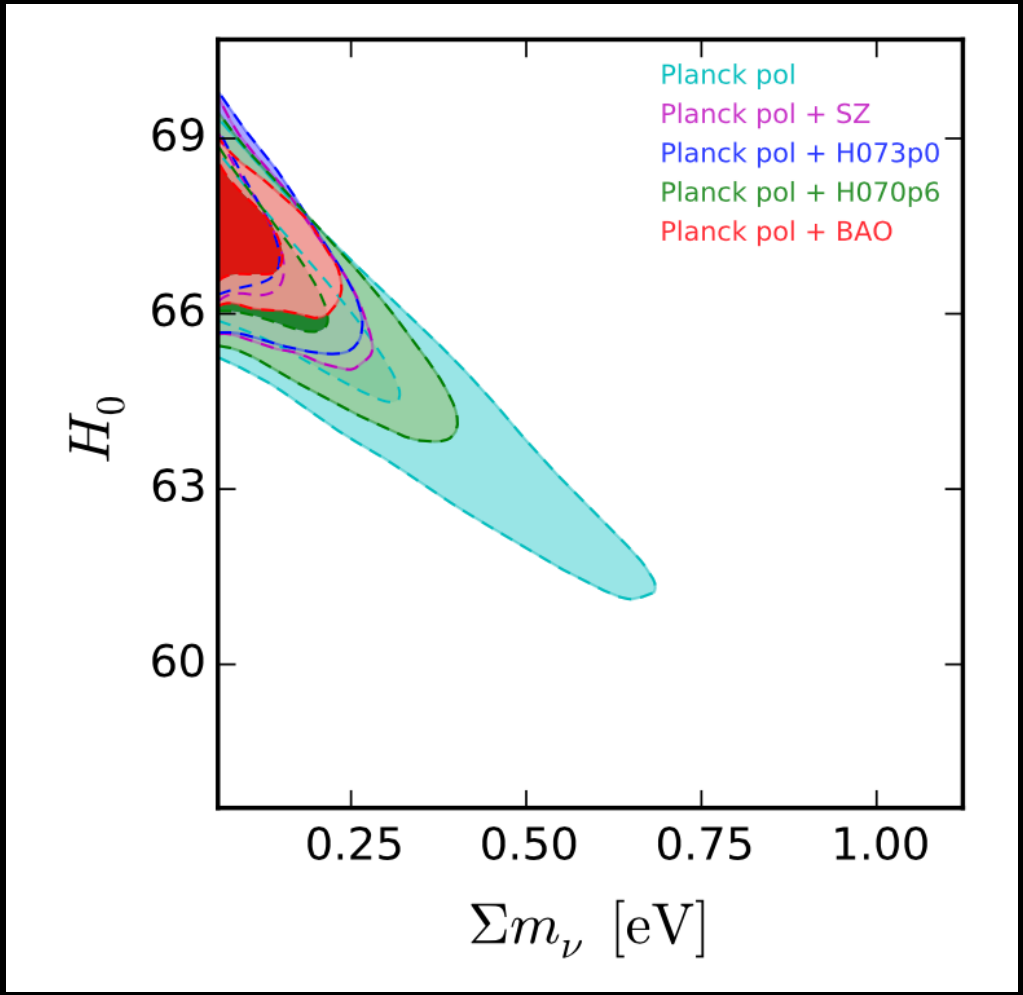

Di Valentino et al. Phys.Rev. D93 (2016) no.8, 083527

2. The Hubble tension

We can see a clear geometrical degeneracy between these two parameters. To reconcile the SH0ES measurement of H0 with Planck we need a negative effective neutrino mass of

$$\sum m_{\nu,\mathrm{eff}} = -0.5 \pm 0.1\ \mathrm{eV}$$

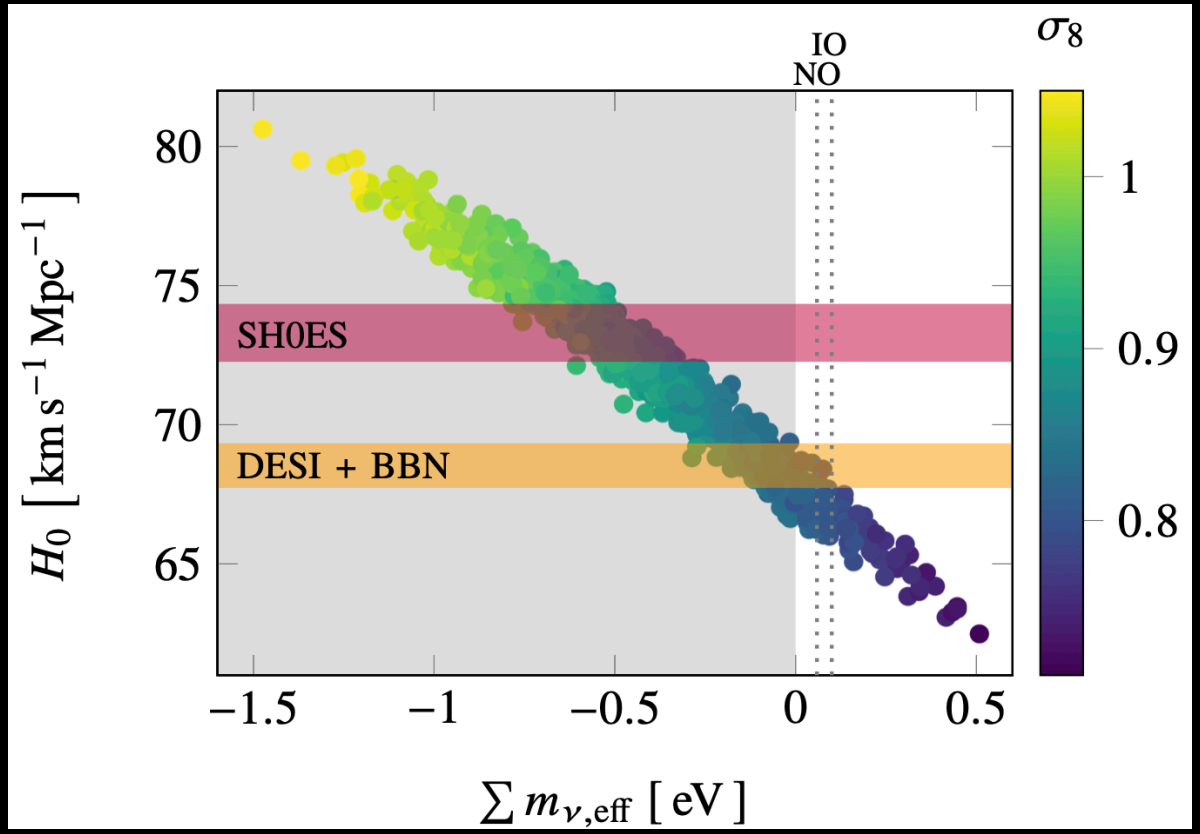

Elbers al., arXiv:2407.10965

2. The Hubble tension

Moreover, there is a very strong positive correlation between H0 and the neutrino effective number. Therefore, imposing an H0 prior as obtained by SH0ES can give an indication for extra particles at recombination. In particular, Neff=4 (excluded at many standard deviations) could completely solve the Hubble tension.

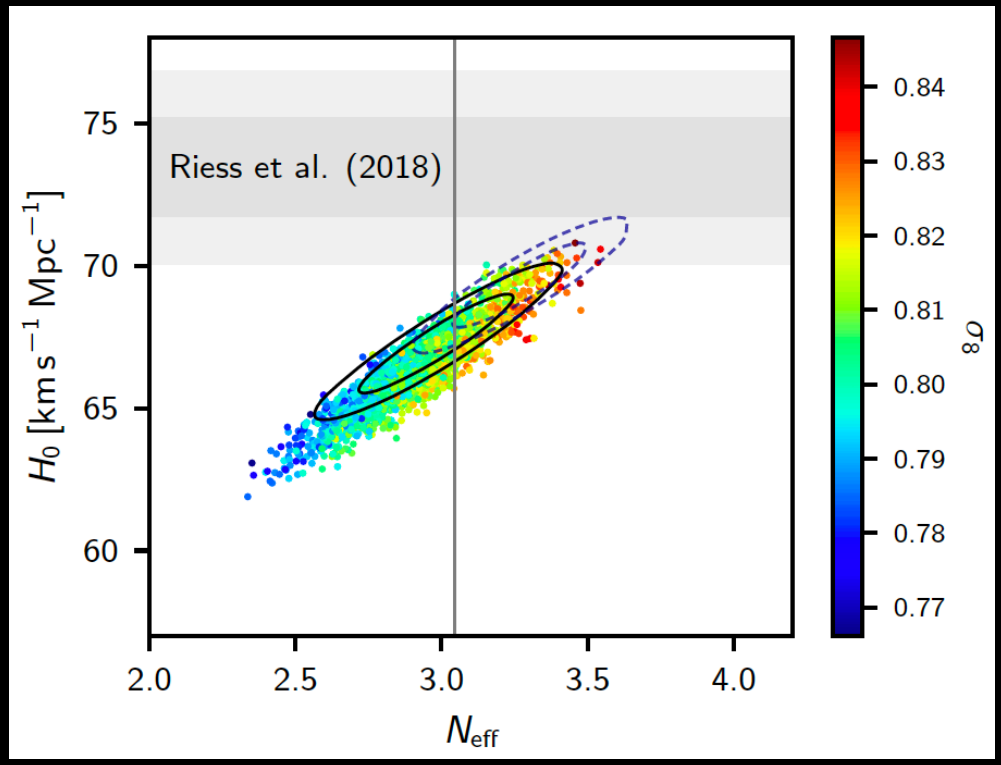

Planck 2018, Aghanim et al., arXiv:1807.06209 [astro-ph.CO]

The Sterile Neutrino

A fully thermalised 4th sterile neutrino with ΔNeff=1 is excluded at about 6σ regardless of its mass.

$$N_{\rm eff} = 2.92^{+0.36}_{-0.37} \quad (95\,\%,\ \textit{Planck}\ \text{TT,TE,EE+lowE}),$$

Therefore, the presence of a sterile neutrino is
in strong contradiction with cosmological data,
so that the production of sterile neutrinos would need to be suppressed by some non-standard interactions (Archidiacono et al. 2016, JCAP, 1608, 067; Chu et al. 2015, JCAP, 1510, 011), low-temperature reheating (de Salas et al. 2015, Phys. Rev., D92, 123534), or other special mechanisms.

The Sterile Neutrino

With the CMB we can only constrain the effective sterile neutrino mass, but fixing the model, we can infer also the physical mass of the particle.
The relationship between Neff and meff is model dependent.

Thermally distributed with an arbitrary temperature Ts

$$m^{\rm eff}_{\nu,\,\rm sterile} = (T_{\rm s}/T_\nu)^3 m^{\rm thermal}_{\rm sterile} = (\Delta N_{\rm eff})^{3/4} m^{\rm thermal}_{\rm sterile}$$

Produced via the mechanism described by Dodelson & Widrow, 1994, PRL, 72,17.

$$m^{\rm eff}_{\nu,\,\rm sterile} = \chi_{\rm s}\, m^{\rm DW}_{\rm sterile} = \Delta N_{\rm eff}\ m^{\rm DW}_{\rm sterile}$$

and distributed proportionally to the active neutrinos with an arbitrary scaling factor, that is a function of the active-sterile neutrino mixing angle.

For low ΔNeff the physical mass can therefore become large and in that case the particles behave as cold dark matter.
For this reason in Planck are excluded all the sterile neutrino masses >10eV.

The Sterile Neutrino

Planck 2018, Aghanim et al., arXiv:1807.06209 [astro-ph.CO]

Contribution of the sterile neutrino when it is massless.

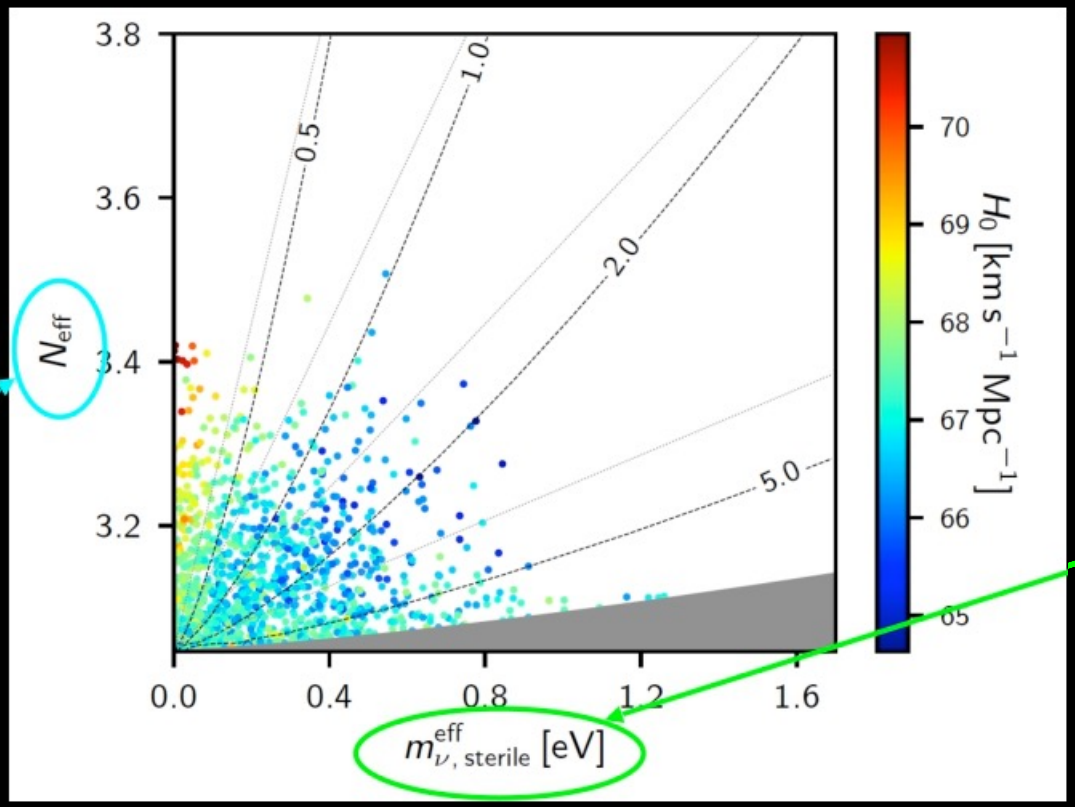

Contribution of the sterile neutrino when it is massive.

$$m^{\rm eff}_{\nu,\,\rm sterile} \equiv (94.1\,\Omega_{\nu,\rm sterile}h^2)\ \text{eV}$$

$$\left.\begin{array}{r} N_{\rm eff} < 3.29, \\ m^{\rm eff}_{\nu,\,\rm sterile} < 0.65\ \text{eV}, \end{array}\right\} \begin{array}{l} 95\,\%,\ \textit{Planck}\ \text{TT,TE,EE+lowE} \\ \text{+lensing+BAO}, \end{array}$$

The physical mass for thermally-produced sterile neutrinos is constant along the grey lines labelled by the mass in eV, while the equivalent result for sterile neutrinos produced via the Dodelson-Widrow mechanism is shown by the adjacent thinner lines. The dark grey shaded region shows the part of parameter space excluded by the default prior $m_{\rm thermal}$ sterile < 10 eV.

The Sterile Neutrino

Planck 2018, Aghanim et al., arXiv:1807.06209 [astro-ph.CO]

Contribution of the sterile neutrino when it is massless.

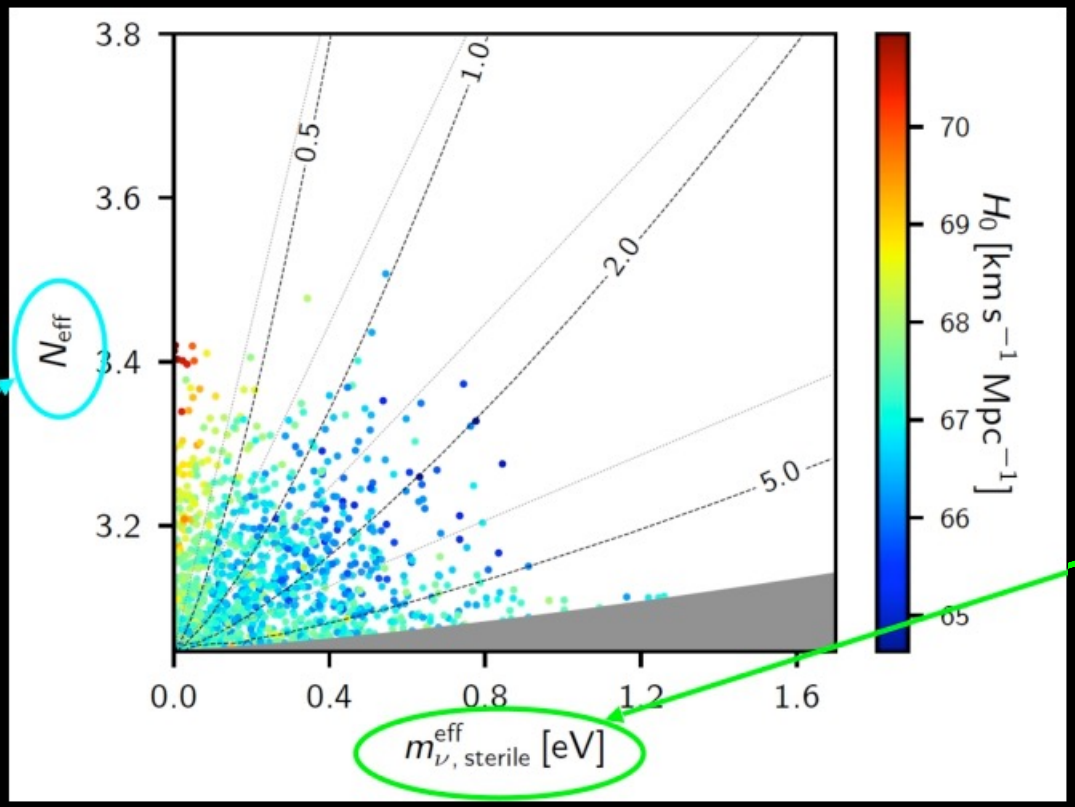

Contribution of the sterile neutrino when it is massive.

$$m^{\rm eff}_{\nu,\,\rm sterile} \equiv (94.1\,\Omega_{\nu,\rm sterile}h^2)\ \text{eV}$$

$$\left.\begin{array}{r} N_{\rm eff} < 3.34, \\ m^{\rm eff}_{\nu,\,\rm sterile} < 0.23\ \text{eV}, \end{array}\right\} \quad 95\,\%,\ \textit{Planck}\ \text{TT,TE,EE+lowE +lensing+BAO.}$$

However also these constraints depend on the choice of the prior: adopting a stronger prior of $m_{\rm thermal}$ sterile < 2 eV, we obtain a stronger constraint.

Self-Interacting sterile neutrino

If one considers neutrino oscillations between active and sterile neutrinos, sterile neutrinos would have been fully thermalised in the early universe preferring Neff=4, and would be strongly disfavoured by the cosmological data.
This problem can be bypassed if by some unknown mechanism they can be either prevented from thermalizing in the early Universe or removed by subsequent annihilation.

The authors of Archidiacono et al., Phys.Rev.D 91 (2015) 6, 065021 suggested a possible revision in the sterile neutrino sector in which the sterile neutrino self-interacts through the exchange of a new very light (effectively massless $m_\phi \ll 1eV$) pseudoscalar degree of freedom:

$$\mathcal{L} \sim g_s \phi \bar{\nu} \gamma_5 \nu$$

Such an additional interaction ($\phi\phi$ <—> $\nu_s\nu_s$) leads to rapid pair-annihilation and disappearance of the sterile neutrinos below a temperature corresponding to their mass.
In this model the active neutrinos are instead not interacting.

Self-Interacting sterile neutrino

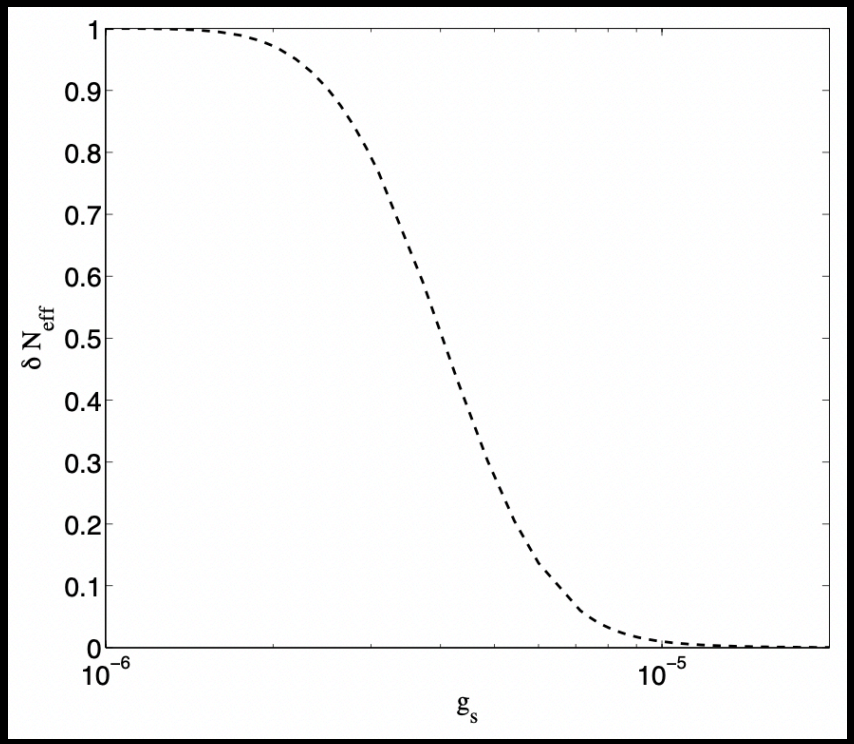

Archidiacono et al., *Phys.Rev.D* 91 (2015) 6, 065021

This is the contribution of the sterile neutrino to the relativistic energy density N_{eff} - 3.044 as a function of the coupling parameter g_s.
We can see that the transition from the full thermalisation to zero thermalisation happens in the range $10^{-6} < g_s < 10^{-5}$.
This implies that if $g_s > 10^{-6}$ sterile neutrinos are not produced until the decoupling of the active neutrinos and the BBN bounds are evaded.

In the data analysis the neutrino sector is parametrised by the overall energy density after thermalisation, N_{eff} and a sterile mass of 1 eV.
The active sector will have a fraction 21/32 N_{eff} of the total energy density, while the remaining fraction 11/32 N_{eff} will end up in the sterile+pseudoscalar fluid, because of the redistribution of energy by oscillations.

Self-Interacting sterile neutrino

	Pseudo		Planck TTTEEE	Planck TTTEEE	... + lensing + BAO
Parameter	Planck TT	Planck TTTEEE	... + R19	... + lensing + BAO	... + R19
$\Delta N_{\rm eff}$	< 0.86	< 0.56	$0.38^{+0.15}_{-0.15}$	< 0.41	$0.34^{+0.14}_{-0.15}$
m_s [eV]	$3.1^{+1.3}_{-1.1}$	< 1.14	< 1.19	< 1.03	< 1.08
H_0 [km/s/Mpc]	$72.2^{+1.7}_{-2.9}$	$71.6^{+1.1}_{-1.6}$	$72.8^{+1.1}_{-1.2}$	$70.0^{+0.7}_{-1.1}$	$71.4^{+0.9}_{-1.0}$
n_s	$0.971^{+0.014}_{-0.013}$	$0.951^{+0.006}_{-0.008}$	$0.957^{+0.006}_{-0.006}$	$0.944^{+0.005}_{-0.006}$	$0.950^{+0.005}_{-0.005}$

Archidiacono et al., *JCAP* 12 (2020) 029

If the pseudoscalar couples only to the sterile neutrino, this model alleviates the H0 tension within 3σ, also when the BAO data are considered.

Constraints at 68% cl and upper limits at 95% cl

3. The S8 tension

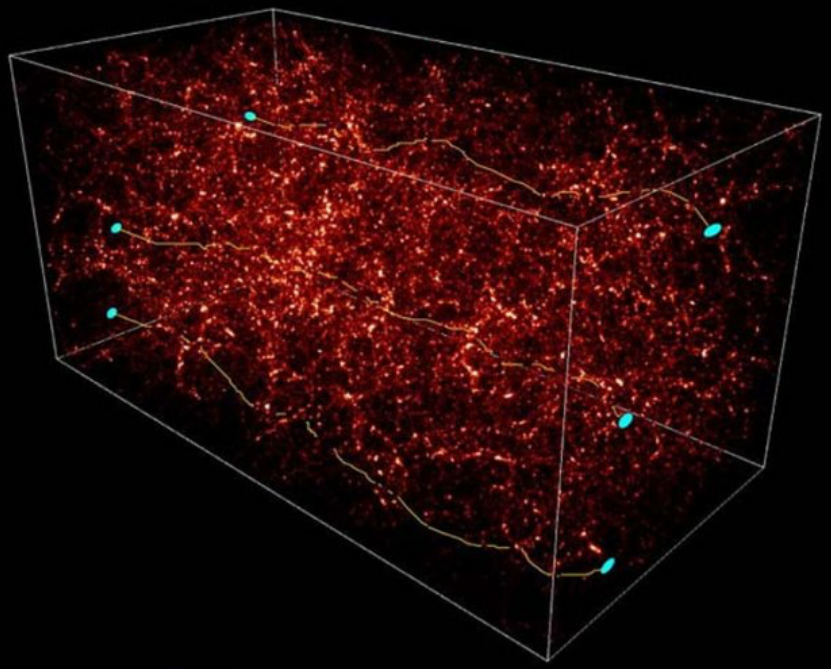

$$S_8 \equiv \sigma_8 \sqrt{\Omega_m / 0.3}$$

A tension on S8 is present between the Planck data in the ΛCDM scenario and the cosmic shear data.

3. The S8 tension

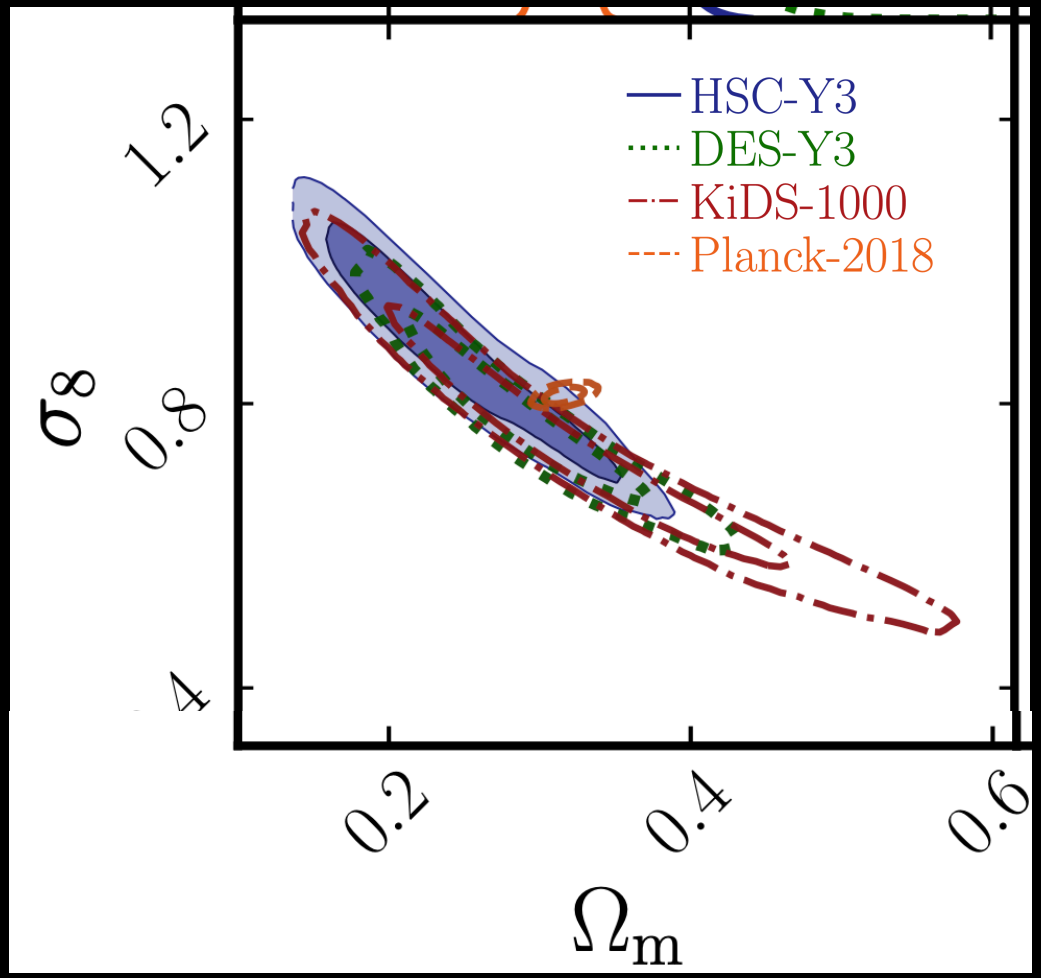

HSC-Y3, Dalal et al., arXiv:2304.00701 [astro-ph.CO]

The S8 tension is present at about 2σ between Planck assuming ΛCDM and HSC-Y3, 3.1σ with KiDS-1000, and 2.5σ with DES-Y3.

$S_8 = 0.834 \pm 0.016$

Planck 2018, Aghanim et al., arXiv:1807.06209 [astro-ph.CO]

$S_8 = 0.776^{+0.032}_{-0.033}$

HSC-Y3, Dalal et al., arXiv:2304.00701 [astro-ph.CO]

$S_8 = 0.766^{+0.020}_{-0.014}$

KiDS-1000, Heymans et al., arXiv:2007.15632 [astro-ph.CO]

$S_8 = 0.776^{+0.017}_{-0.017}$

DES-Y3, Abbott et al., arXiv:2105.13549 [astro-ph.CO]

3. The S8 tension

The S8 value can depend on the total neutrino mass.

In fact, massive neutrinos lower the clustering amplitude preferring a smaller value for S8.

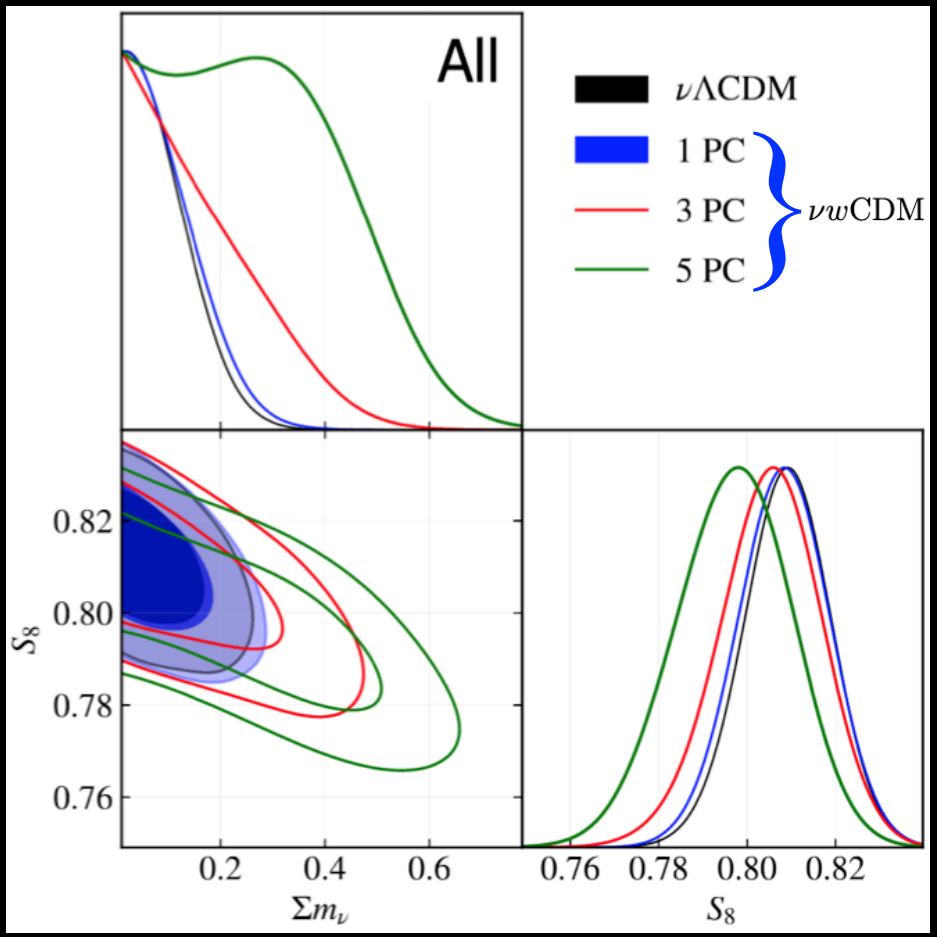

Diaz Rivero et al., *arXiv:1903.03125*

4. A_L : a failed consistency check

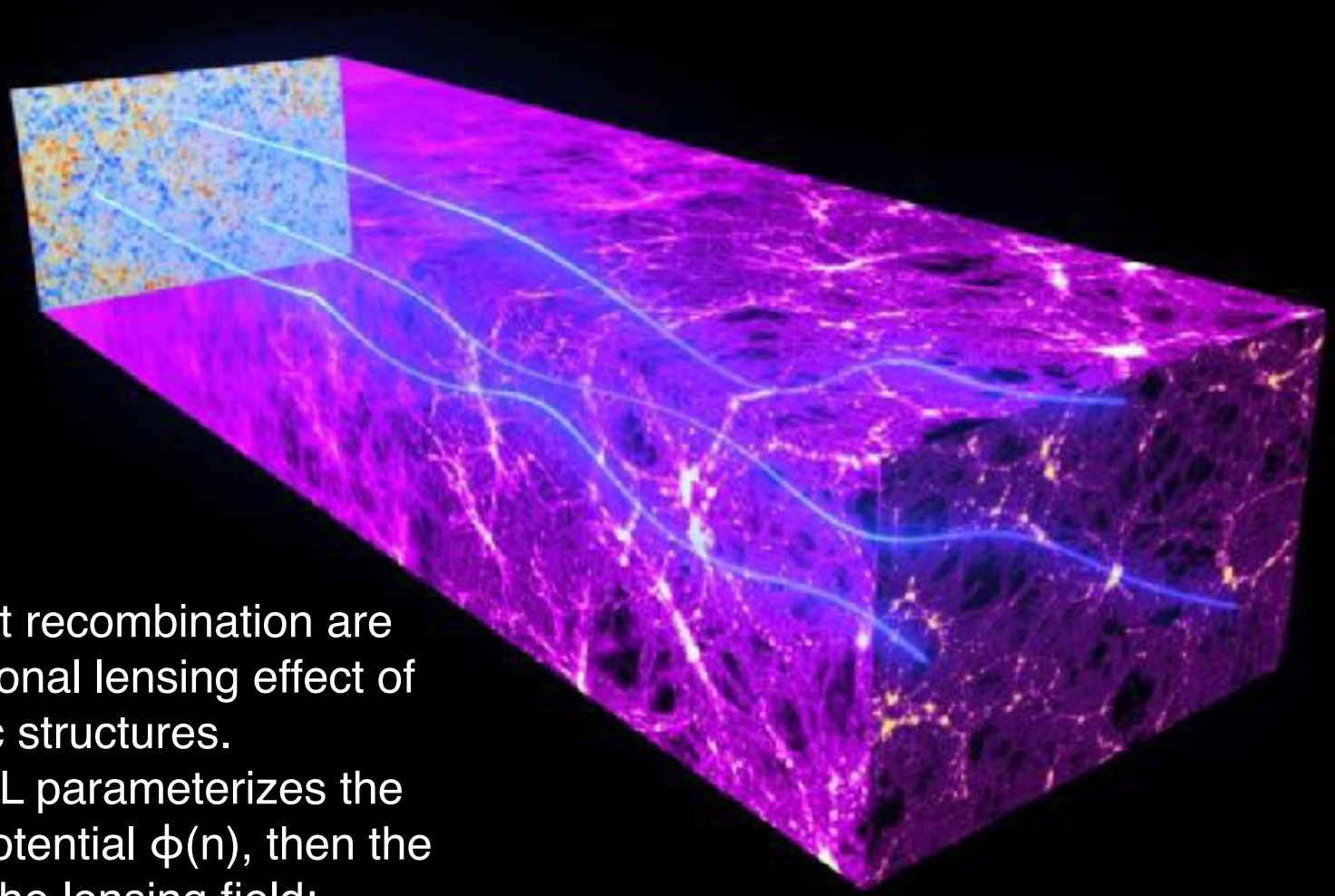

CMB photons emitted at recombination are deflected by the gravitational lensing effect of massive cosmic structures.
The lensing amplitude AL parameterizes the rescaling of the lensing potential ϕ(n), then the power spectrum of the lensing field:

$$C_\ell^{\phi\phi} \rightarrow A_L C_\ell^{\phi\phi}$$

The gravitational lensing deflects the photon path by a quantity defined by the gradient of the lensing potential ϕ(n), integrated along the line of sight n, remapping the temperature field.

4. A_L : a failed consistency check

Its effect on the power spectrum is the smoothing of the acoustic peaks, increasing AL.

Interesting consistency checks is if the amplitude of the smoothing effect in the CMB power spectra matches the theoretical expectation AL = 1 and whether the amplitude of the smoothing is consistent with that measured by the lensing reconstruction.

If AL =1 then the theory is correct, otherwise we have a new physics or systematics.

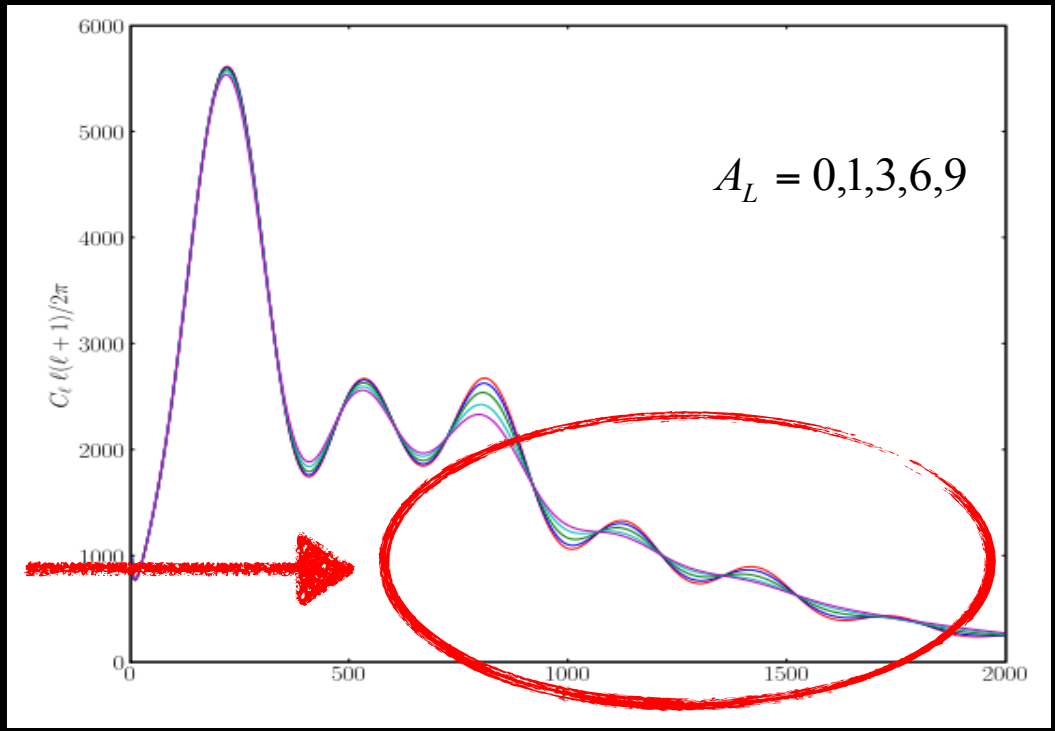

Calabrese et al., Phys. Rev. D, 77, 123531

4. A_L : a failed consistency check

The Planck lensing-reconstruction power spectrum is consistent with the amplitude expected for ΛCDM models that fit the CMB spectra, so the Planck lensing measurement is compatible with AL = 1.

However, the distributions of AL inferred from the CMB power spectra alone indicate a preference for AL > 1.

The joint combined likelihood shifts the value preferred by the TT data downwards towards AL = 1, but the error also shrinks, increasing the significance of AL > 1 to 2.8σ.

The preference for high AL is not just a volume effect in the full parameter space, with the best fit improved by $\Delta\chi^2 \sim 9$ when adding AL for TT+lowE and 10 for TTTEEE+lowE.

Planck 2018, Astron.Astrophys. 641 (2020) A6

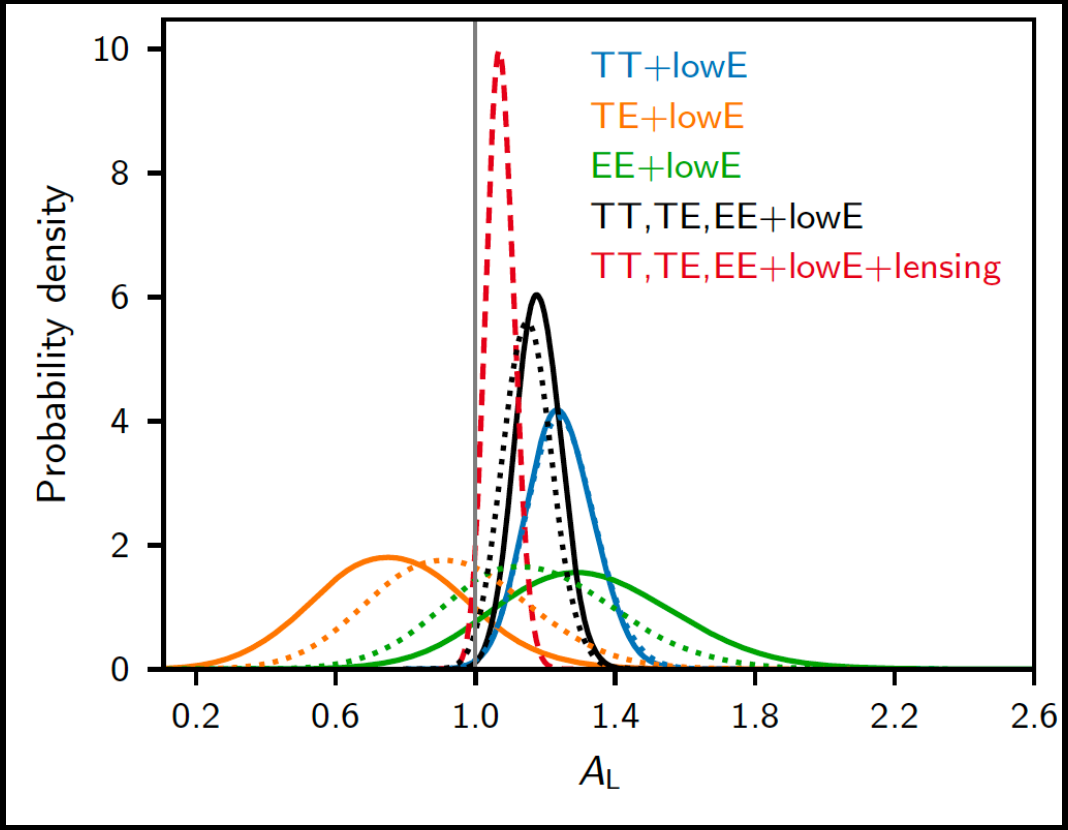

$$A_L = 1.243 \pm 0.096 \quad (68\,\%,\ \textit{Planck}\ \text{TT+lowE}),$$
$$A_L = 1.180 \pm 0.065 \quad (68\,\%,\ \textit{Planck}\ \text{TT,TE,EE+lowE}),$$

4. A_L : a failed consistency check

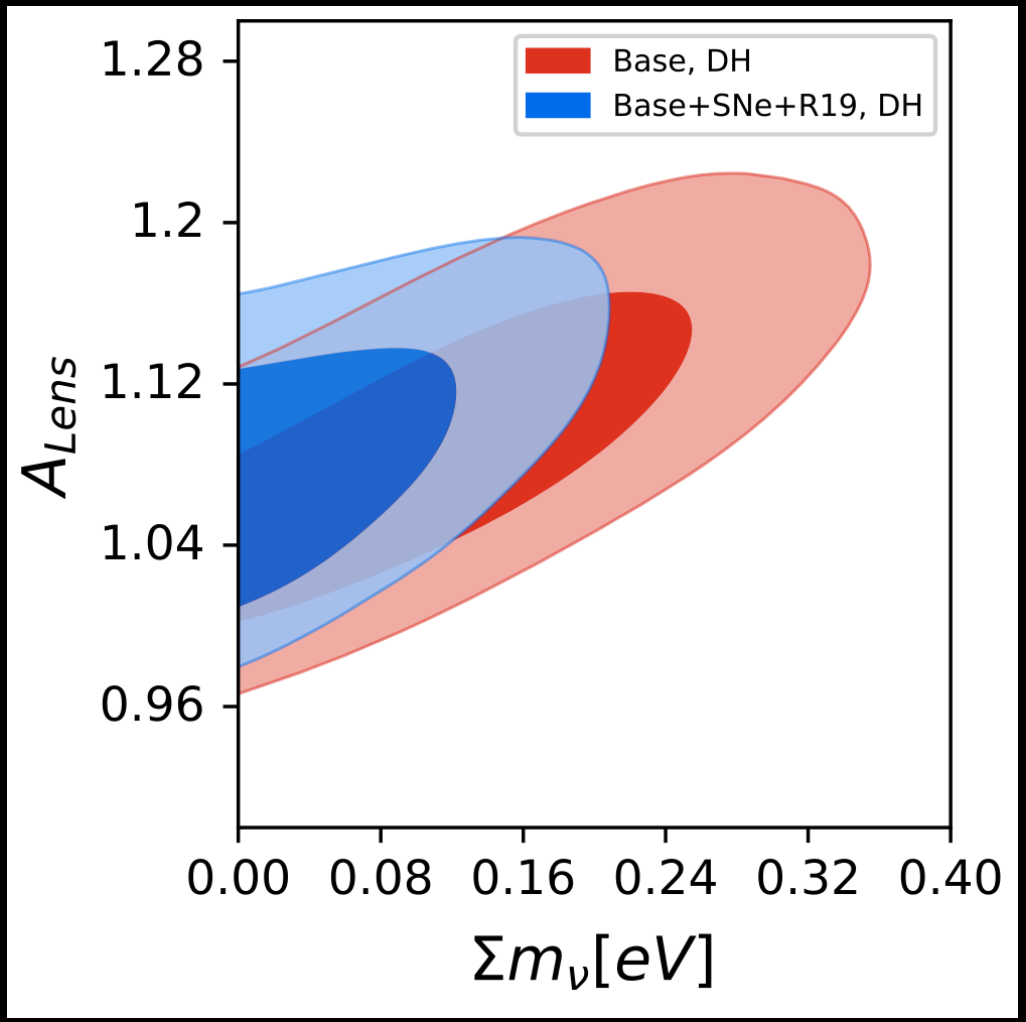

Choudhury and Hannestad, arXiv:1907.12598 [astro-ph.CO]

There is a very strong positive correlation between Alens and the total neutrino mass.
Therefore, to be conservative, we need to take into account this wrong amount of lensing when constraining Σm_ν.

4. A_L : a failed consistency check

Cosmological inputs for nonoscillation data analysis			Results: Cosmo only		Cosmo + m_β + $m_{\beta\beta}$	
#	Model	Data set	Σ (2σ)	$\Delta\chi^2_{\rm IO-NO}$	Σ (2σ)	$\Delta\chi^2_{\rm IO-NO}$
0	ΛCDM + Σ	Planck TT, TE, EE	< 0.34 eV	0.9	< 0.32 eV	1.0
1	ΛCDM + Σ	Planck TT, TE, EE + lensing	< 0.30 eV	0.8	< 0.28 eV	0.9
2	ΛCDM + Σ	Planck TT, TE, EE + BAO	< 0.17 eV	1.6	< 0.17 eV	1.8
3	ΛCDM + Σ	Planck TT, TE, EE + BAO + lensing	< 0.15 eV	2.0	< 0.15 eV	2.2
4	ΛCDM + Σ	Planck TT, TE, EE + lensing + H_0(R19)	< 0.13 eV	3.9	< 0.13 eV	4.0
5	ΛCDM + Σ	Planck TT, TE, EE + BAO + H_0(R19)	< 0.13 eV	3.1	< 0.13 eV	3.2
6	ΛCDM + Σ	Planck TT, TE, EE + BAO + lensing + H_0(R19)	< 0.12 eV	3.7	< 0.12 eV	3.8
7	ΛCDM + Σ + $A_{\rm lens}$	Planck TT, TE, EE + lensing	< 0.77 eV	0.1	< 0.66 eV	0.1
8	ΛCDM + Σ + $A_{\rm lens}$	Planck TT, TE, EE + BAO	< 0.31 eV	0.2	< 0.30 eV	0.3
9	ΛCDM + Σ + $A_{\rm lens}$	Planck TT, TE, EE + BAO + lensing	< 0.31 eV	0.1	< 0.30 eV	0.2

For example, when A_{lens} is free to vary, because of their correlation, the bounds on the total neutrino mass are strongly weakened, up to a factor of ~2.

As a consequence, in these cases there is no more the preference for the normal ordering we have in the LCDM scenario.

Capozzi, Di Valentino et al., *Phys.Rev.D* 104 (2021) 8, 083031

4. A_L : a failed consistency check

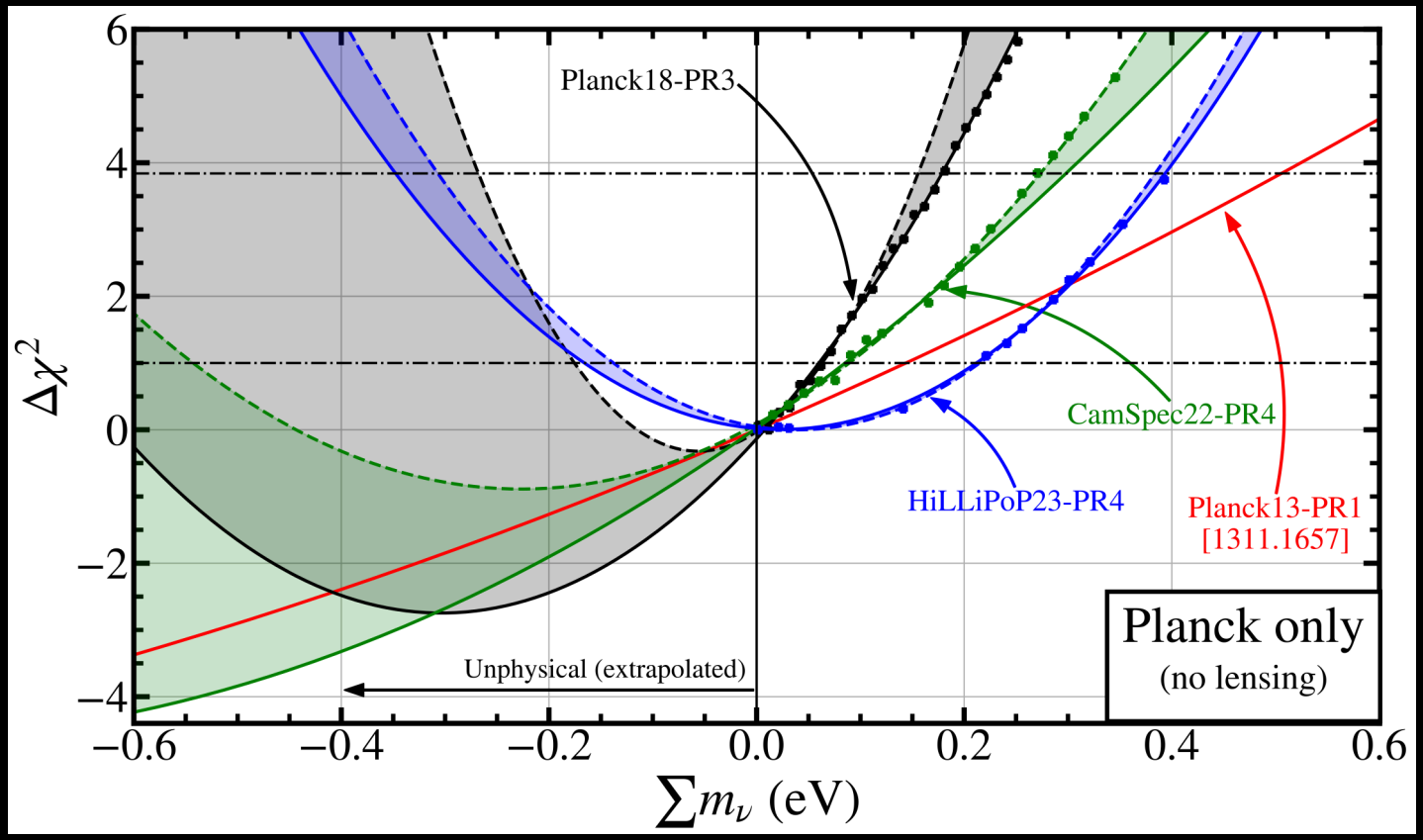

Naredo-Tuero et al., arXiv:2407.13831

The preference for negative neutrino masses is primarily seen in the Planck 2018 data, which is known to be influenced by the AL problem. This preference vanishes when using the new Planck 2023 HiLLiPoP data, resulting in significantly weaker constraints. Additionally, the pull towards negative masses in the DESI data comes from the z = 0.7 bin, which shows a ~3σ tension with Planck's expectations. Excluding these outliers and combining the data with HiLLiPoP, the constraint on neutrino mass relaxes to:

$$\sum m_\nu < 0.11\,\text{eV at } 95\%\ \text{CL}$$

4. A_L : a failed consistency check

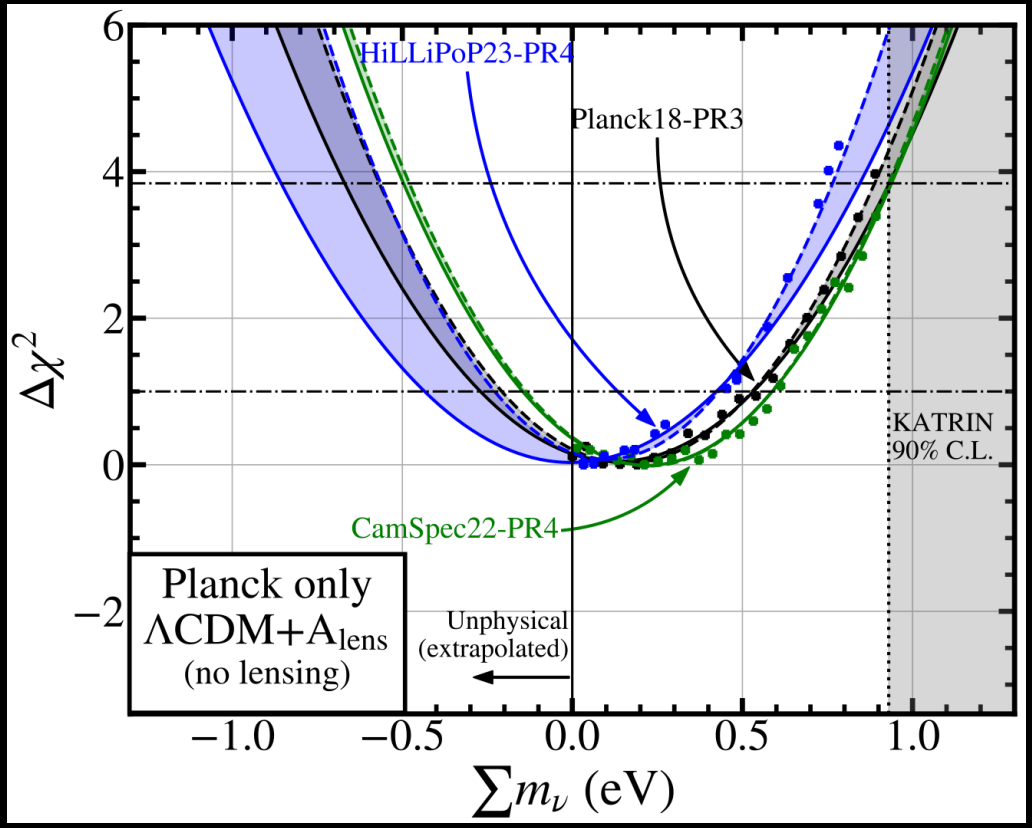

Naredo-Tuero et al., arXiv:2407.13831

Neutrino mass profile likelihoods using the full Planck temperature and polarization data in the ΛCDM model, while allowing the unphysical AL parameter to vary, show that the bounds are significantly relaxed.

Astronomy & Astrophysics manuscript no. ms
September 24, 2019

Planck 2018 results. VI. Cosmological parameters

Planck Collaboration: N. Aghanim[54], Y. Akrami[15,57,59], M. Ashdown[65,5], J. Aumont[95], C. Baccigalupi[78], M. Ballardini[21,41], A. J. Banday[95,8], R. B. Barreiro[61], N. Bartolo[29,62], S. Basak[85], R. Battye[64], K. Benabed[55,90], J.-P. Bernard[95,8], M. Bersanelli[32,45], P. Bielewicz[75,78], J. J. Bock[63,10], J. R. Bond[7], J. Borrill[12,93], F. R. Bouchet[55,90], F. Bou
J.-F. Cardoso[55,90], J. Carron[23], A. Challinor[58,65,11], H. C. Chi
F. Cuttaia[41], P. de Bernardis[31], G. de Zotti[42], J. Delabroui
A. Ducout[66], X. Dupac[35], S. Dusini[62], G. Efstathiou[6
J. Fergusson[11], R. Fernandez-Cobos[61], F. Finelli[41,47], F. For
S. Galli[55,90†], K. Ganga[2], R. T. Génova-Santos[60,16], M.
A. Gruppuso[41,47], J. E. Gudmundsson[94,25], J. Hamann[86],
Z. Huang[83], A. H. Jaffe[53], W. C. Jones[25], A. Karakci[59],
N. Krachmalnicoff[78], M. Kunz[14,54,3], H. Kurki-Suonio[24,40],
M. Le Jeune[2], P. Lemos[58,65], J. Lesgourgues[56], F. Levri
M. López-Caniego[35], P. M. Lubin[28], Y.-Z. Ma[77,80,74], J.
A. Marcos-Caballero[61], M. Maris[43], P. G. Martin[7], M. Mar
P. R. Meinhold[28], A. Melchiorri[31,50], A. Mennella[32,45],
D. Molinari[30,41,48], L. Montier[95,8], G. Morgante[41], A. Mo
B. Partridge[39], G. Patanchon[2], H. V. Peiris[22], F. Perrot
J. P. Rachen[18], M. Reinecke[72], M. Remazeilles[64], A.
B. Ruiz-Granados[60,16], L. Salvati[54], M. Sandri[41], M. Savelain
R. Sunyaev[72,91], A.-S. Suur-Uski[24,40], J. A. Tauber[36], D.
L. Valenziano[41], J. Valiviita[24,40], B. Van Tent[69], L. Vibert[54,5
S. D. M. W
(Affiliation

We present cosmological parameter results from the final f
isotropies, combining information from the temperature an
improved measurements of large-scale polarization allow th
cant gains in the precision of other correlated parameters. In
many parameters, with residual modelling uncertainties estin
spatially-flat 6-parameter ΛCDM cosmology having a power
from polarization, temperature, and lensing, separately and i
baryon density $\Omega_b h^2 = 0.0224 \pm 0.0001$, scalar spectral inde
68 % confidence regions on measured parameters and 95 %
$100\theta_* = 1.0411 \pm 0.0003$. These results are only weakly depe
in many commonly considered extensions. Assuming the ba
Hubble constant $H_0 = (67.4 \pm 0.5)$ km s^{-1}Mpc^{-1}; matter densi
We find no compelling evidence for extensions to the base-ΛCDM model. Combining with baryon acoustic oscillation (BAO) measurements (and
considering single-parameter extensions) we constrain the ef
the Standard Model prediction $N_{\rm eff} = 3.046$, and find that th
to prefer higher lensing amplitudes than predicted in base ΛC
from the ΛCDM model; however, this is not supported by t
BAO data. The joint constraint with BAO measurements on s
with Type Ia supernovae (SNe), the dark-energy equation of
constant. We find no evidence for deviations from a purely
Keck Array data, we place a limit on the tensor-to-scalar ra
deuterium abundances for the base-ΛCDM cosmology are i
agreement with BAO, SNe, and some galaxy lensing observ
including galaxy clustering (which prefers lower fluctuation
measurements of the Hubble constant (which prefer a high
favoured by the *Planck* data.

Key words. Cosmology: observations – Cosmology: theory – Cosmic background radiation – cosmological parameters

*Corresponding author: G. Efstathiou, gpe@ast.cam.ac.uk
†Corresponding author: S. Galli, gallis@iap.fr
‡Corresponding author: A. Lewis, antony@cosmologist.info

Page 40

$$\Omega_K = -0.044^{+0.018}_{-0.015} \quad (68\,\%,\ \textit{Planck}\ \text{TT,TE,EE+lowE}), \qquad (46b)$$

a detection of curvature at about 3.4σ

an apparent detection of curvature at well over $2\,\sigma$. The 99 % probability region for the TT,TE,EE+lowE result is $-0.095 < \Omega_K < -0.007$, with only about 1/10000 samples at $\Omega_K \geq 0$. This is not entirely a volume effect, since the best-fit χ^2 changes by $\Delta\chi^2_{\rm eff} = -11$ compared to base ΛCDM when adding the one additional curvature parameter. The reasons for the pull towards

*Corresponding author: G. Efstathiou, gpe@ast.cam.ac.uk
†Corresponding author: S. Galli, gallis@iap.fr
‡Corresponding author: A. Lewis, antony@cosmologist.info

5. Curvature of the universe

5. Curvature of the universe

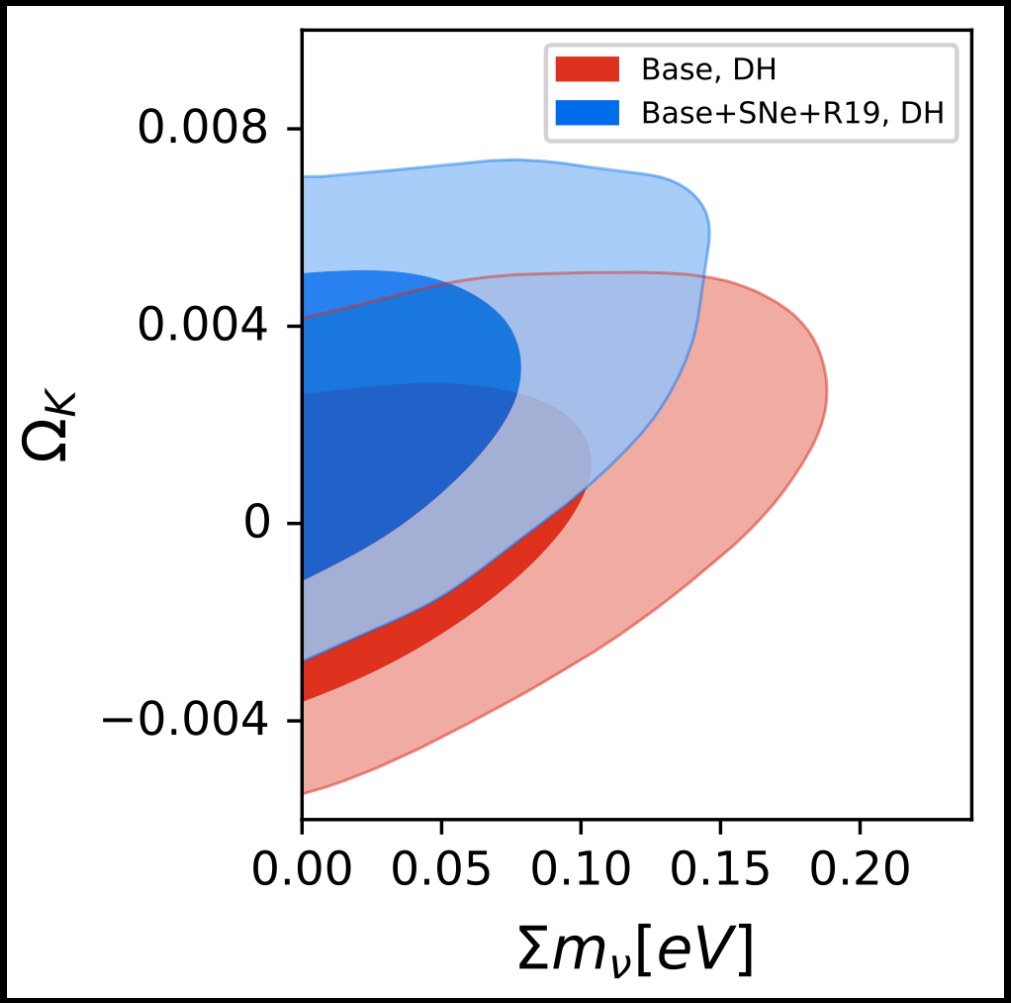

Choudhury and Hannestad, arXiv:1907.12598 [astro-ph.CO]

There is a positive correlation between the curvature and the total neutrino mass.

6. CMB tension

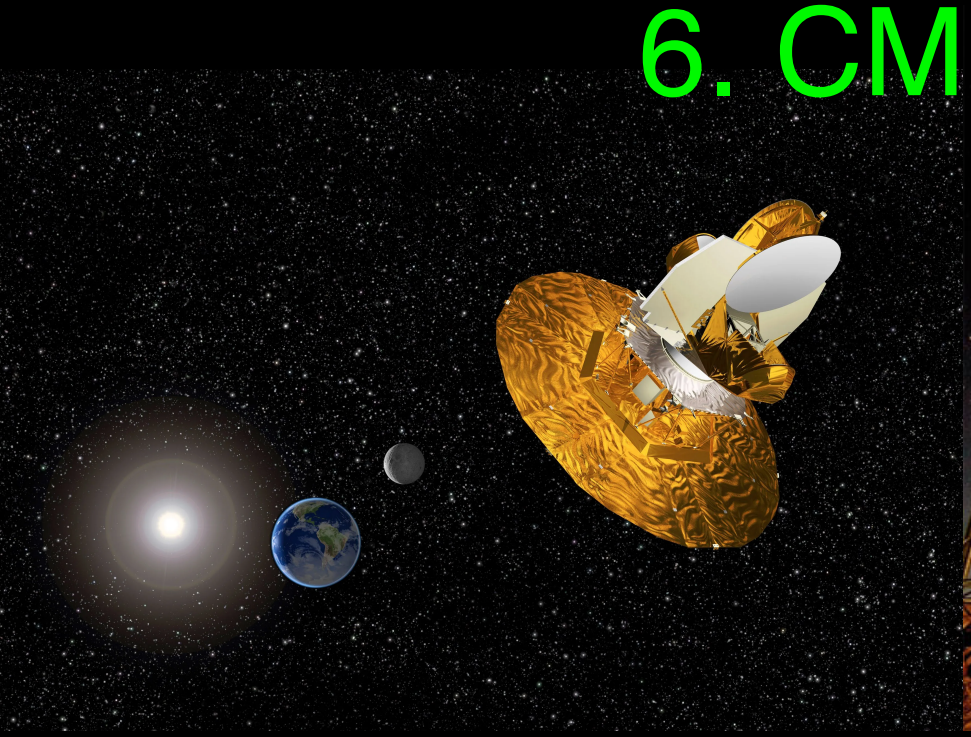

Satellite CMB telescopes

Ground based CMB telescopes

6. CMB tension

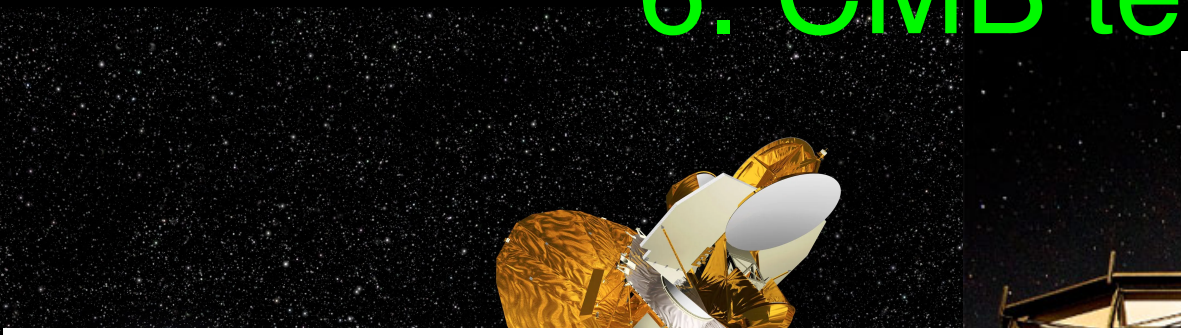

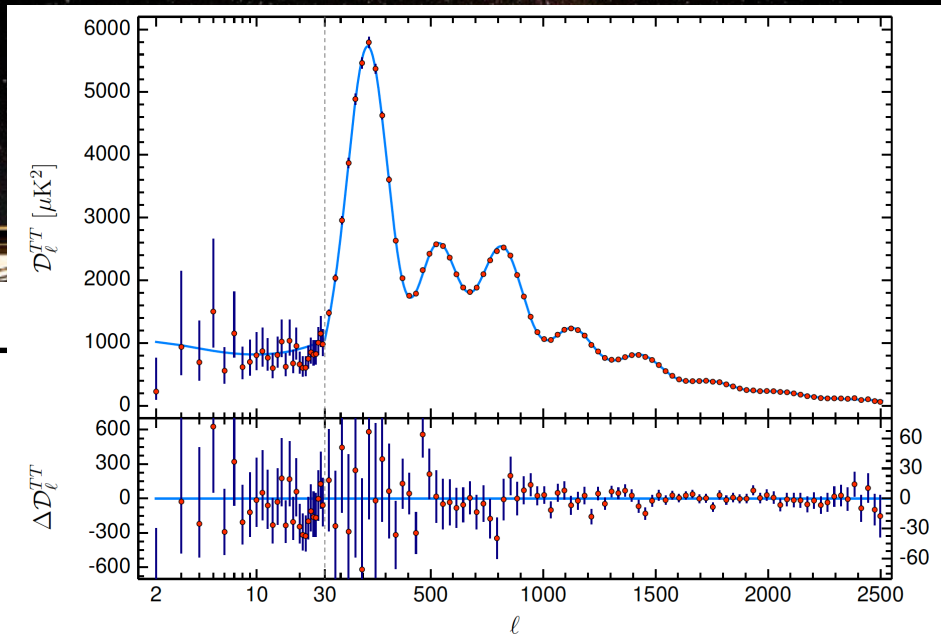

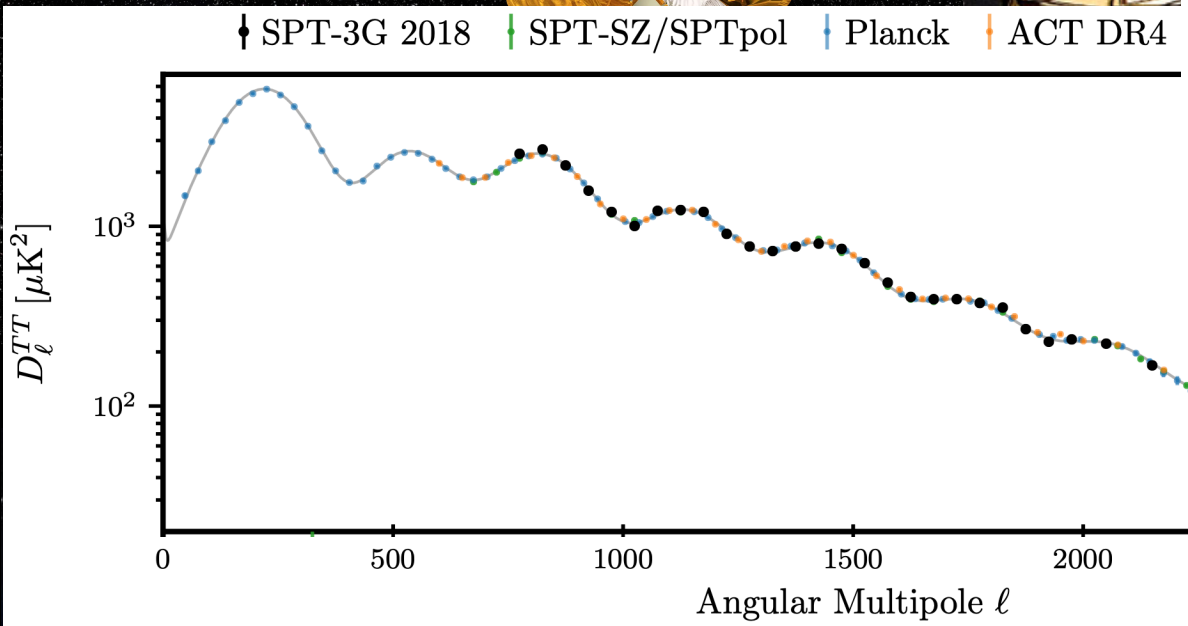

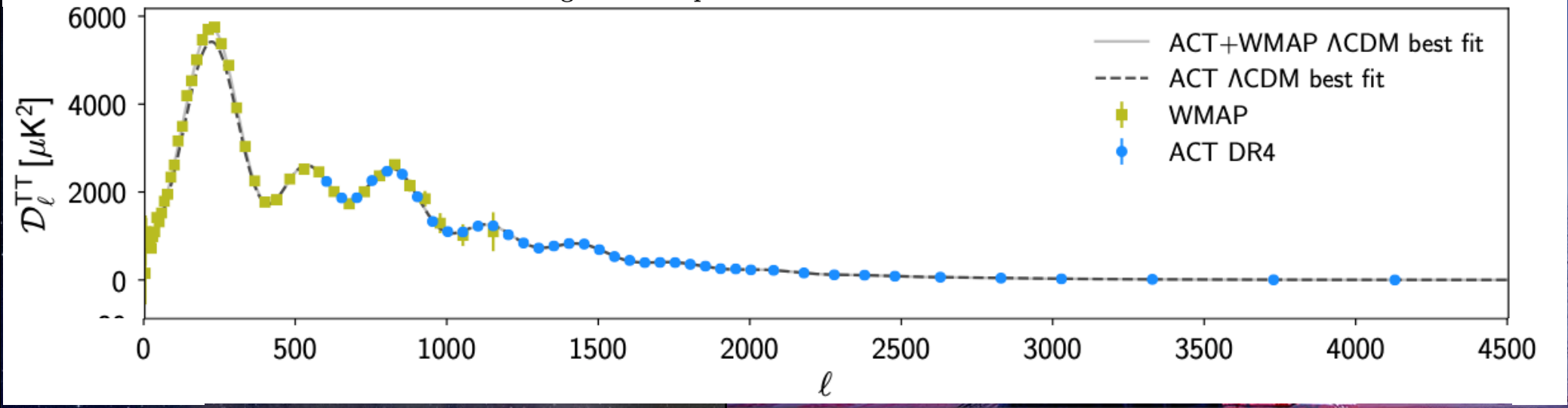

6. CMB tension

Handley and Lemos, arXiv:2007.08496 [astro-ph.CO]

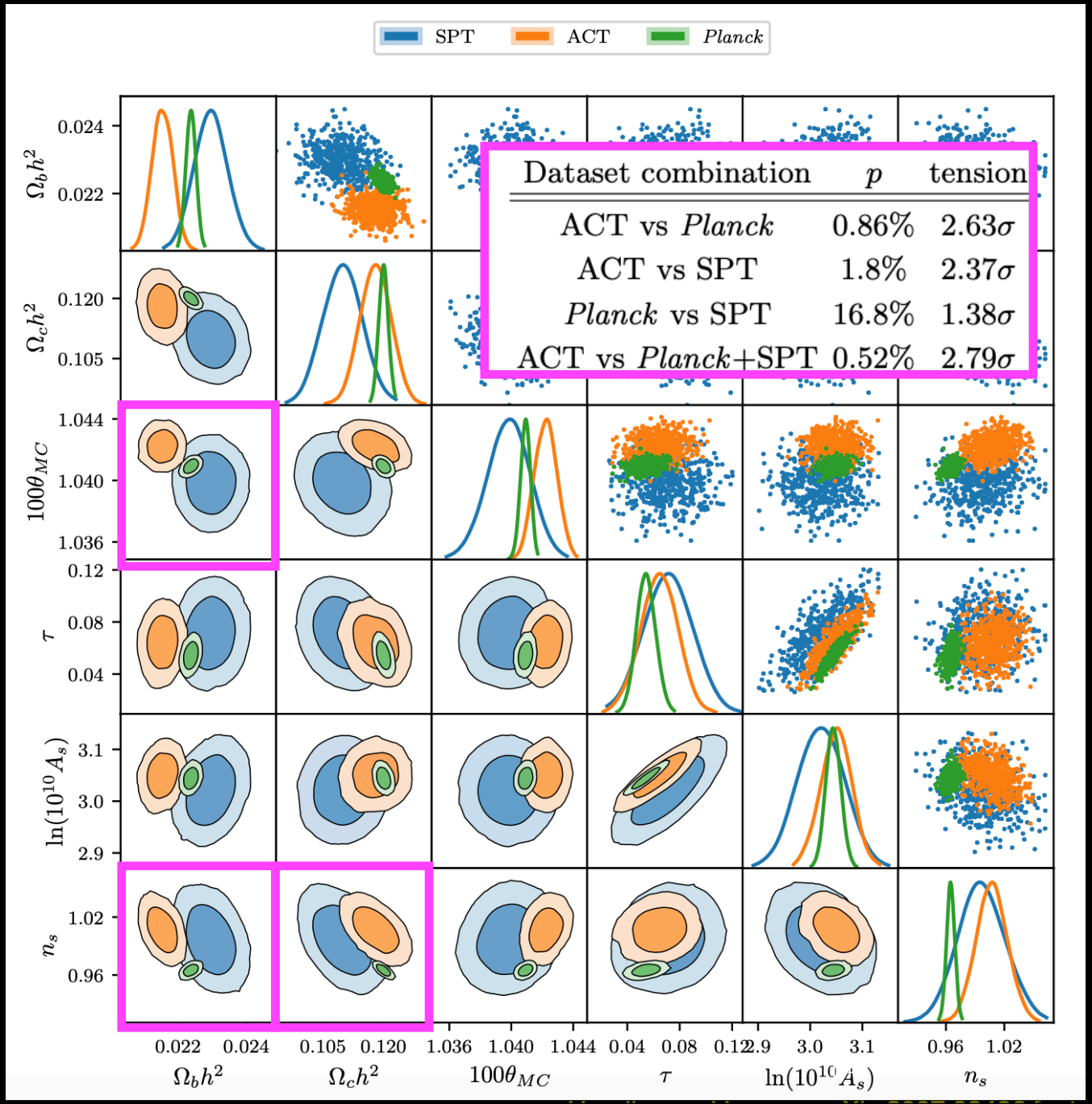

Dataset combination	p	tension
ACT vs *Planck*	0.86%	2.63σ
ACT vs SPT	1.8%	2.37σ
Planck vs SPT	16.8%	1.38σ
ACT vs *Planck*+SPT	0.52%	2.79σ

Global tensions between CMB datasets.

For each pairing of datasets this is the tension probability p that such datasets would be this discordant by (Bayesian) chance, as well as a conversion into a Gaussian-equivalent tension.

Between Planck and ACT there is a 2.6σ tension.

Assuming LCDM

6. CMB tension

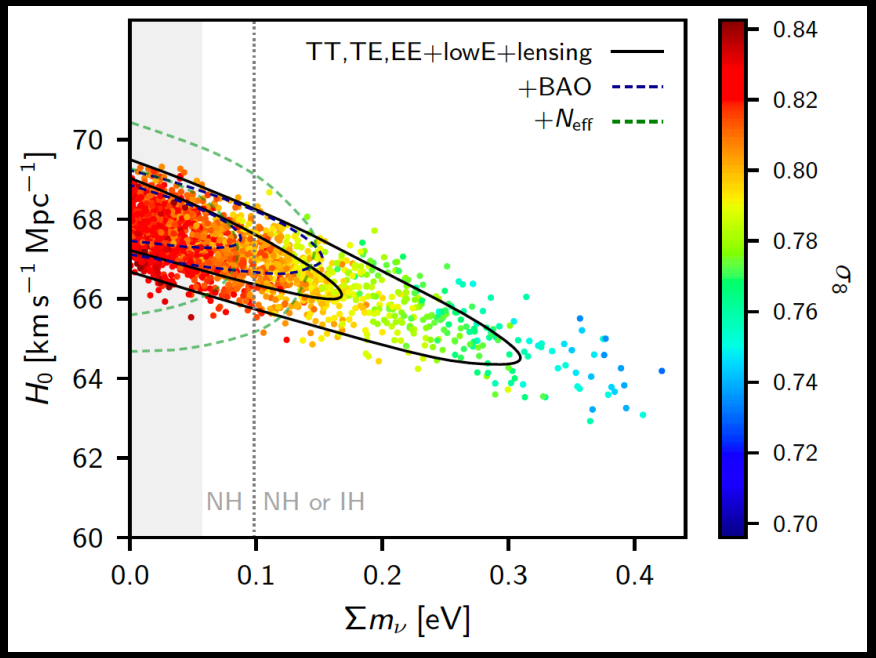

$$\sum m_\nu < 0.24 \text{ eV} \quad (95\,\%,\ \text{TT,TE,EE+lowE+lensing})$$

Planck 2018 collaboration, arXiv:1807.06209 [astro-ph.CO]

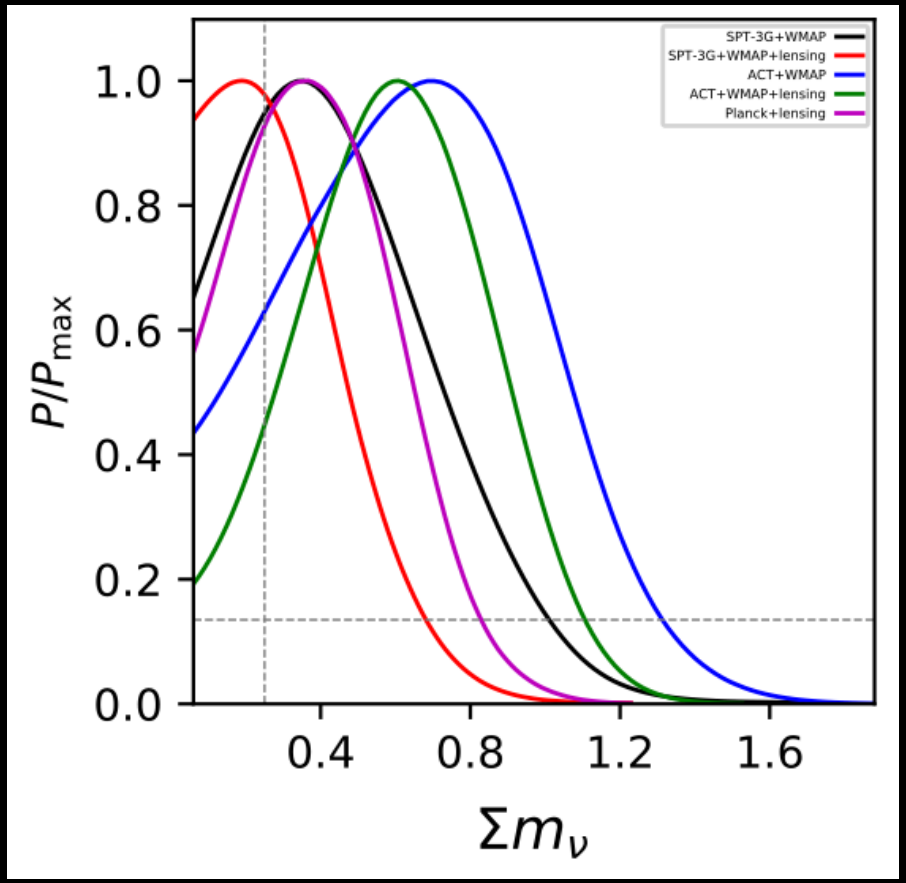

Di Valentino and Melchiorri, 2022 *ApJL* **931** L18

While we have only an upper limit for Planck on the total neutrino mass, ACT-DR4, when combined with WMAP and lensing, prefers a neutrino mass different from zero at more than 95% CL.

Constraints at 68% CL

Dataset	Σm_ν [eV]
ACT-DR4+WMAP+Lensing	0.60 ± 0.25
SPT-3G+WMAP	$0.46^{+0.14}_{-0.36}$
Planck+Lensing ($+A_{\rm lens}$)	$0.41^{+0.17}_{-0.25}$

6. CMB tension

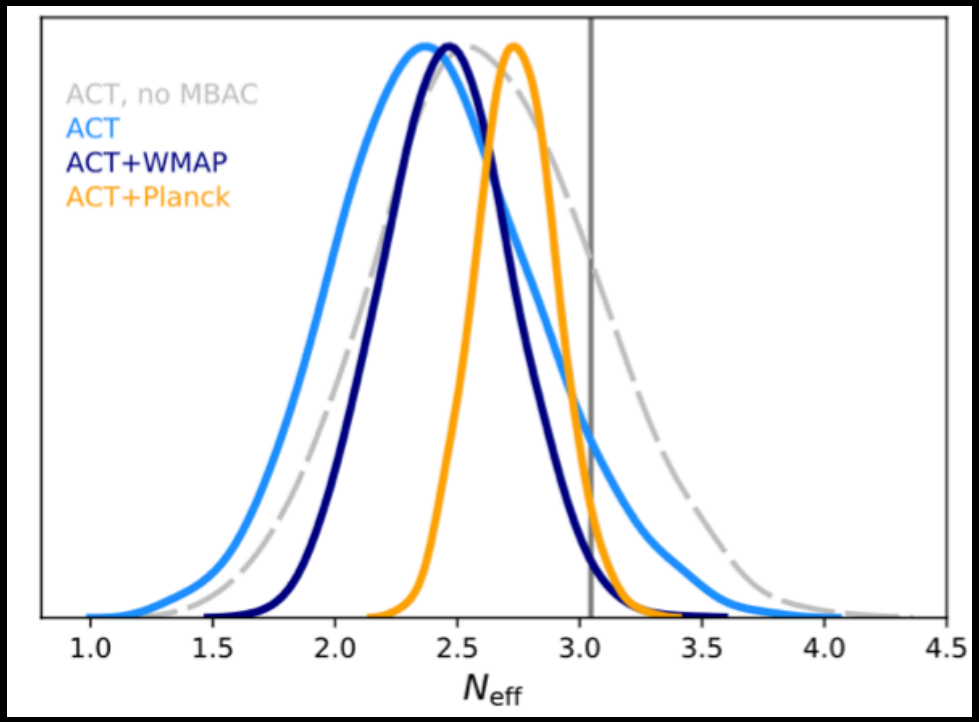

ACT-DR4 2020, Aiola et al., arXiv:2007.07288 [astro-ph.CO]

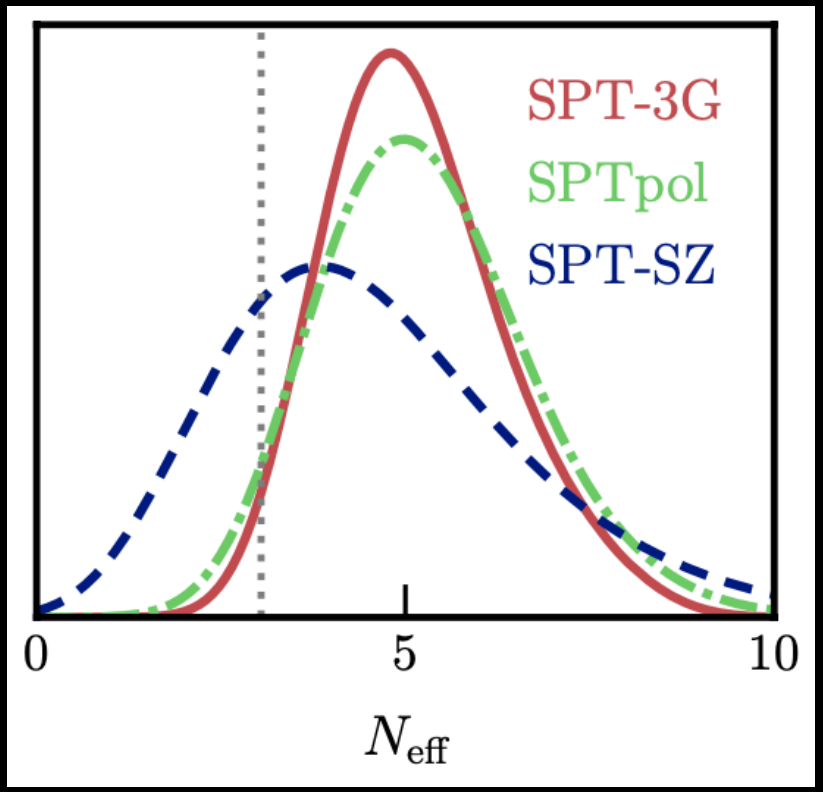

SPT-3G, arXiv:2103.13618 [astro-ph.CO]

Parameter	ACT	**ACT+WMAP**	ACT+Planck
$N_{\rm eff}$	2.42 ± 0.41	$\mathbf{2.46 \pm 0.26}$	2.74 ± 0.17

$$N_{\rm eff} = 3.70 \pm 0.70$$

6. CMB tension

Constraints at 68% CL

	Σm_ν [eV]
Planck ($+A_{\rm lens}$)	< 0.50
Planck+BAO ($+A_{\rm lens}$)	< 0.22
Planck+Pantheon ($+A_{\rm lens}$)	< 0.47
Planck+Lensing ($+A_{\rm lens}$)	$0.38^{+0.12}_{-0.28}$
ACT-DR4+WMAP	0.81 ± 0.28
ACT-DR4+WMAP+BAO	< 0.27
ACT-DR4+WMAP+Pantheon	0.71 ± 0.28
ACT-DR4+WMAP+Lensing	0.56 ± 0.21
ACT-DR4+WMAP+R20	0.83 ± 0.230
ACT-DR4+WMAP+F21	$0.85^{+0.27}_{-0.33}$
ACT-DR4+WMAP+BAO+R20	$0.39^{+0.13}_{-0.25}$
ACT-DR4+WMAP+BAO+F21	< 0.34
SPT-3G+WMAP	< 0.56
SPT-3G+WMAP+BAO	< 0.28
SPT-3G+WMAP+Pantheon	$0.46^{+0.11}_{-0.39}$
SPT-3G+WMAP+Lensing	< 0.39
SPT-3G+WMAP+R20	$0.49^{+0.12}_{-0.42}$
SPT-3G+WMAP+F21	< 0.60
SPT-3G+WMAP+BAO+R20	$0.37^{+0.13}_{-0.25}$
SPT-3G+WMAP+BAO+F21	< 0.32

Di Valentino and Melchiorri,
2022 *ApJL* **931** L18

What about the 10 parameters extended model?

ACT-DR4 suggests a neutrino mass with $\Sigma m_\nu = 0.81 \pm 0.28$ eV and SPT-3G

$\Sigma m_\nu < 0.56$ eV at 68% CL.

6. CMB tension

Constraints at 68% CL

	Σm_ν [eV]
Planck ($+A_{\rm lens}$)	< 0.50
SPT-3G+WMAP+R20	$0.49^{+0.12}_{-0.42}$
SPT-3G+WMAP+F21	< 0.60
SPT-3G+WMAP+BAO+R20	$0.37^{+0.13}_{-0.25}$
SPT-3G+WMAP+BAO+F21	< 0.32

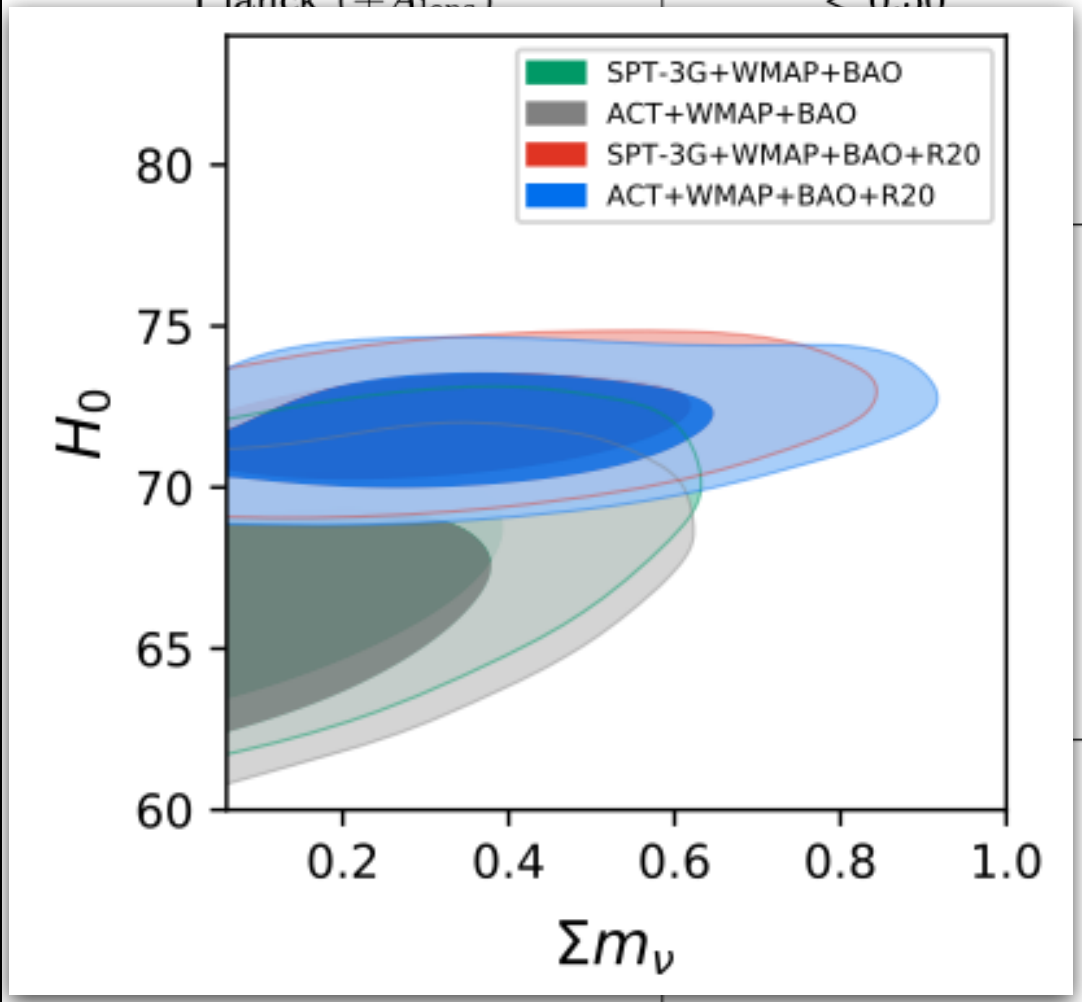

Di Valentino and Melchiorri, 2022 *ApJL* **931** L18

When CMB and BAO constraints are considered in these extended cosmologies, they provide constraints on the Σm_ν vs H0 plane that clearly show a correlation between these two parameters, that is exactly the opposite of what is obtained under standard LCDM.

6. CMB tension

10 parameters

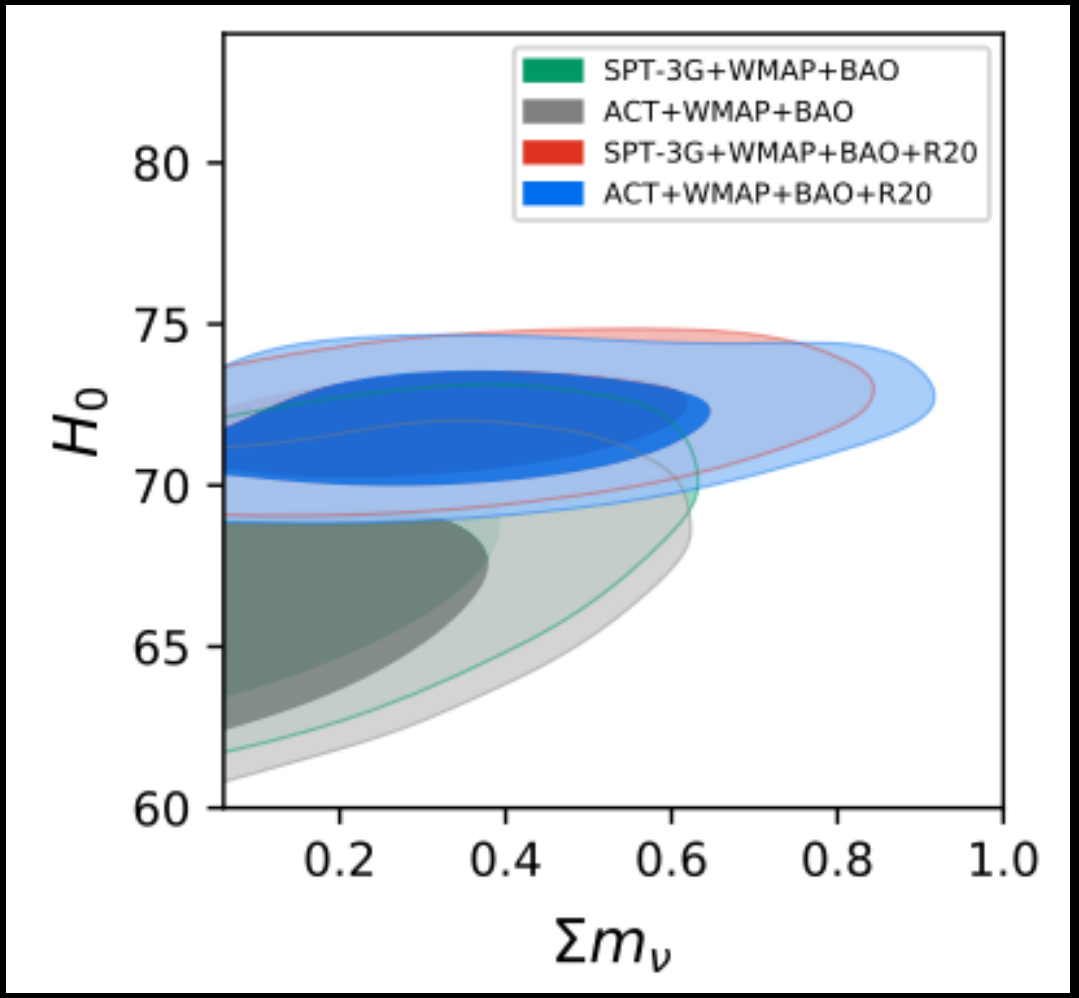

Di Valentino and Melchiorri, 2022 *ApJL* **931** L18

standard LCDM

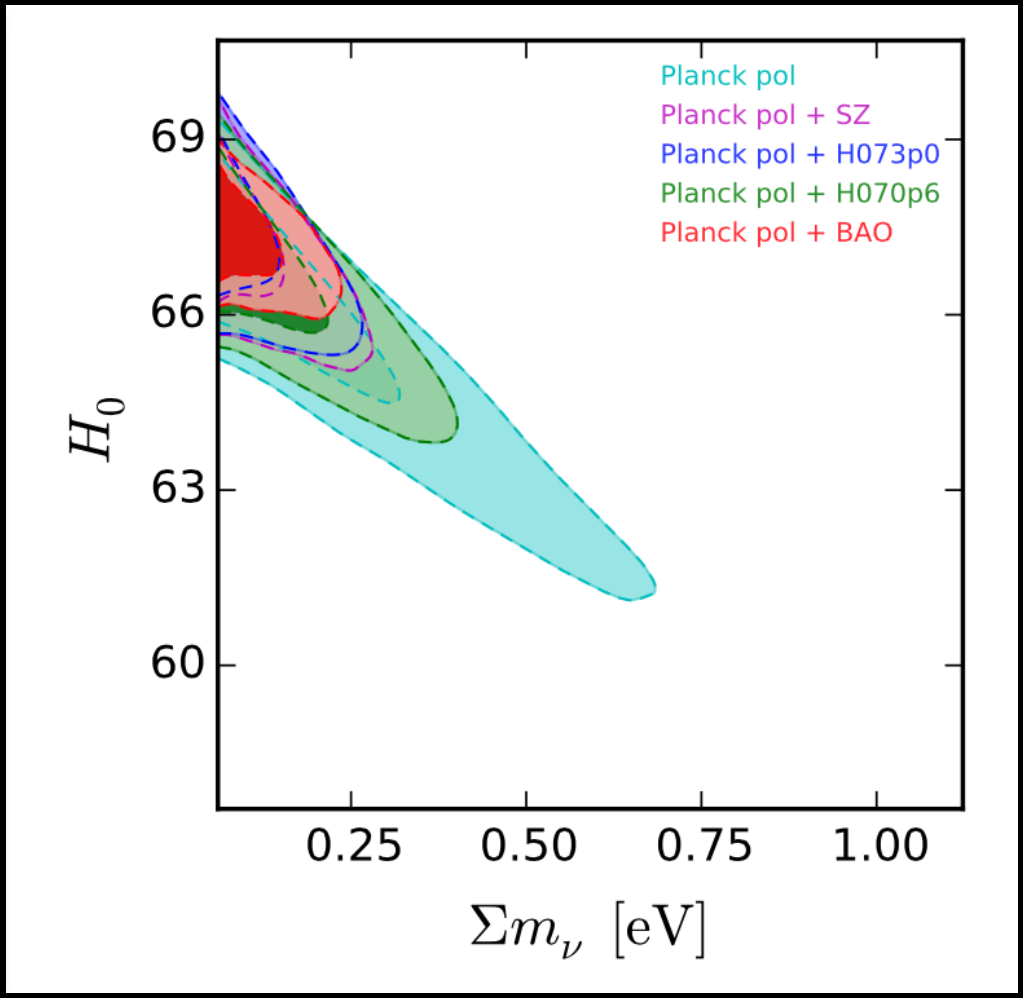

Di Valentino et al. Phys.Rev. D93 (2016) no.8, 083527

6. CMB tension

Dataset	Σm_ν [eV]
Plan	0.50
Planck+	0.22
Planck+P	0.47
Planck+	$^{+0.12}_{-0.28}$
ACT-	$\pm$ 0.28
ACT-DR4	0.27
ACT-DR4+	$\pm$ 0.28
ACT-DR4-	$\pm$ 0.21
ACT-DR4+WMAP+R20	0.83 $\pm$ 0.230
ACT-DR4+WMAP+F21	$0.85^{+0.27}_{-0.33}$
ACT-DR4+WMAP+BAO+R20	$0.39^{+0.13}_{-0.25}$
ACT-DR4+WMAP+BAO+F21	< 0.34
SPT-3G+WMAP	< 0.56
SPT-3G+WMAP+BAO	< 0.28
SPT-3G+WMAP+Pantheon	$0.46^{+0.11}_{-0.39}$
SPT-3G+WMAP+Lensing	< 0.39
SPT-3G+WMAP+R20	$0.49^{+0.12}_{-0.42}$
SPT-3G+WMAP+F21	< 0.60
SPT-3G+WMAP+BAO+R20	$0.37^{+0.13}_{-0.25}$
SPT-3G+WMAP+BAO+F21	< 0.32

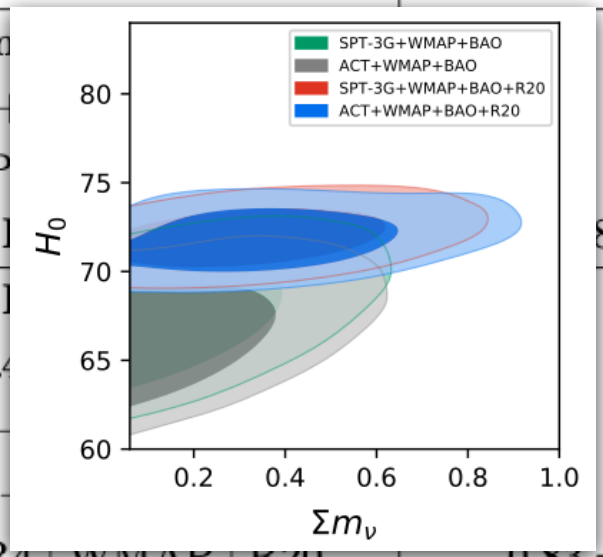

Di Valentino and Melchiorri,
arXiv:2112.02993 [astro-ph.CO]

What about the 10 parameters extended model?

Therefore, in extended cosmologies, a neutrino mass is preferred by the cosmological data:

ACT-DR4+BAO+R20 gives

$\Sigma m_\nu = 0.39^{+0.13}_{-0.25}$ eV,

while SPT-3G+BAO+R20

$\Sigma m_\nu = 0.60^{+0.44}_{-0.50}$ eV at 68% CL.

Constraints at 68% CL

6. CMB tension

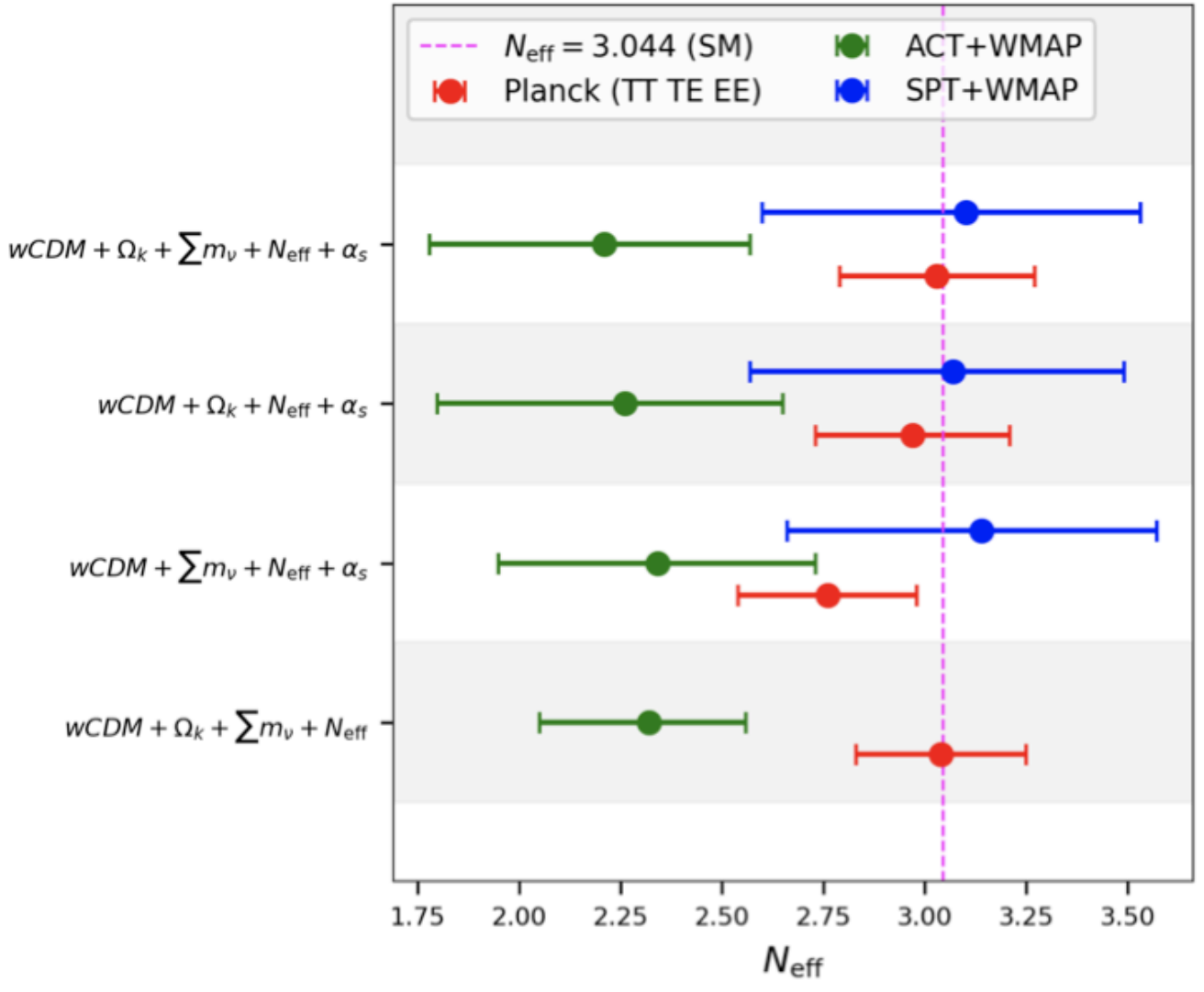

Di Valentino et al., *Phys.Rev.D* 106 (2022) 10, 103506

And the indication for Neff significantly less than 3.044 from ACT is robust also in its extensions.

Conclusions:

With the cosmological data, we can constrain important neutrino parameters:
the total neutrino mass, where there is no evidence for a neutrino mass different from zero, and the neutrino effective number, where there is no evidence for extra species.

We expect to have a CNB that has not been detected yet.
However, we have indirect evidence from measurements of Neff.
This can be done at BBN with the abundance of light elements or at the CMB through the damping tail and ISW effect.

We can measure a total neutrino mass with the CMB and LSS and the most stringent bound is $\Sigma m_\nu < 0.043$eV at 95% CL (pushing for a negative number) for a combination of cosmological and astrophysical probes,
which is in tension with the terrestrial measurements.

Warning!!

Some indication for anomalies and tensions are present in the cosmological data, and these could significantly affect the current Planck constraints on the fundamental physics quantities, presenting a serious limitation to precision cosmology.
Until the nature of these anomalies (if new physics or systematic errors) is clear, we should be very conservative when considering cosmological constraints.

Thank you!

e.divalentino@sheffield.ac.uk

MENU

COSMOVERSE • COST ACTION CA21136

Addressing observational tensions in cosmology with systematics and fundamental physics

https://cosmoversetensions.eu/

WG1 – Observational Cosmology and systematics

Unveiling the nature of the existing cosmological tensions and other possible anomalies discovered in the future will require a multi-path approach involving a wide range of cosmological probes, various multiwavelength observations and diverse strategies for data analysis.

READ MORE

WG2 – Data Analysis in Cosmology

Presently, cosmological models are largely tested by using well-established methods, such as Bayesian approaches, that are usually combined with Monte Carlo Markov Chain (MCMC) methods as a standard tool to provide parameter constraints.

READ MORE

WG3 – Fundamental Physics

Given the observational tensions among different data sets, and the unknown quantities on which the model is based, alternative scenarios should be considered.

READ MORE

The total neutrino mass and BAO

To simplify let's consider an ensemble of galaxy pairs at a specific redshift z.
When the pairs are oriented across the line-of-sight,
a preferred angular separation of galaxies Δθ can be observed.
This allows us to measure the comoving distance DM(z) = rd/Δθ to this redshift,
which is an integrated quantity of the expansion rate of the universe.

$$D_{\rm M}(z) = \frac{c}{H_0}\int_0^z {\rm d}z' \frac{H_0}{H(z')}$$

The angular diameter distance will be DA(z) = DM(z)/(1 + z).
Conversely, when the pairs are aligned along the line-of-sight, a preferred redshift separation Δz can be observed. This measures a comoving distance interval that, for small values, provides a redshift dependent measurement of the Hubble parameter, represented by the equivalent distance variable DH(z) = c/H(z) = rd/Δz.
Hence BAO measurements constrain the quantities DM(z)/rd and DH(z)/rd.
This interpretation holds under standard assumptions and models similar to ΛCDM.
For measurements in redshift bins with low signal-to-noise ratios,
the angle-averaged quantity DV(z)/rd can be constrained,
where DV(z) is the angle-average distance that represents the average of the distances measured along and perpendicular to the line-of-sight.

$$D_{\rm V}(z) = \left(zD_{\rm M}(z)^2 D_H(z)\right)^{1/3}$$

DESI collaboration, arXiv:2404.03002